Late Miocene Uplift at

Wheeler Ridge,

Kern County, California

Gary Henley II

June 2011

CSUB

Late Miocene Uplift at

Wheeler Ridge,

Kern County, California

Gary Henley II

June 2011

CSUB

Thesis completion represents part of fulfilling Masters in Geology requirements at CSUB.

Late Miocene Uplift at

Wheeler Ridge,

Kern County, California

Gary Henley II

June 2011

This thesis has been accepted on behalf of the Department of Geology by their supervisory committee:

Dr. Robert Negrini, Committee Chair

Stuart Gordon, Committee Member

Brian Hirst, Committee Member

Table of Contents

Table of Contents (cont.)

Acknowledgements

I would like to thank my family and friends that encouraged me along the way to finish this project. I would like to thank Morgann, my daughter, for reminding when it was time to play and put aside my work. I would like to thank Brandon for his unending words of encouragement and his simple wisdom that some day this would be finished. I would like to thank my father, big Gary, and my grandparents, Goldie and Charles, for teaching me that anything is possible with the right attitude and a little bit of hard work. Without them none of this would have been possible, or enjoyable.

I would like to thank Vintage Production, LLC (Oxy) for allowing me access to their data and allowing me to publish my results. I would also like to thank all of my colleagues at Oxy who were always willing to give their time to help me with this project. Special acknowledgements are given to Jana McIntyre, Don Miller, Robert Bridges, Jaime Roig, Jeff Gartland, Kristal Bennett, Robert Privett, and Harry Angell.

Last, but certainly not least, I would like to thank my thesis advisors who tirelessly pushed me to expect more out of myself and their selfless sacrifice of their time to review my work. I would like to thank Rob for encouraging me along the way and keeping my head out of the weeds. I would like to thank Stuart for teaching me how to be a subsurface geologist. I would like to thank Brian for giving me the clue that helped me unravel this puzzle. I was truly blessed these three gentlemen took the time to be a part of this thesis and can only hope to accomplish half of what these men have in their careers.

Abstract

A stratigraphic and structural study from the late Miocene to the present at Wheeler Ridge oil field, Kern County, CA gives new insight into the formation of the Wheeler Ridge anticline and refines previous interpretations. Well log correlations of the lower Fruitvale, upper Fruitvale, and Santa Margarita formations show evidence of at least two late Miocene compressional events. Both of these late Miocene events are associated with unconformities and folding within the lower and upper Fruitvale and suggest southwest to northeast shortening. The lower Santa Margarita sands terminate near the edge of the late Miocene Wheeler Ridge anticline. The upper Santa Margarita sands and Etchegoin, San Joaquin, Tulare (undifferentiated) sands overtop the late Miocene Wheeler Ridge anticline and are continuous throughout the study area, thus suggesting no uplift during the Pliocene.

Quaternary uplift resulted in the currently observed Wheeler Ridge thrust fault and Wheeler Ridge anticline. The Wheeler Ridge thrust fault accommodates north to south shortening, strikes roughly east to west, dips to the south at approximately 30 degrees, is approximately 30,000 feet along strike, and has a maximum of 1,300 feet of throw.

A model of the late Miocene to recent uplift, deposition, and erosion is put forward to explain stratigraphic thickness variation observed in the lower Fruitvale, upper Fruitvale, and Santa Margarita formations. The model explains the erosion patterns observed in the lower Fruitvale and upper Fruitvale formations. The model also explains why the lower Santa Margarita sands are not continuous throughout the area, due to uplift of the late Miocene Wheeler Ridge anticline. This new model does not require a wedge thrust or back thrust solution, used in previous interpretations, to explain the faulting and folding in the Wheeler Ridge area.

Introduction

The Wheeler Ridge anticline, located in the southern San Joaquin Valley, north of the San Emigdio Mountains (Figures 1 & 2), is a fault propagation fold at the northward end of the Plio-Pleistocene fold and thrust belt responsible for San Emigdio Mountain uplift (Figure 3) (Davis, 1983; Dibblee, 1986; Medwedeff, 1992). The Wheeler Ridge anticline and the San Emigdio Mountains have been interpreted as the result of transpression along the "Big Bend" in the San Andreas Fault to the south (Namson and Davis, 1988; Medwedeff, 1992).

The Wheeler Ridge anticline and fault forms a structural trap for hydrocarbons and, as a result, numerous oil wells have been drilled in the Wheeler Ridge Anticline (Figure 2) (DOGGR, 1992). The primary study area for this research includes the Wheeler Ridge oil field (Figure 2). However, interpretations made in the Wheeler Ridge oil field are extended eastward into the North Tejon and Wind Gap oil fields for the purpose of comparison with previous interpretations.

This study will focus on the middle Miocene to present structure and stratigraphy of the Wheeler Ridge anticline. The objective is to evaluate the stratigraphy at the Wheeler Ridge oil field and develop a model to explain the stratigraphic variation therein (Figure 4). The model will be used to interpret the structure of the Wheeler Ridge anticline, Wheeler Ridge fault, and the new interpretation will be compared with previous interpretations.

Understanding of the Wheeler Ridge fault and anticline is important for academic, seismic hazard, and economic reasons. Wheeler Ridge is an example of a youthful

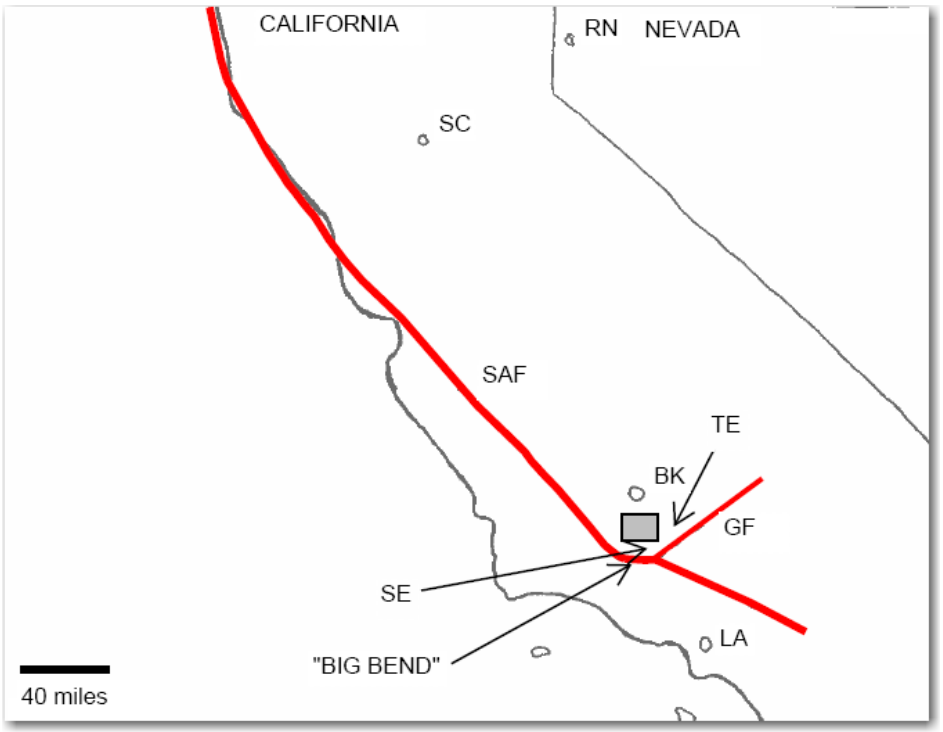

Figure 1. Wheeler Ridge study area shown in grey box. RN = Reno, SC = Sacramento, BK = Bakersfield, GF = Garlock Fault, LA = Los Angeles, SAF = San Andreas Fault, SE = San Emigdio Mountains, TE = Tejon Embayment.

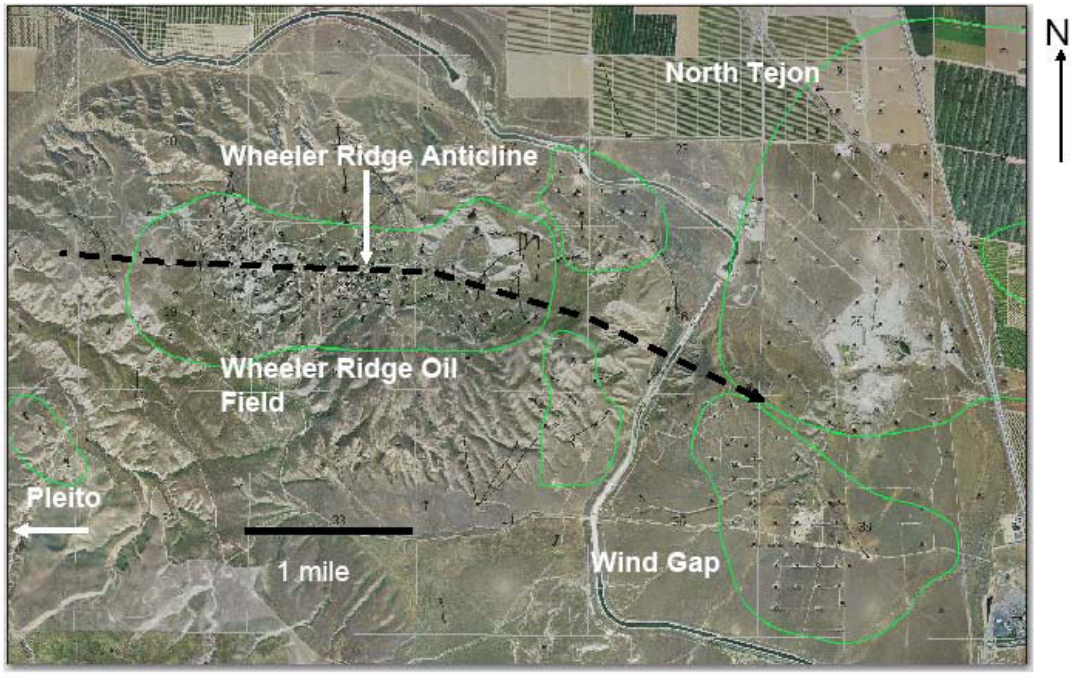

Figure 2. Wheeler Ridge field area with DOGGR field outlines and well locations. Green outlines are oil field outlines from DOGGR, 1992.

growing anticline. Understanding the mechanics of a fault propagation fold and the stratigraphic consequences is important when evaluating older structures in other parts of the world and predicting their geometry given minimal data. The 1952 magnitude 7.8 earthquake is one of the largest earth quakes in the United States (Bawden et al, 1997). The earthquake occurred on the White Wolf fault to the immediate north of Wheeler Ridge oil field. Understanding accurately the amount of fault slip possible and rate of fault propagation will place useful constraints on seismic hazard at Wheeler Ridge. Finally, the Wheeler Ridge oil field has 56 million barrels of estimated oil in place and improved knowledge of the geometry of folded beds and faults and their timing of deformation will lead to better exploitation of the remaining reserves (Gordon and Gerke, 2009).

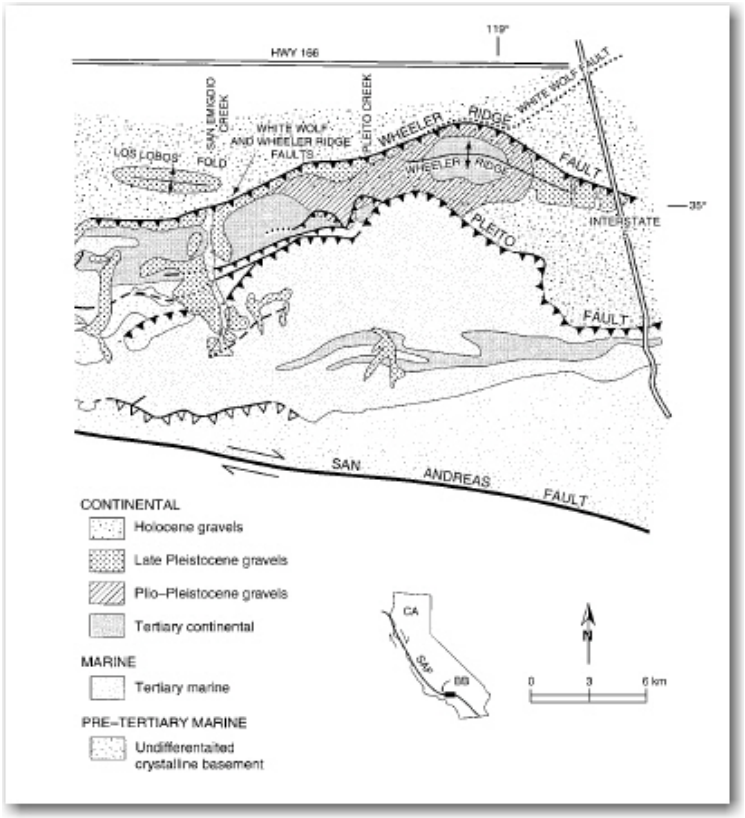

Figure 3. Approximate surface location of Wheeler Ridge Fault and other faults near study area (Modified from Keller et al., 1998).

Previous Work

Stratigraphy

The stratigraphy present at Wheeler Ridge represents approximately 140 million years of regional history (Figure 4) (Childs, 1985; Decelles, 1988; Dibblee, 1986; DOGGR, 1992; Hirst, 1986; Hirst, 1988). The basement rock is Cretaceous in age and is unconformably overlain by the Tejon Formation, which is late Paleocene to Eocene in age (Decelles, 1988; Dibblee, 1986; DOGGR, 1992; Hirst, 1986; Hirst, 1988). The Tejon Formation is composed of the Live Oak Silt and the Metrella sands (Decelles, 1988; Dibblee, 1986; DOGGR, 1992; Hirst, 1986; Hirst, 1988). The San Emigdio formation conformably sits on top of the Tejon Formation, is upper Eocene to lower Oligocene in age, and is interpreted as a regressive sequence (Decelles, 1988; Dibblee, 1986; DOGGR, 1992; Hirst, 1986; Hirst, 1988; Tye et al, 1993). The San Emigdio Formation is locally composed of the Refugian sands, "R" sands, and the unnamed lower Zemorrian sands and silts (Childs, 1985; Decelles, 1988; Dibblee, 1986; DOGGR, 1992; Hirst, 1986; Hirst, 1988). The Pleito Formation, locally equivalent to the Vedder Formation, overlies the San Emigdio Formation (Childs, 1985; Decelles, 1988; Dibblee, 1986; DOGGR, 1992; Hirst, 1986; Hirst, 1988). The Pleito Formation conformably overlies the San Emigdio Formation, is upper Oligocene to lower Miocene in age, and is composed of the Vedder sands (Z), silts, and claystone (Childs, 1985; Decelles, 1988; Dibblee, 1986; DOGGR, 1992; Hirst, 1986; Hirst, 1988; Tye et al, 1993). The Temblor Formation, with Freeman-Jewitt sands and silts, are Saucesian to Relizian in age, and overly the Pleito Formation (Childs, 1985; Dibblee, 1986; DOGGR, 1992; Hirst, 1986; Hirst, 1988). The Temblor Formation contains volcanic deposits to the east and south of the North Tejon

oil field (DOGGR, 1992; Goodman, 1988; Goodman, 1992; Hirst, 1986; Hirst, 1988). The Monterey Formation, overall a fine-grained siliceous rich unit, locally referred to as the Fruitvale Formation, overlies the Temblor Formation, is shallow to deep marine, contains the Olcese and Reserve sands, and is Relizian to Delmonitian in age (Childs, 1985; Dibblee, 1986; DOGGR, 1992; Hirst, 1986; Hirst, 1988). The Santa Margarita sands, shallow marine and Upper Mohnian in age, unconformably overly the Fruitvale shale (Childs, 1985; Dibblee, 1986; DOGGR, 1992;Gordon and Gerke, 2009; Hirst, 1986; Hirst, 1988) (Figure 5). The Etchegoin Formation, shallow marine to nonmarine, overlies the Santa Margarita formation.

Structure

The San Joaquin valley in California is a hydrocarbon rich basin (DOGGR, 1992). As such, it has been the focus of numerous studies. The formation and evolution of the southern San Joaquin basin has been studied in detail (e.g. Atwater and Stock, 1998; Davis, 1983; Davis and Lagoe, 1988; Dibblee, 1986; Goodman and Malin, 1992; Goodman et al, 1990; Gordon and Gerke, 2009; Hirst, 1986; Hirst, 1988; Loomis and Glazner, 1986; Namson and Davis, 1988; Namson and Davis, 2004).

The southern San Joaquin basin has had a complex history of compression and extension. An early period of compression occurred during the Paleogene related to the convergence of the North American and Farallon plates (Davis and Lagoe, 1988; Goodman and Malin, 1992). The middle Oligocene to middle Miocene was a period of active extension attributed to the passage of the Pacific / Farallon / North American triple

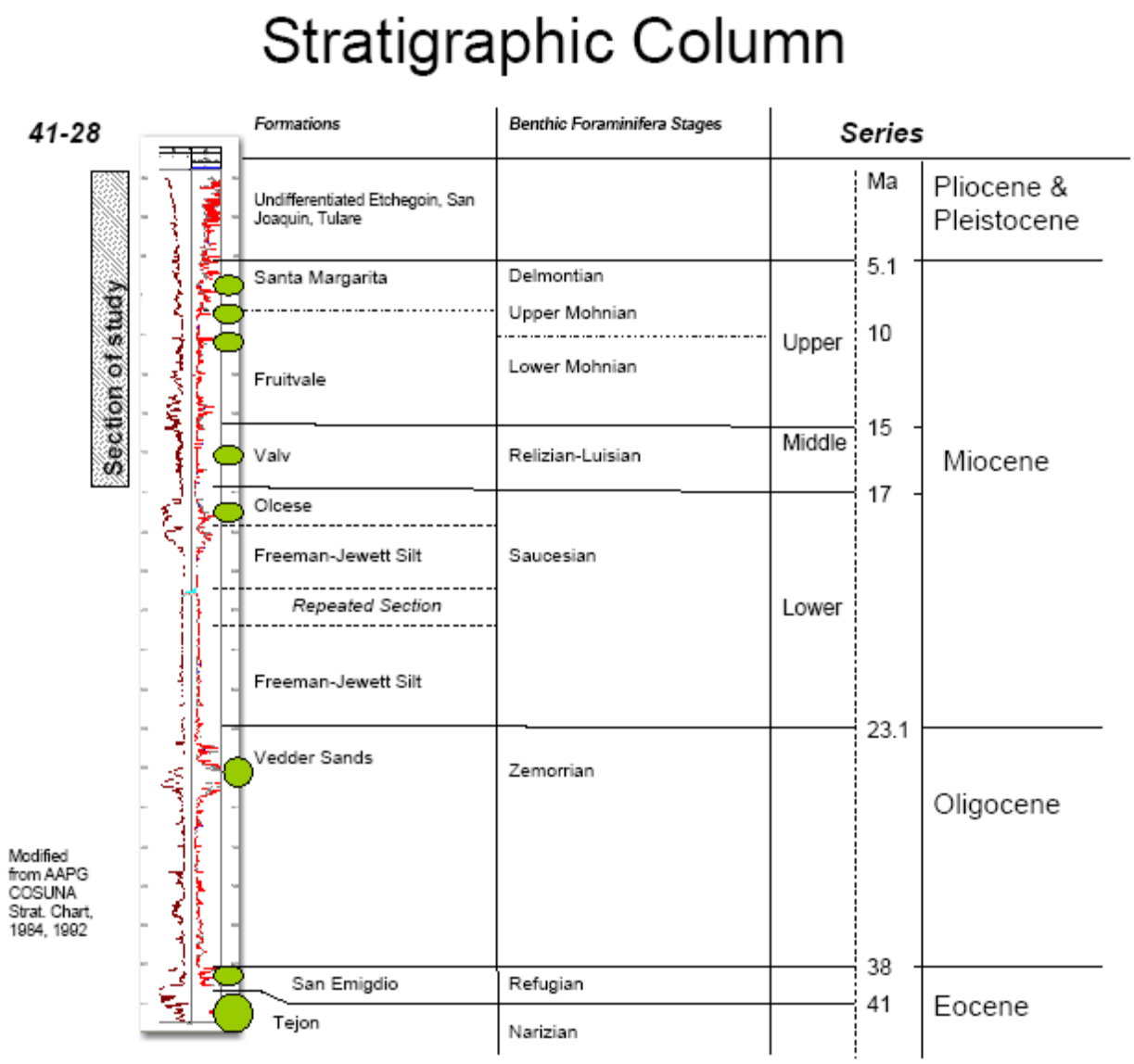

Figure 4. Stratigraphic column of Wheeler Ridge with a type log from well 41-28. Modified from AAPG COS UNA Strat. Chart. (Childs, 1985). Hydrocarbon bearing formations have been identified by green eclipses.

junction in the southern San Joaquin Valley by Bohannon and Parsons, (1995), Davis and Lagoe, (1988), Dibblee and Nilsen, (1973), Goodman and Malin, (1992), Glazner and Bartley, (1984), Gordon and Gerke, (2009), Hirst, (1986), Hirst, (1988), Luyendyk, (1991). The timing of the extension in the San Joaquin basin is similar to the timing of

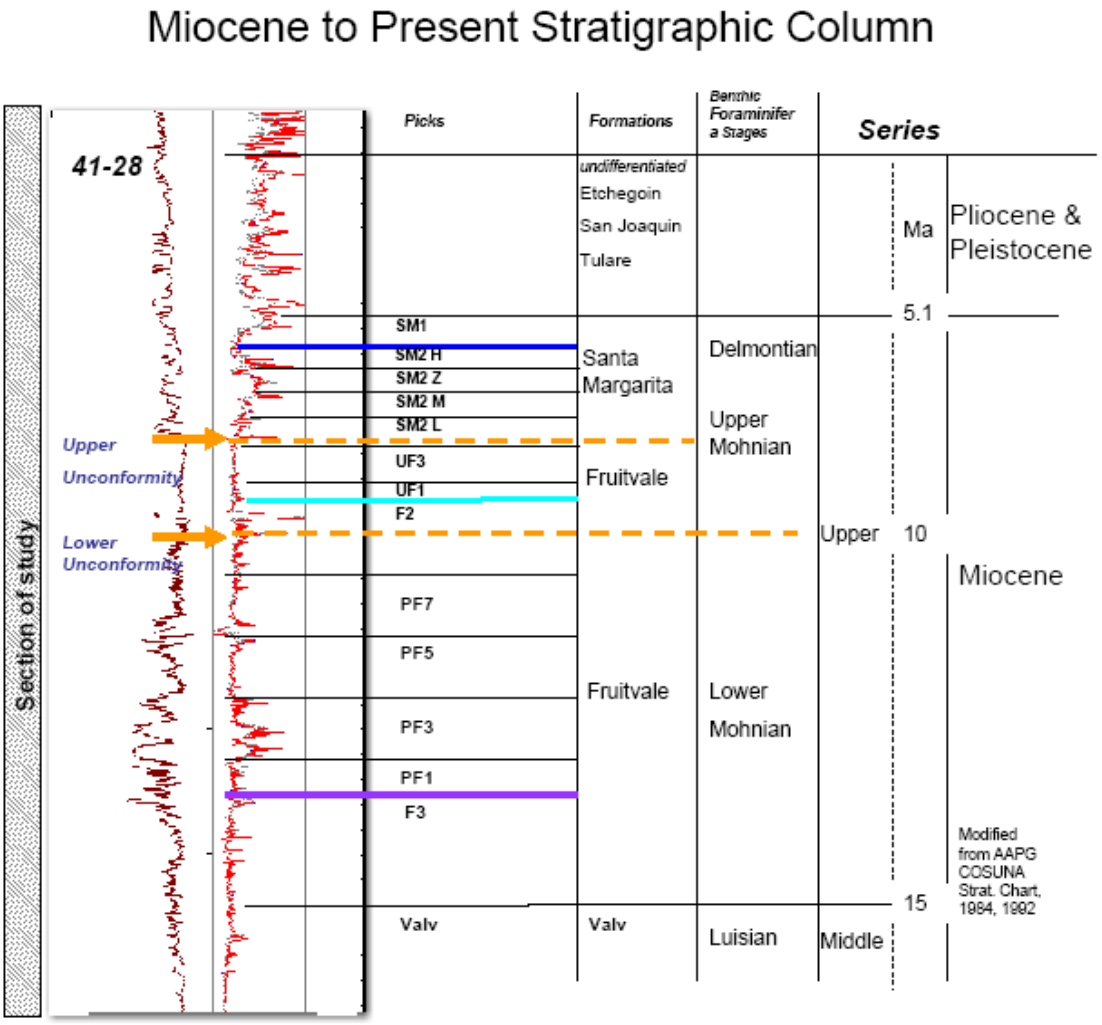

Figure 5. Stratigraphic column of section of study. In this study dark blue will be used to signify the SM2 top, light blue will be used for the F2 top, and purple will be used for the F3 top. The dashed blue lines are the upper and lower Miocene unconformities. The lower Fruitvale is shown from the F3 to the lower unconformity. The upper Fruitvale is shown from the F2 to the upper unconformity. Modified from AAPG COS UNA Strat. Chart. (Childs, 1985).

the extension in the Mojave basin (Dokka and Ross, 1995; Goodman and Malin, 1989; Luyendyk, 1991; Walker et al, 1995). It is possible then, the southern part of the San Joaquin Valley was a part of the Mojave extensional belt during the Miocene (Dokka and Ross, 1995; Luyendyk, 1991).

The extensional period, middle Oligocene to middle Miocene, produced high angle normal faults that potentially have been reactivated as tear faults (discussed in a

later section). The middle Miocene to present interval has been interpreted as to have been dominated by tectonics with a component of strike-slip convergence (Atwater and Stock, 1998; Davis, 1983; Davis and Lagoe, 1988; Dibblee, 1986; Goodman and Malin, 1992; Gordon and Gerke, 2009; Loomis and Glazner, 1986; Medwedeff, 1992; Namson and Davis, 1988, Namson and Davis, 2004). This paper will focus mainly on the middle Miocene to present period.

Wheeler Ridge is to the west of the Tejon Embayment area and northeast of the San Emigdio Mountains (Figure 1). Wheeler Ridge is the largest and easternmost fold north of the San Emigio Mountains (Dibblee, 1986). The Tejon Embayment area shows evidence of syndepositional normal faulting that produced growth stratigraphy (Goodman and Malin, 1989; Goodman and Malin, 1992; Gordon and Gerke, 2009; Hirst, 1986; Hirst, 1988). Syndepositional normal faulting is characterized by increased thickness of stratigraphic units on the footwall (Thorsen, 1963). The North Tejon field has sets of north-south trending growth normal faults dipping both to the east and west (Hirst, 1986; Hirst, 1988). The normal faults terminate upward in the middle Miocene section, before the F3 marker in the Fruitvale (Hirst, 1986; Hirst, 1988).

Another prominent normal fault is the White Wolf fault to the north of the Wheeler Ridge oil field. The slip history of the White Wolf fault is poorly constrained despite being the subject of numerous studies (Castillo and Zoback, 1995; Davis, 1986; Dibblee, 1986; Goodman and Malin, 1992). The White Wolf fault is currently active and was the epicenter of the 7.8 magnitude 1952 earthquake, one of the largest earthquakes California (Bawden et al, 1997). The White Wolf fault does not cut middle Miocene to

present stratigraphy within the Wheeler Ridge, Wind Gap, and North Tejon oil fields and is not discussed in this study.

Previous studies of the Wheeler Ridge fault system have interpreted all of the uplift to be Quaternary in age and related to north-south transpression from the "Big Bend" in the San Andreas fault (Figure 1) (Davis, 1983; Gordon and Gerke, 2009; Medwedeff, 1992; Namson and Davis, 1988). Well-bore breakout data suggests a rotation in the stress field from compression northeast – southwest to north - south in the southern San Joaquin Valley near the "Big Bend" in the San Andreas fault (Castillo and Zoback, 1994). The change in stress fields can be seen in the change of fold trends from southeast-northwest to east-west progressing from north to south in the southern San Joaquin Valley (Castillo and Zoback, 1995). The Wheeler Ridge anticline has been interpreted as a east-west trending structure that is doubly plunging to the east and west (Dibblee, 1986; Keller et al, 1998; Keller et al, 1999; Keller et al, 2000; Medwedeff, 1992). The Wheeler Ridge is actively growing and laterally propagating to the east (Keller et al, 1998; Medwedeff, 1992). Previous interpretations have suggested the Wheeler Ridge is a part of a larger fault system, with a depth of decollement at the brittle-ductile transition zone (Namson and Davis, 1988; Namson and Davis, 2004). This study will focus on the shallow faulting within 12,000 feet of the ground surface, representing the limit of well penetrations.

The eastern edge of the anticline, the North Tejon and Wind Gap oil fields, was studied in detail with five roughly north-south balanced cross-sections were created therein (Medwedeff, 1992). This work was focused on the North Tejon and Wind Gap oil fields to the east of the Wheeler Ridge oil field. A wedge thrust geometry was used to

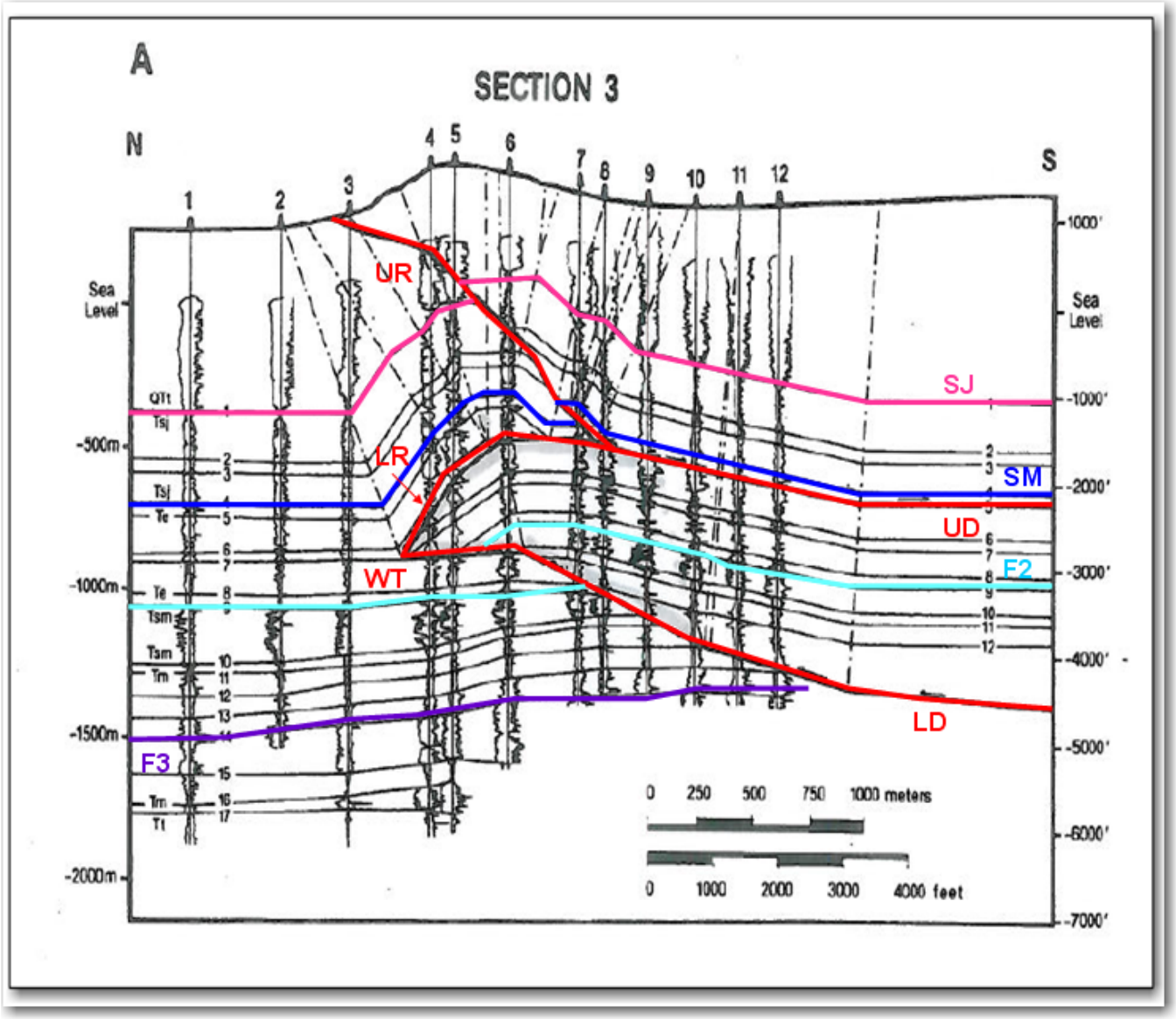

Figure 6. Wedge thrust solution (Medwedeff, 1992). LD = lower decollement, LR = lower ramp, UD = upper decollement, UR = upper ramp, WT = wedge tip. Red line represents faults, pink line is the San Joaquin top, blue is the Santa Margarita top, light blue is the F2 marker and the purple line is the F3 marker.

model the present geometry of the Neogene units (Figure 6) (Medwedeff, 1992). A wedge thrust is a subset of the fault bend fold theory (Groshrong, 1999; Medwedeff, 1992; Mitra, 1993; Mount et al, 1990; Suppe, 1983). Key characteristics of a wedge thrust solution are a wedge tip, a lower decollement, possibly an upper decollement, and folded growth strata (Medwedeff, 1992).

More specifically, Medwedeff (1992) interpreted the Wheeler Ridge fault system as a doubly vergent wedge thrust at the western edge of the North Tejon oil field that changes to a single wedge thrust eastward and finally into a simple fault bend fold at the eastern edge of the North Tejon oil field. North-south striking, nearly vertical faults in the Wheeler Ridge anticline were interpreted as tear faults related to the Quaternary compression (Keller et al, 1998; Medwedeff, 1992). The change from doubly verging wedge thrust to single wedge thrust to simple fault bend fold occurred when crossing the tear faults (Medwedeff, 1992). The reason for the change in fault style was interpreted to be related to the mechanical integrity of the individual tear fault bounded blocks (Medwedeff, 1992). However, kinematic graph of the crestal structural relief and fold area versus shortening do not suggest a kinematic evolution of the fault styles from east to west (Poblet et al, 2004).

An important assumption of the wedge thrust solution is that all of the compressional uplift is Quaternary in age (Medwedeff, 1992). Previous literature suggest that this might not be the case, at least in the vicinity of the study area. Evidence for regional uplift beginning at the upper Miocene to the early Pliocene has been documented in the Pioneer oil field, approximately ten miles to the west of the Wheeler Ridge oil field (Gordon and Gerke, 2009). In the nearby Pioneer oil field an estimated 1500 feet of erosion of upper Monterey Antelope and McDonald strata occurred (Gordon and Gerke, 2009). Uplift in the San Emigdio Mountains, to the south, is documented in the upper Miocene to early Pliocene as well (Davis, 1983; Davis and Lagoe, 1988; Dibblee, 1986). At a larger regional scale, a change in the relative plate motions between North America and the Pacific plate from ~N60W to N37W occurred approximately eight Ma (Atwater

and Stocke, 1998). The change in relative plate motions is approximately coincident with observed upper Miocene to early Pliocene erosion.

Studies of the geomorphic character of the Wheeler Ridge anticline have shown the presence of wind and water gaps and a range of soil ages across the anticline (Keller et al, 1998; Keller et al, 1999; Keller et al, 2000). Five different Quaternary soil ages were found, with the progression from relatively old to young going from west to east (Keller et al, 1998). The soil ages ranged from 185 ka to Holocene (Keller et al, 1998). The wind and water gap geomorphic features were found to be evidence of stream defeat as the anticline grew and began to propagate to the east (Keller et al, 1998). The soils were found to cluster in age between the wind and water gaps leading to the conclusion the wind and water gaps were coincident with tear faults that bounded the propagating fold and thrust system (Keller et al, 1998). The streams cuts at the surface of the tear faults were interpreted to be the result of the tear faults being relatively stable and occurring in discrete steps as the Wheeler Ridge fault propagated eastward (Keller et al, 1998). Quaternary uplift was estimated to have initiated at 400 ka, based on estimating the rate of eastward propagation at 30 mm/yr and back calculating the current length of the anticline (Keller et al, 1998). The current rate of uplift was estimated to be at a minimum of 3 mm/yr (Keller et al, 1998).

Methods

Well logs

Wheeler Ridge oil field has been a producing oil field over the last 80 years (DOGGR, 1992; DOGGR, 2011). The majority of the associated wells have resistivity and spontaneous potential logs. By tradition, spontaneous potential logs are shown on the left and resistivity logs are shown on the right (e.g., Figure 7). Spontaneous potential is a qualitative measurement of the relative spontaneous electrical potential between two objects, in this case the formation where the tool is measuring and a mud pit at the surface. Spontaneous potential deflections to the left, more negative potential, typically indicate sandier formations. The resistivity tools measure the resistance of the formation to accept a current. Resistivity is affected by lithology, porosity, fluid in the pores, and many other factors. A typical sand will show both an increase in resistivity and a deflection of the spontaneous potential relative to shaly formations (Figure 7).

As part of this study every well log in the field area was studied in detail and all picks of contacts used in this study originate from the author. The picks were tied into lithologic descriptions, production data, and paleontological data, where available, to confirm suspected geological formations and sequences. The best and most correlative markers are shales due to their greater areal continuity. The F2, F3, and SM2 markers were picked in shales and represent depositional sequence boundaries (Emery and Myers, 2009; Mitchum et al, 1977). Maximum flooding surfaces are sequence boundaries and are defined as surfaces separating younger from older strata with evidence of erosion or truncation and a long hiatus of deposition (Emery and Myers, 2009; Mitchum et al, 1977; Van Wagoner et al., 1988).

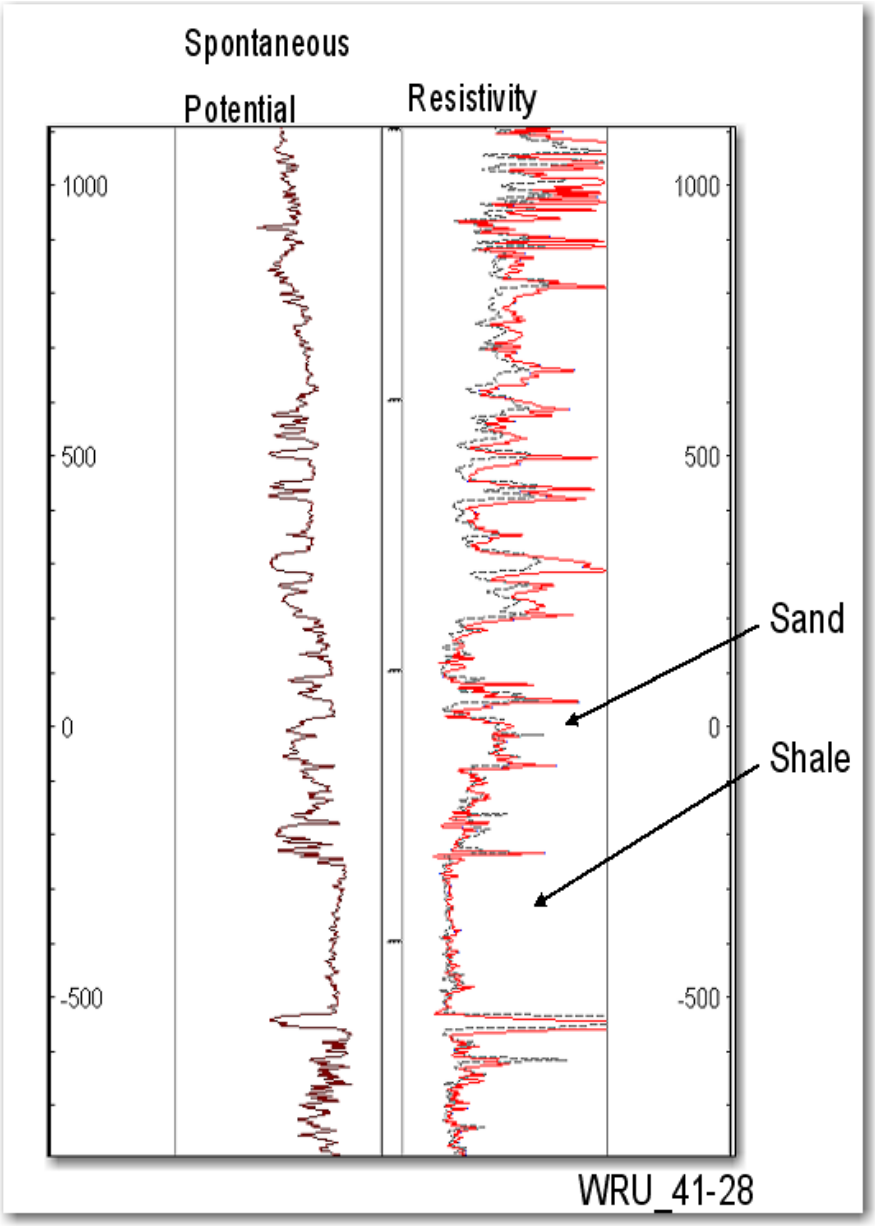

Figure 7. Log segment of a well, WRU_41-28, from the field area showing characteristic signatures of sandy and shaly intervals.

Stratigraphic cross-sections were created to assist with correlation. A stratigraphic cross-section is built on a profile line containing a number of wells. They are usually flattened on a datum, typically a key marker bed. Such cross-sections greatly assist in identifying time markers within well logs, and help one to avoid falling into the

trap of correlating lithologies that typically transgress time surfaces (Emery and Myers, 2009). Stratigraphic cross-sections also help to identify sequence boundaries, unconformities, and stratigraphic variation.

Key markers within this study are the F3, F2, SM2, and SM1 picks. The name F3 refers to a marker within the Fruitvale and the SM2 would be a marker within the Santa Margarita (DOGGR, 1992). Typically sands or productive horizons have been named in this manner, however it is important to note that in a time stratigraphic sense a sand may correlate to a shale because both are being deposited at the same time (Emery and Myers, 2009). That is why it is easiest to correlate flooding surfaces, since shales are deposited across a wide area in a near shore marine environment (Emery and Myers, 2009). All correlation in this project was done using Geographix ®, a geologic interpretation software package.

Cross-sections

After correlation was completed structural cross-sections were created perpendicular to fault and fold trends. All cross sections used in this research are scaled one to one with no vertical exaggeration. The cross sections were used to identify faults by identifying missing and repeated section. Repeated section was measured in each well and saved to create vertical separation, i.e. fault throw, maps.

Mapping

Structure Maps

Structure maps were created for all key horizons. Initially, structure maps identify correlation busts, obvious errors that create bulls eyes of high or low spots, that are fixed and, iteratively, a final structure map for that contact is attained. Structure maps

are important in identifying fault locations, fault trends, folding style, and unconformities. The structure maps in this project were created in the GeoAtlas ® module of Geographix ®. Typical structure contour maps in this study have 50 foot contours and were created using a minimum curvature algorithm that incorporated data from wells up to 4000 feet apart and resolved structures down to 400 feet wide.

Missing section, where identified, is shown on the appropriate structure contour maps as perimeters enclosed areas where the section is not found. Missing section is defined as section that is not present in well logs when flattening on the appropriate key marker bed, within each depositional sequence, i.e. lower Fruitvale, upper Fruitvale, Santa Margarita, and Etchegoin, San Joaquin, Tulare (undifferentiated).

Fault and Unconformity Maps

Fault maps were created by contouring x,y, and z coordinates of the fault picks identified in the well logs. The fault maps were used to estimate the strike and dip of the Wheeler Ridge fault and associated structures. The throw of the Wheeler Ridge fault was then mapped to show the area of the fault with the most ramping, therefore greatest throw, and to identify the limits of the fault.

A footwall cutoff map was created for the Wheeler Ridge Fault to identify the formation directly below the fault surface. Subcrop maps were created by identifying the last pick in a well before crossing an unconformity. Unconformities can be caused by incision related to sedimentary, climatic, or tectonically driven forces. Each type of unconformity will have its own specific pattern of erosion. The importance of subcrop maps in unconformities is they show the pattern of erosion and allow interpretations of the structure causing them.

Unconformity maps were generated by putting together the missing section in structure maps, showing the formations directly below and above the unconformities. The unconformity maps are important, because they show the pattern of erosion and future burial of structures.

Research

The main focus of this research was to understand the stratigraphic variation in the upper Miocene and the related structural history of the Wheeler Ridge anticline. This paper will focus mainly on the stratigraphy and structure of the upper Miocene to present.

Stratigraphy

Fruitvale

The late Miocene Fruitvale Formation has been divided into two depositional sequences in the Wheeler Ridge area in this study. The two depositional sequences are separated by an unconformity that is late Miocene in age (Figure 5). Stratigraphic cross sections flattened on the F3 marker show the stratigraphic variation within the Fruitvale (Figures 8 - 10). Figure 11 shows the net thickness isochore map of the lower Fruitvale. The isochore shows an increasing thickness of the Fruitvale to the north.

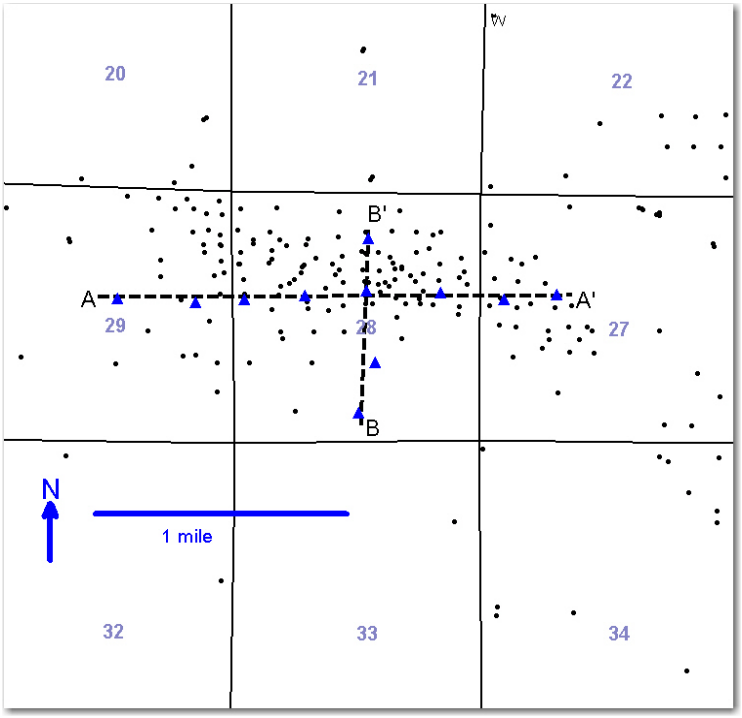

Figure 8. Location of E-W stratigraphic cross section of the Fruitvale (A-A'). Location of N-S stratigraphic cross section of the Fruitvale (B-B'). Triangles are wells included in cross sections (see Appendix I for a list of well names used in cross sections).

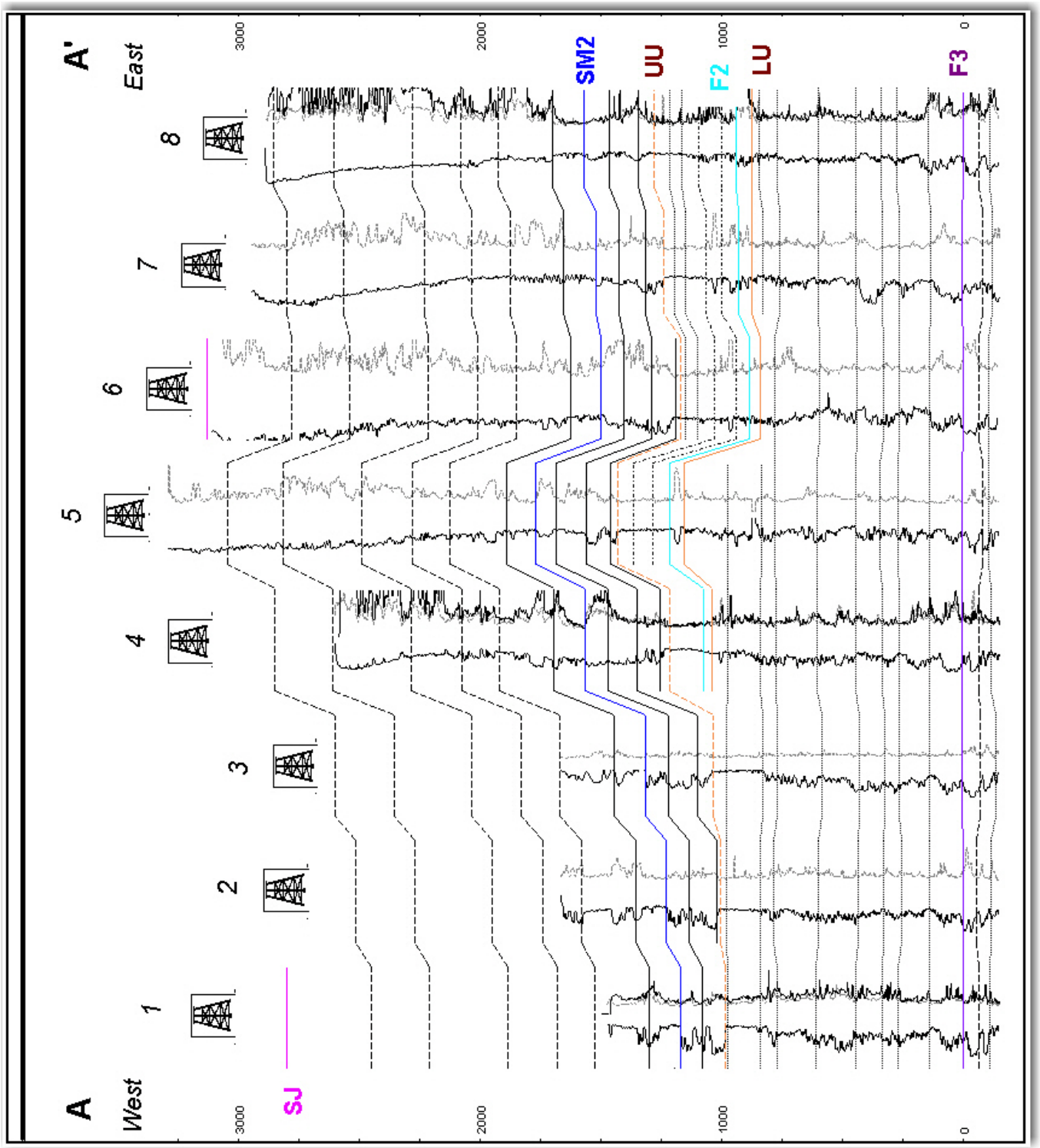

Figure 9. Stratigraphic cross section of the Fruitvale flattened on the F3 marker, east to west. Note absence of F2 marker in the three wells on the left. Oil derricks are at ground level. Depths are relative to F3 marker. LU = lower unconformity, UU = upper unconformity.

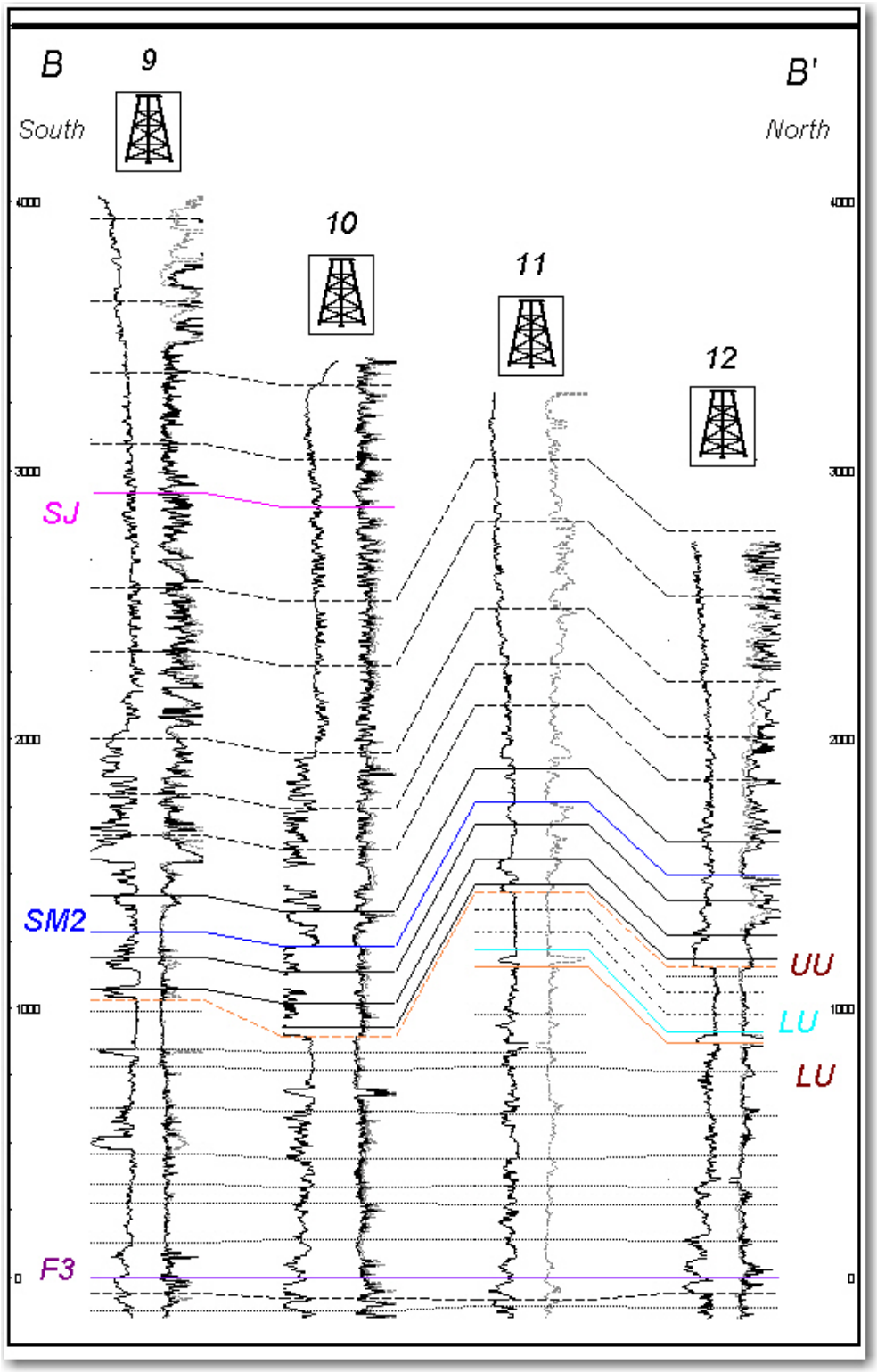

Figure 10. Stratigraphic cross section of the Fruitvale flattened on the F3 marker, north to south. Note absence of F2 marker in the two wells on the right. Oil derricks are at ground level. Depths are relative to F3 marker. LU = lower unconformity, UU = upper unconformity.

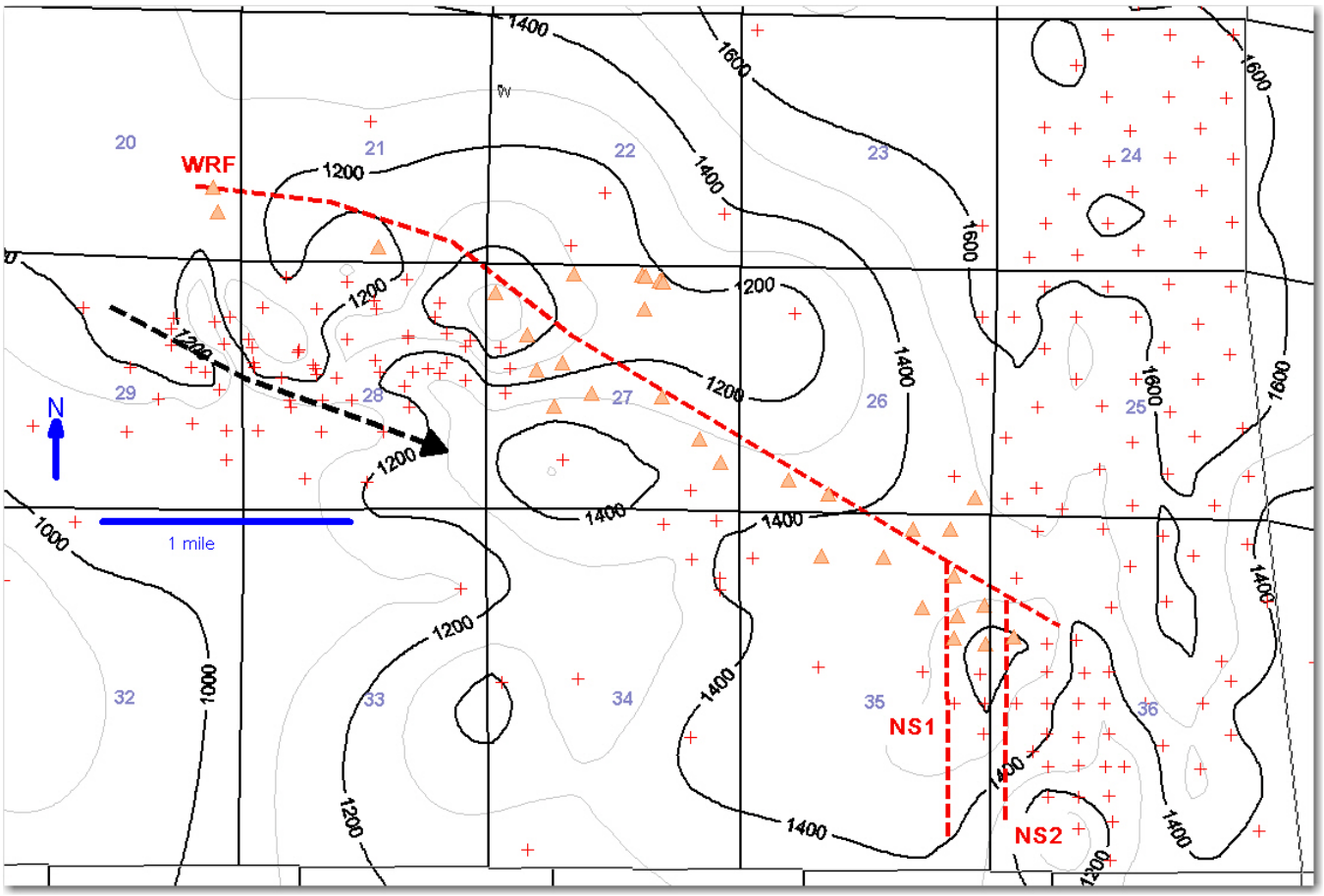

Figure 11. Isochore of the lower Fruitvale. Dashed red line shows fault intersections with F3 marker. Isochore shows decreasing thickness to the southwest due to cut out section related to the upper and lower unconformities. Triangles represent wells with increased thickness related to faulting and were not included in contouring. Dashed arrow represents approximate location of late Miocene anticline axis.

Lower Fruitvale

The lower Fruitvale depositional sequence is upper Miocene, lower Mohnian, in age (Childs, 1985; Dibblee, 1986; DOGGR, 1992; Hirst, 1986; Hirst, 1988). The depositional sequence is defined by the F3 marker, lower limit, to the lower unconformity, upper limit (Figure 5). The top of the lower Fruitvale from conventional core data showed thin highly fractured chert layers (see Appendix II). The Thorium/Uranium ratio in the upper portion of the lower Fruitvale is ~0.5 with Uranium

values ranging from 8-18 ppm and Potassium at ~1 percent (Wheeler Ridge F1). The lower Fruitvale is interpreted to be a deep marine depositional sequence.

An unconformity is apparent on the isochore maps between the upper and lower Fruitvale that removes part of the PF6-PF8 sections to the southwest (Figure 12). The structure contour map of the PF6 marker shows an east to west trending anticline that is cut by the Wheeler Ridge fault and missing section near the center of section 28 (Figure 12). The PF8 markers show similar structures with and increase area of missing section from PF6 to PF8 (Figures 12 and 13). The PF8 structure map indicates missing section to the north of the Wheeler Ridge fault and to the southwest of the Wheeler Ridge anticline. The missing section decreases with stratigraphic depth, i.e. from PF8 to PF7, and resembles a hole being eroded into the center of the Wheeler Ridge anticline. This is explored in more detail in the discussion section.

The lower Fruitvale is thicker at North Tejon and Wind Gap oil fields than it is at the Wheeler Ridge oil field (Figure 11). In addition to being thicker the lower Fruitvale appears to be sandier to the east, by evaluating the differences in the Spontaneous Potential and Resistivity log character.

Lower Unconformity

The lower unconformity cuts into the lower Fruitvale formation removes up to 500 feet of section (Figure 11). The lower unconformity is the depositional sequence boundary between the lower Fruitvale and upper Fruitvale. As such, the lower unconformity is a structural truncation in a sequence stratigraphy framework (Mitchum et al, 1977). Figure 14 shows a subcrop map of the lower unconformity and the formation

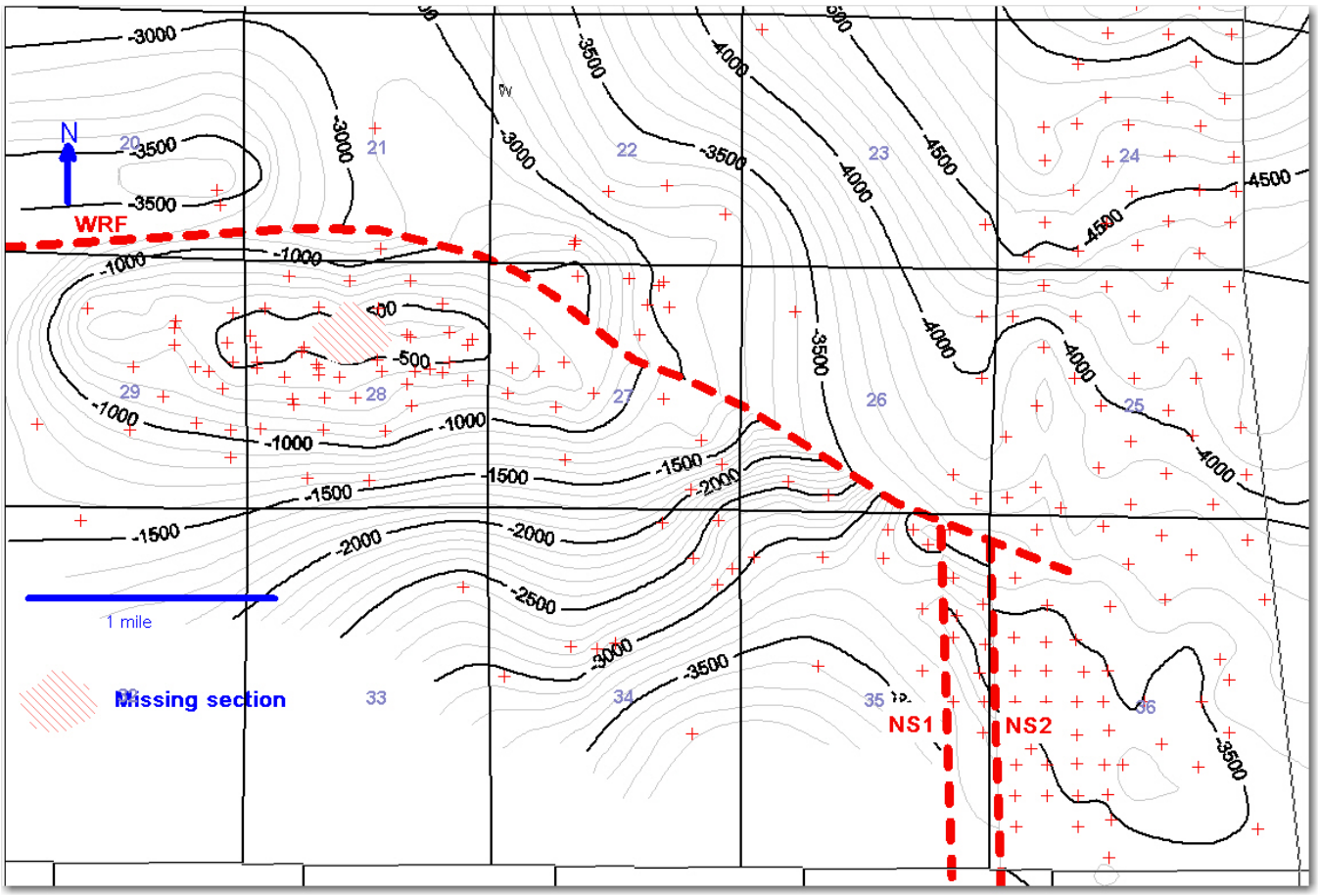

Figure 12. Structure contour map of the PF6 marker showing missing section due to lower unconformity. WRF = Wheeler Ridge Fault , NS1 = north-south trending fault with normal and strike slip separation.

directly below the unconformity. Here, the upper Fruitvale formation lies on top of the lower unconformity. The unconformity cuts the deepest near the crest of the structure, and the north flank appears to have been eroded more than the south flank. However, the erosion history on the southwest flank has been removed by the upper unconformity.

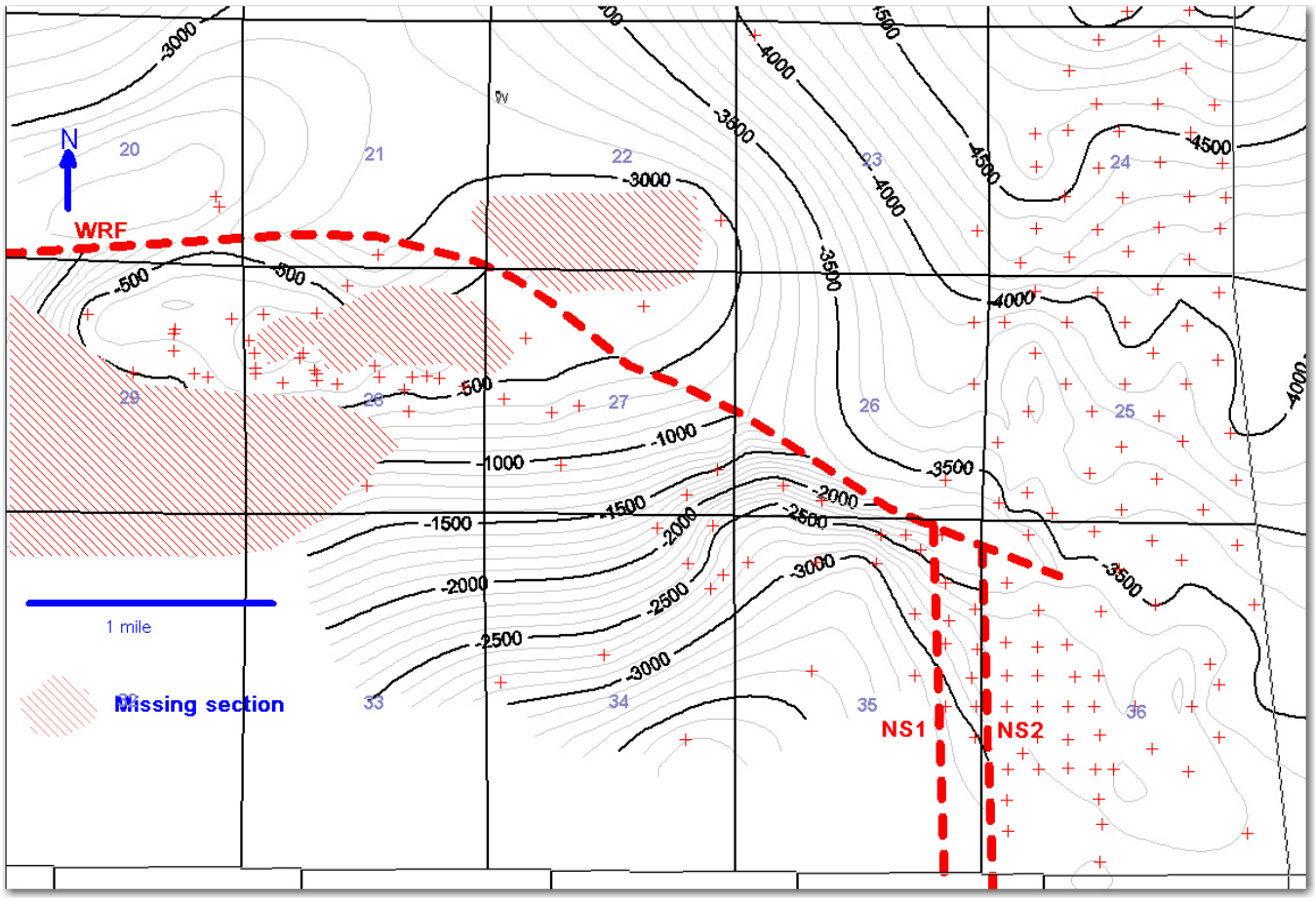

Figure 13. Structure contour map of the PF8 marker showing missing section due to lower unconformity. WRF = Wheeler Ridge Fault , WRF2 = Upper splay of Wheeler Ridge Fault. The upper unconformity cuts out the lower unconformity and the entire upper Fruitvale to the south west.

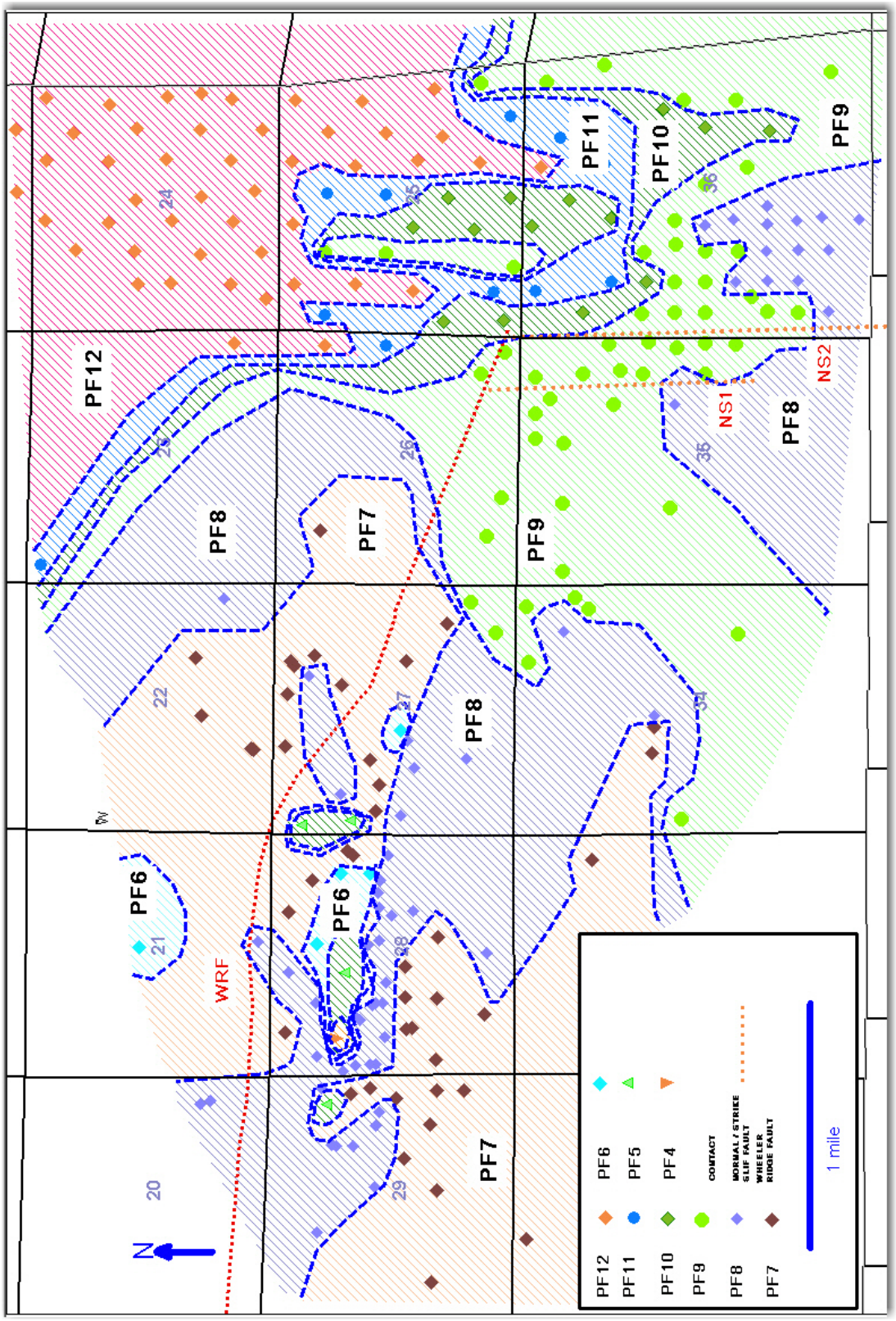

Figure 14. A subcrop map of the unit directly below the lower unconformity. Note the upper unconformity cuts out the lower unconformity along a northwest to southeast trend. Dashed red line shows fault intersections with F3 marker.

Upper Fruitvale

The upper Fruitvale Formation is defined by markers F2-UF5 in the Wheeler Ridge oil field. The upper Fruitvale unconformably overlies the lower Fruitvale. The upper unconformity is the depositional sequence boundary between the upper Fruitvale and Santa Margarita. As with the lower unconformity, the upper unconformity is a structural truncation in a sequence stratigraphy framework (Mitchum et al, 1977).

The upper Fruitvale is interpreted to be shallow to deep marine and is interpreted to be part of a low stand systems tract from the depositional units present. The upper Fruitvale is predominately shaly with intermittent carbonate rich thin sands. The shales are dark black and highly bioturbated above and below the F2 sand (Appendix II). One large fracture was observed in the upper portion of the upper Fruitvale that was three feet in length and one inch wide with no offset of bioturbated shales. The F2 sand at Wheeler Ridge, locally called the Main sand, is here interpreted as a thin bedded turbidite sequence (unpublished core descriptions by the author). The F2 sand in well Wheeler Ridge F1 shows repeating Bouma sequences (Appendix II) (Bouma, 1962). The Ta sand is medium to coarse grained. The Tb and Tc sands are very fine to fine grained. The Td and Te are silt sized grains. The Bouma sequences present suggest an edge of a distal turbidite fan was penetrated by the Wheeler Ridge F1 well. The F2 sand has a horizontal permeability range of 2300-2900 mD and porosity of 27-31 percent, from sidewall data, making it a very high quality reservoir rock. The F2 is a productive horizon throughout the Wheeler Ridge oil field, where present, and to the northeast of the Wheeler Ridge oil field with cumulative oil production in some wells over 200 thousand barrels of oil recovered to date (DOGGR, 2011).

Figure 15 shows an isochore of the upper Fruitvale and its increasing thickness to the north. The upper Fruitvale is also thicker at North Tejon and Wind Gap oil fields than at the Wheeler Ridge oil field. As with the lower unconformity, this may mean more erosion associated with the upper unconformity than estimated at the Wheeler Ridge oil field. The approximate erosion related to the upper unconformity is 1000 feet, from the isochore map (Figure 15). The upper Fruitvale is sandier to the east, from the spontaneous potential and resistivity log character. Figures 16-18 show cross sections illustrating the unconformity between the upper and lower Fruitvale zone. The upper Fruitvale is being cut to the south by another unconformity, which is shown in the Santa Margarita section.

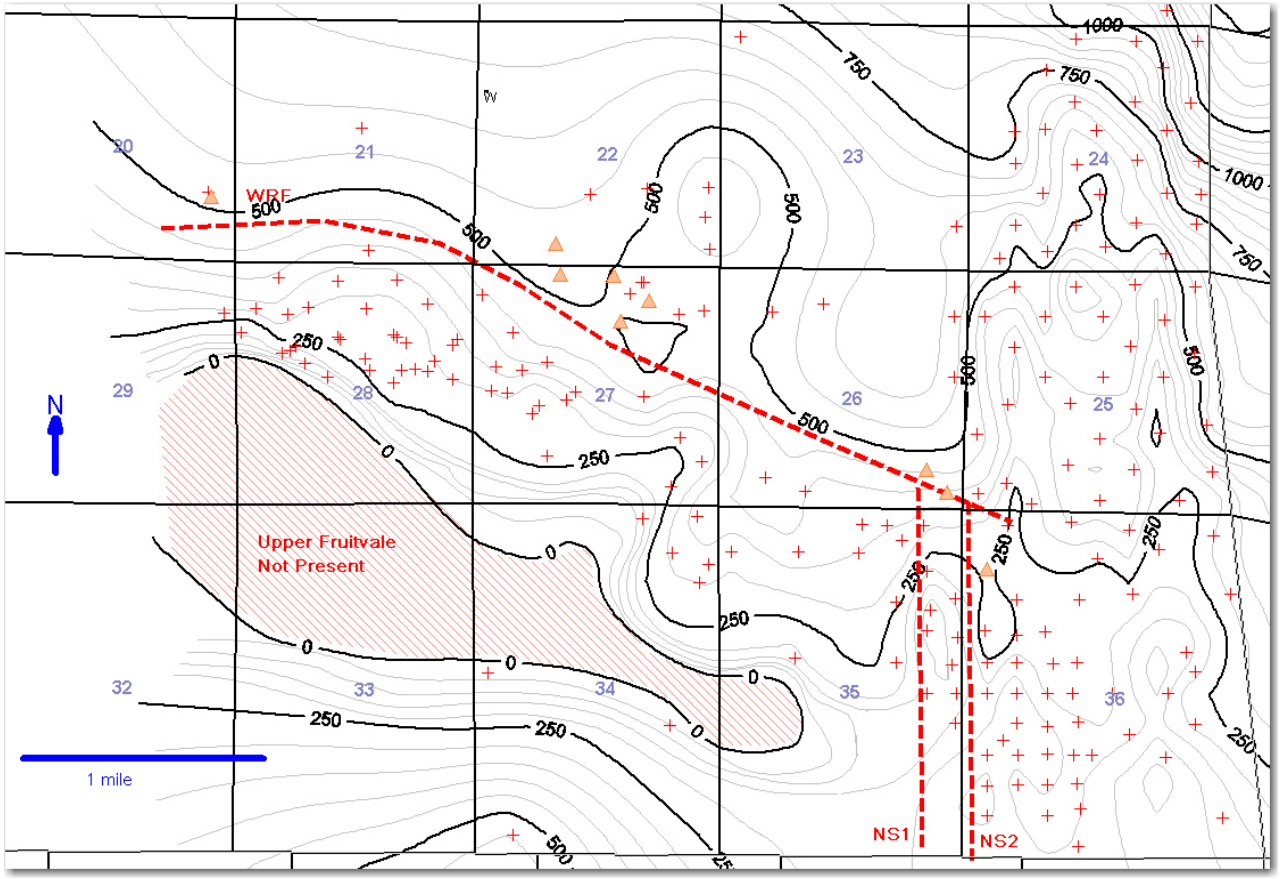

Figure 15. Isochore of the upper Fruitvale, including repeated section related to faulting. Note the increasing thickness to the north. Dashed red line shows fault intersections with F2 marker. WRF = Wheeler Ridge fault, NS1 = Normal fault 1, NS2 = Normal fault 2.

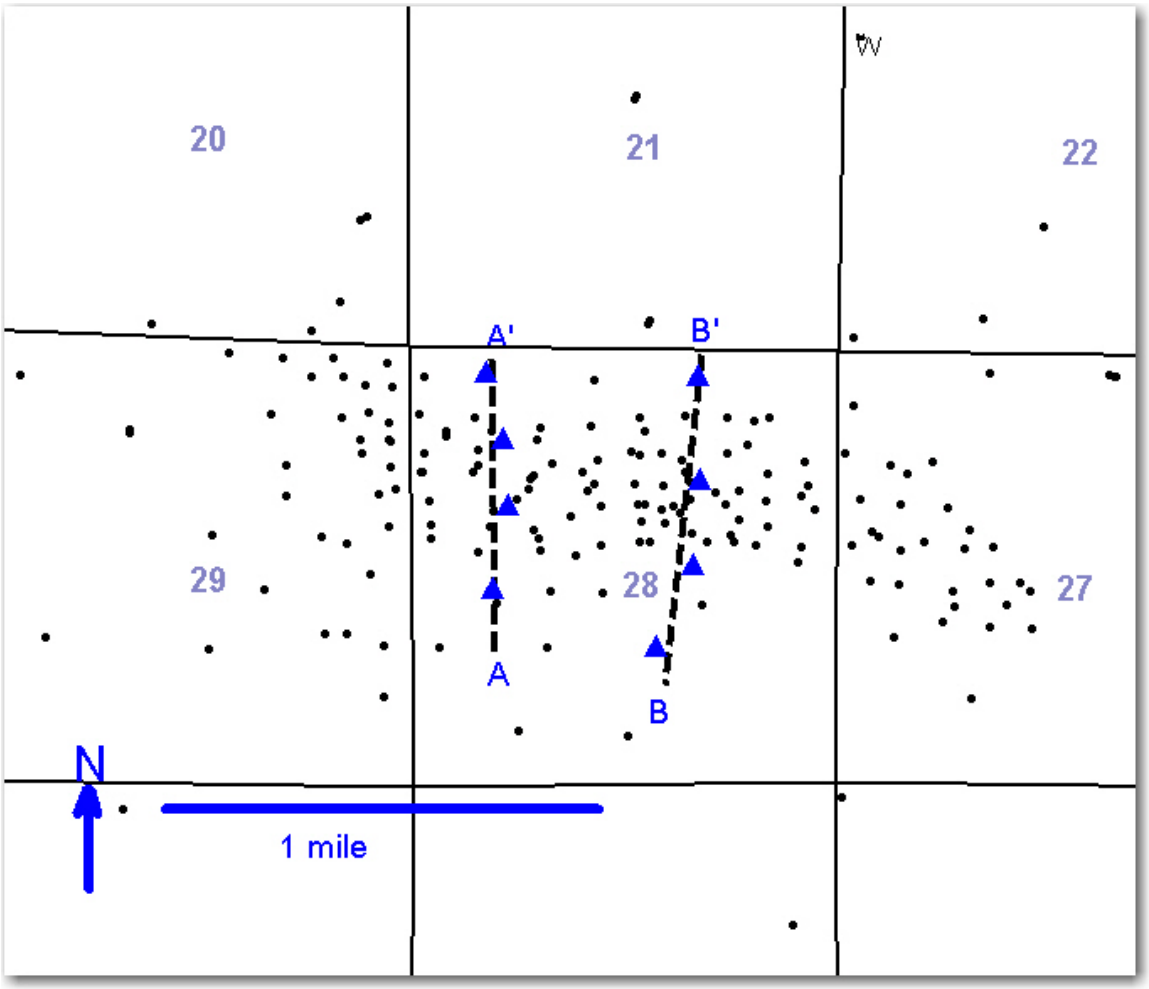

Figure 16. Location of N-S cross sections focused on the upper Fruitvale. Blue triangles signify the location of wells shown in cross sections.

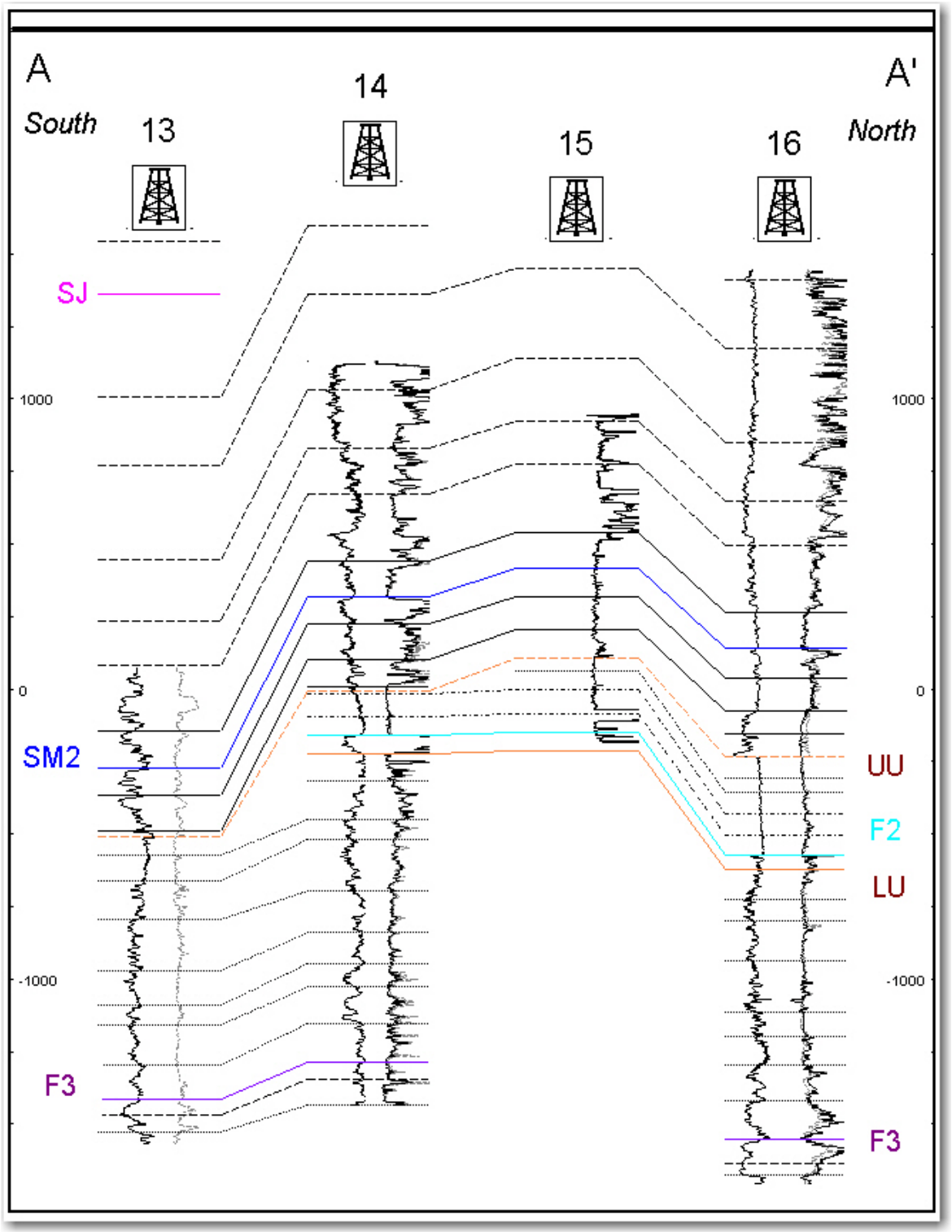

Figure 17. Cross section of the upper Fruitvale formation, south to north. Note the decreased thickness of the upper Fruitvale formation to the south. (Wells are not proportionally spaced).

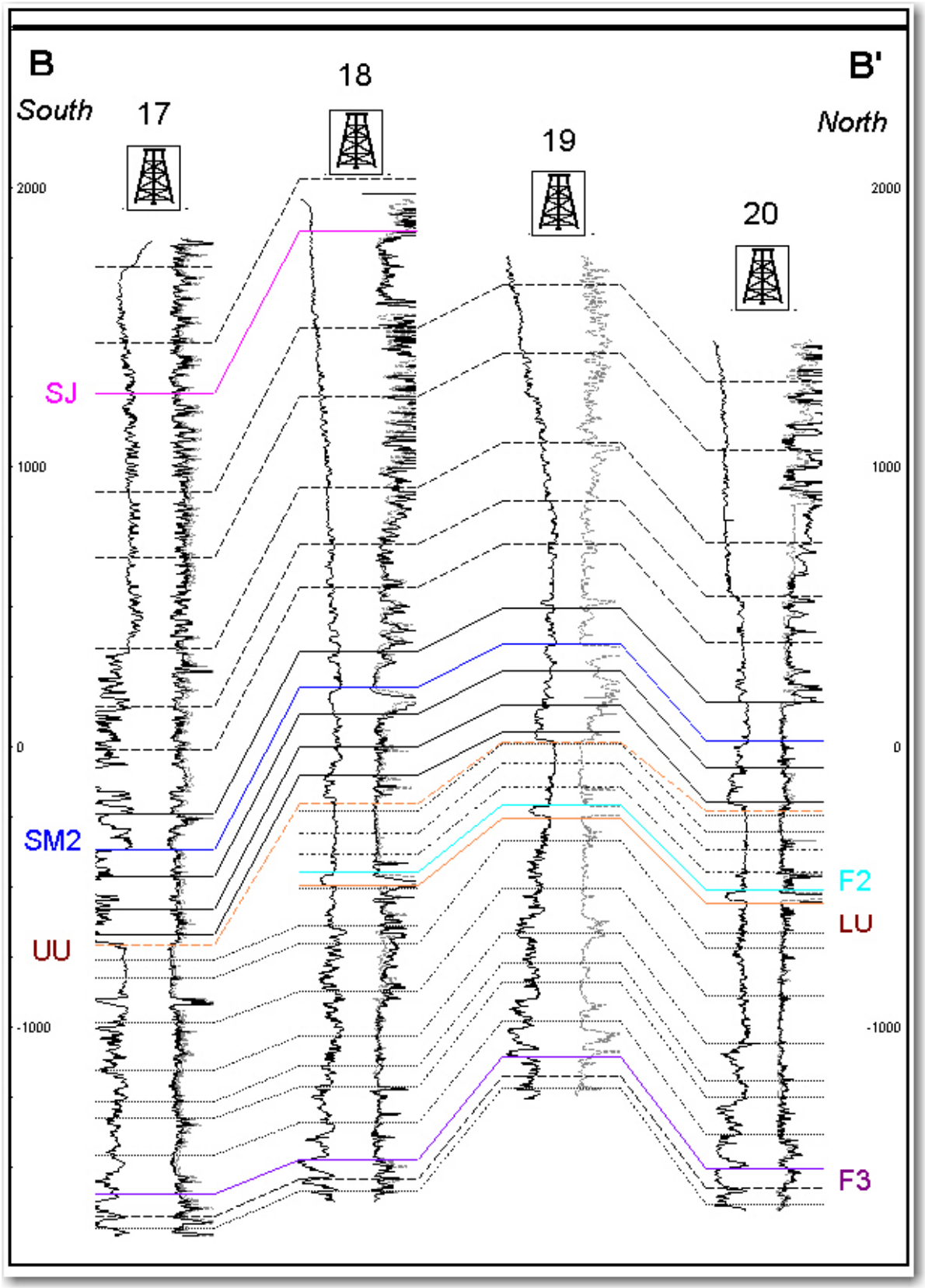

Figure 18. Cross section of the upper Fruitvale formation, south to north. Note the decreased thickness of the upper Fruitvale formation to the south. (Wells are not proportionally spaced).

Structure contour maps of the F2 and UF3 markers show the upper Fruitvale formation cut out by the upper unconformity along a northwest to southeast trend (Figures 19 and 20).

Upper Unconformity

The upper unconformity cuts into the upper Fruitvale formation, removing up to 1000 feet of section (Figures 15). A subcrop map of the upper unconformity shows that the entire upper Fruitvale formation in the southwestern portion of the Wheeler Ridge is missing (Figure 21). The upper unconformity also cuts out the lower unconformity and erodes into the lower Fruitvale formation (shown in cross sections in a later section). The Santa Margarita Formation unconformably overlies the upper Fruitvale.

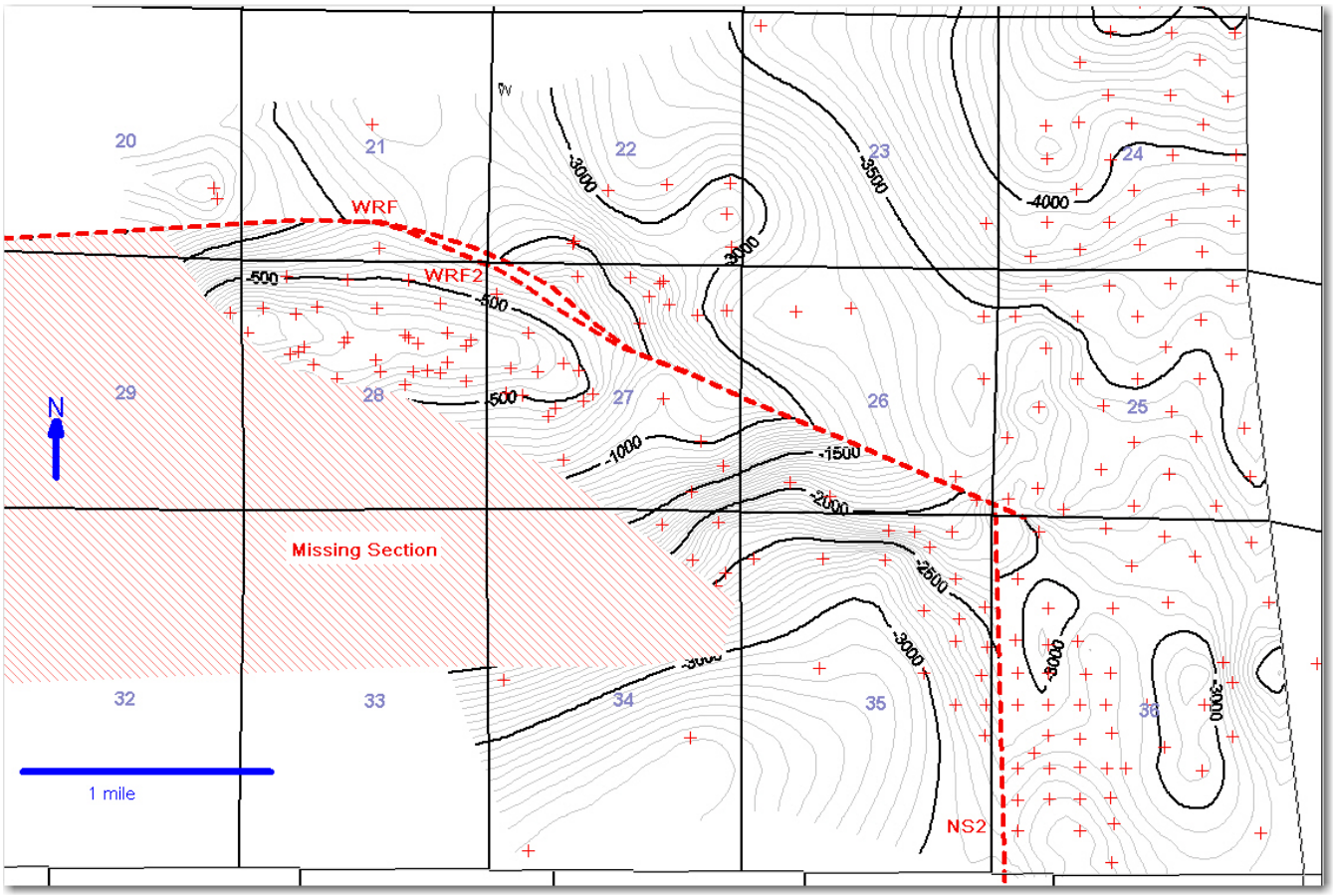

Figure 19. Structure contour map of the F2 marker showing missing section related to upper unconformity. WRF = Wheeler Ridge Fault , WRF2 = Upper splay of Wheeler Ridge Fault.

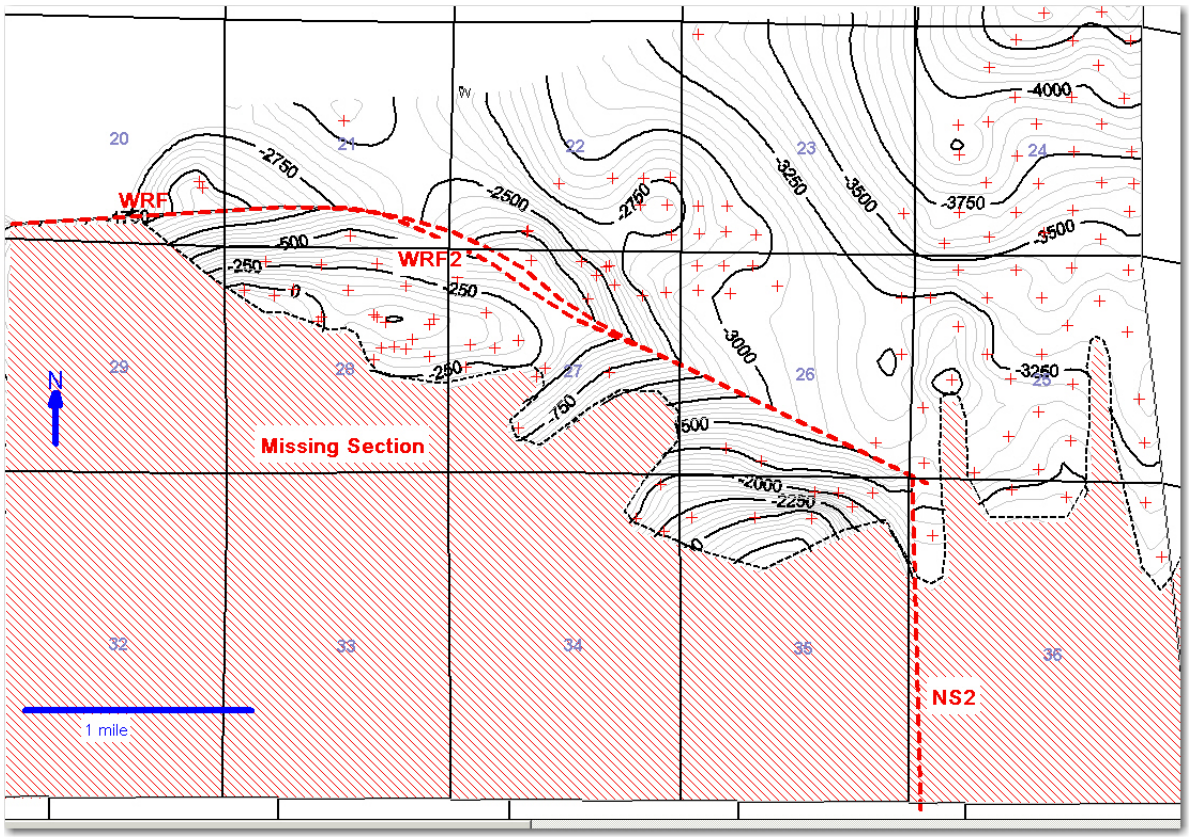

Figure 20. Structure contour map of the UF3 marker showing missing section related to upper unconformity. WRF = Wheeler Ridge Fault , WRF2 = Upper splay of Wheeler Ridge Fault.

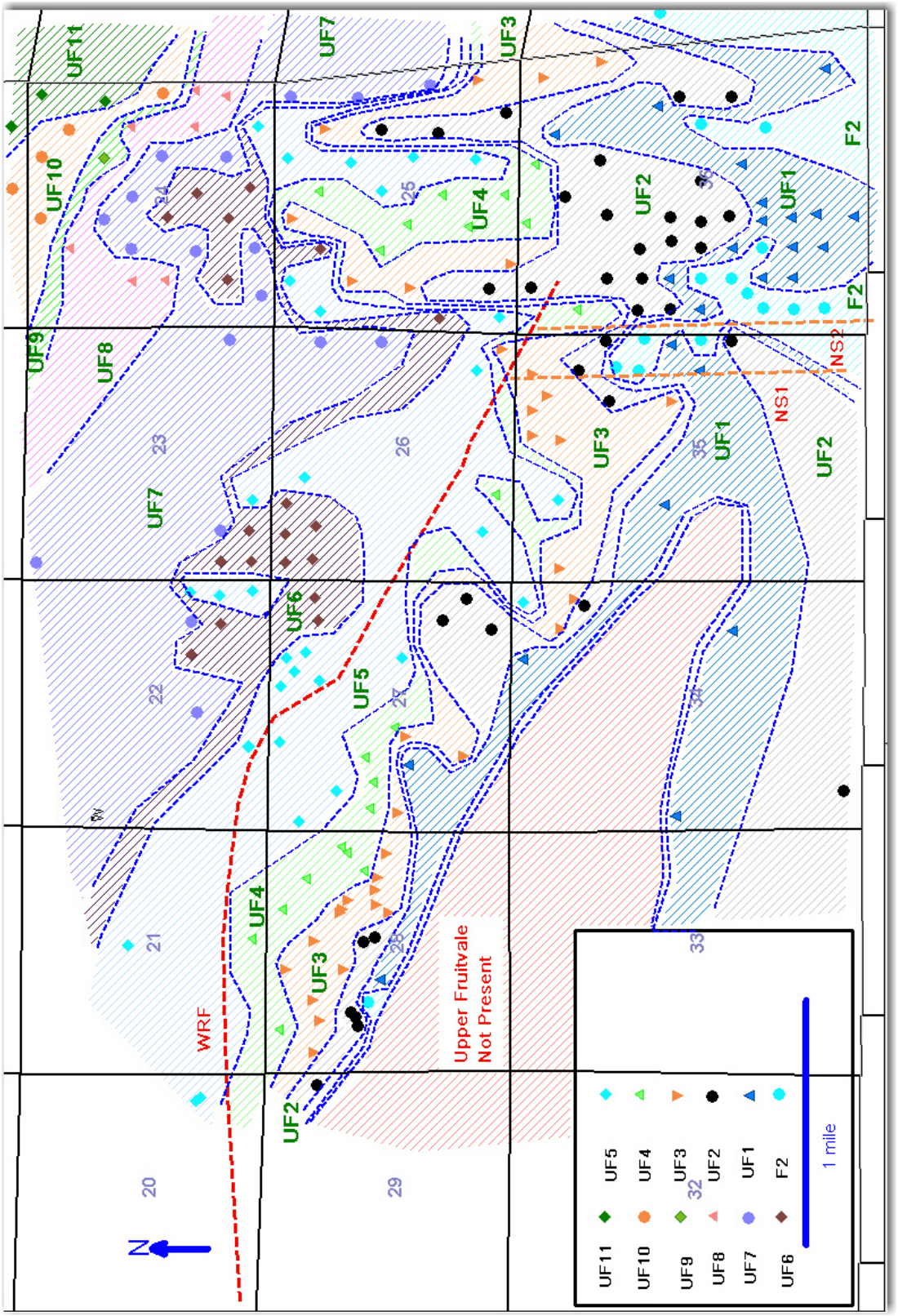

Figure 21. A subcrop map of the upper unconformity. Note the regular manner in which the upper Fruitvale, and into the lower Fruitvale, is eroded out from the northeast to the southwest. Dashed red line shows fault intersections with F2 marker.

Santa Margarita

The Santa Margarita Formation, upper Mohnian in age, unconformably overlies the Fruitvale Formation. The Santa Margarita is typically divided into the SM1 and SM2 sands (DOGGR, 1992). There is a hard, in a mechanical strength sense, continuous shale between the SM1 and the SM2 that can be correlated throughout the field area and is interpreted as a maximum flooding surface herein. The SM2 top is a conformable depositional sequence boundary or concordant upper boundary (Mitchum et al, 1977). The SM1 is a non oil bearing formation in the Wheeler Ridge area (DOGGR, 1992). The SM2 is an actively producing formation. The SM2 has, herein, been divided into four distinct zones. The SM2 H, SM2 Z, SM2 M, and SM2 L subdivision represents a break up of the SM2 zone into its individual parasequences, or reservoir flow units from a production stand point. Each of the individual parasequences show an overall coarsening upward profile on the spontaneous potential and resistivity logs. The gamma ray logs show a rapid coarsening upward into a blocky shape.

Core taken across the SM2 H shows a typical sequence of thin interbedded sands and silts, followed by medium to coarse grained sand with pebbles with either normal or reverse grading, followed by medium to coarse grained sand and no apparent bedding (Appendix II). Occasional crossbeds, roots, shell rich layers (coquina), and a large concretions were found in the core. The SM2 H has a permeability range of 1900 mD to 3300 mD and porosity of 28 to 31 percent from sidewall data. The SM2 H appears to be a deltaic environment from the log response, core data, marine shells, and roots present. From the blocky character of the Gamma Ray and the well sorting of sand grains the deltaic environment may have been wave dominated. A partial core of the SM2 Z shows

similar structures. The top of the SM2 H changes into interbedded sands and silts with 1mm-15mm bed thickness with planar bedding and cementing of the sands.

In general, the sandy intervals from the core were unconsolidated. The only exception was the concretions that ranged in size from 4 to 20 cm. All of the concretions were circular in shape and rigorously fizzed with acid. The shales tended to be very hard and brittle. During coring the shale at the top of the SM2 H jammed the core barrel while the sands cored easily. Within the core itself, all fractures and small faults were observed within the shales and inter bedded thin cemented sands and silts.

Stratigraphic cross sections of the Santa Margarita flattened on the SM2 marker top are shown below (Figures 22-25). An isochore of the Santa Margarita shows a general thinning to the southwest (Figure 26) . Structure contour maps of the Santa Margarita sands show an approximately east to west fold trend (Figures 27-30).

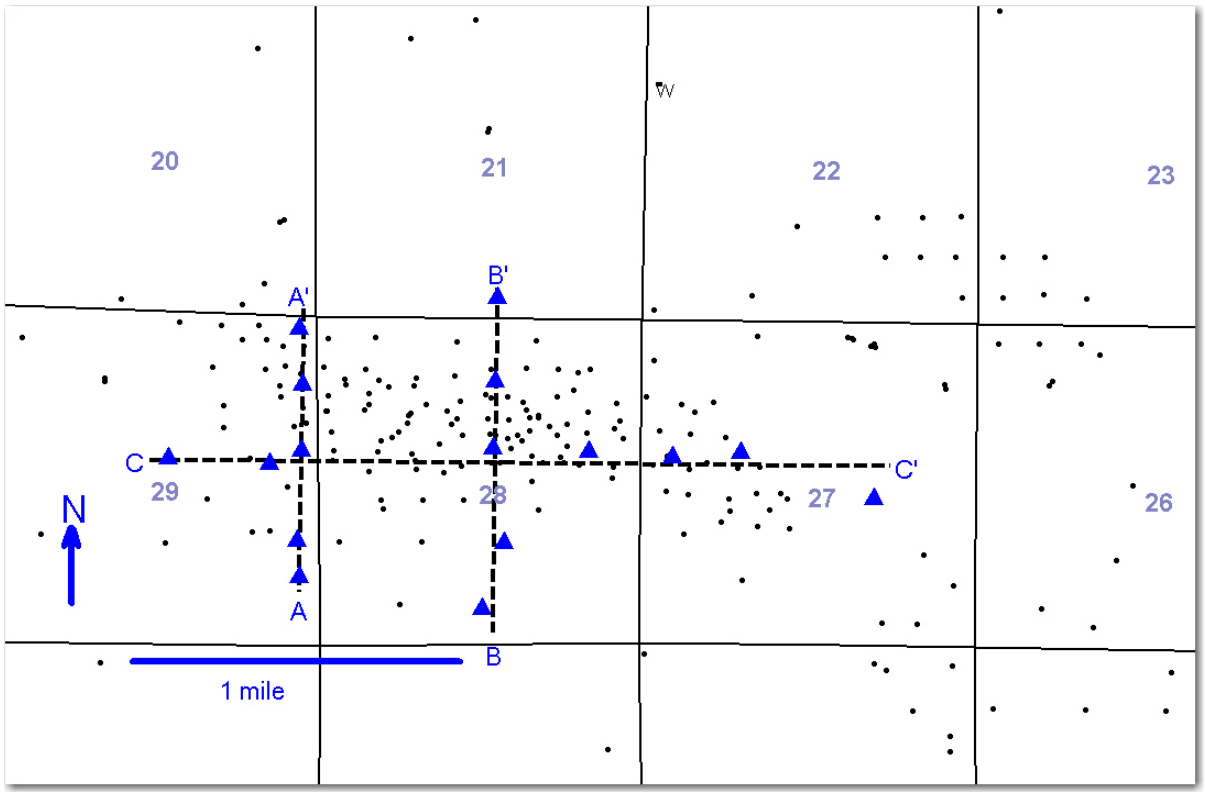

Figure 22. Cross section locations of the Santa Margarita.

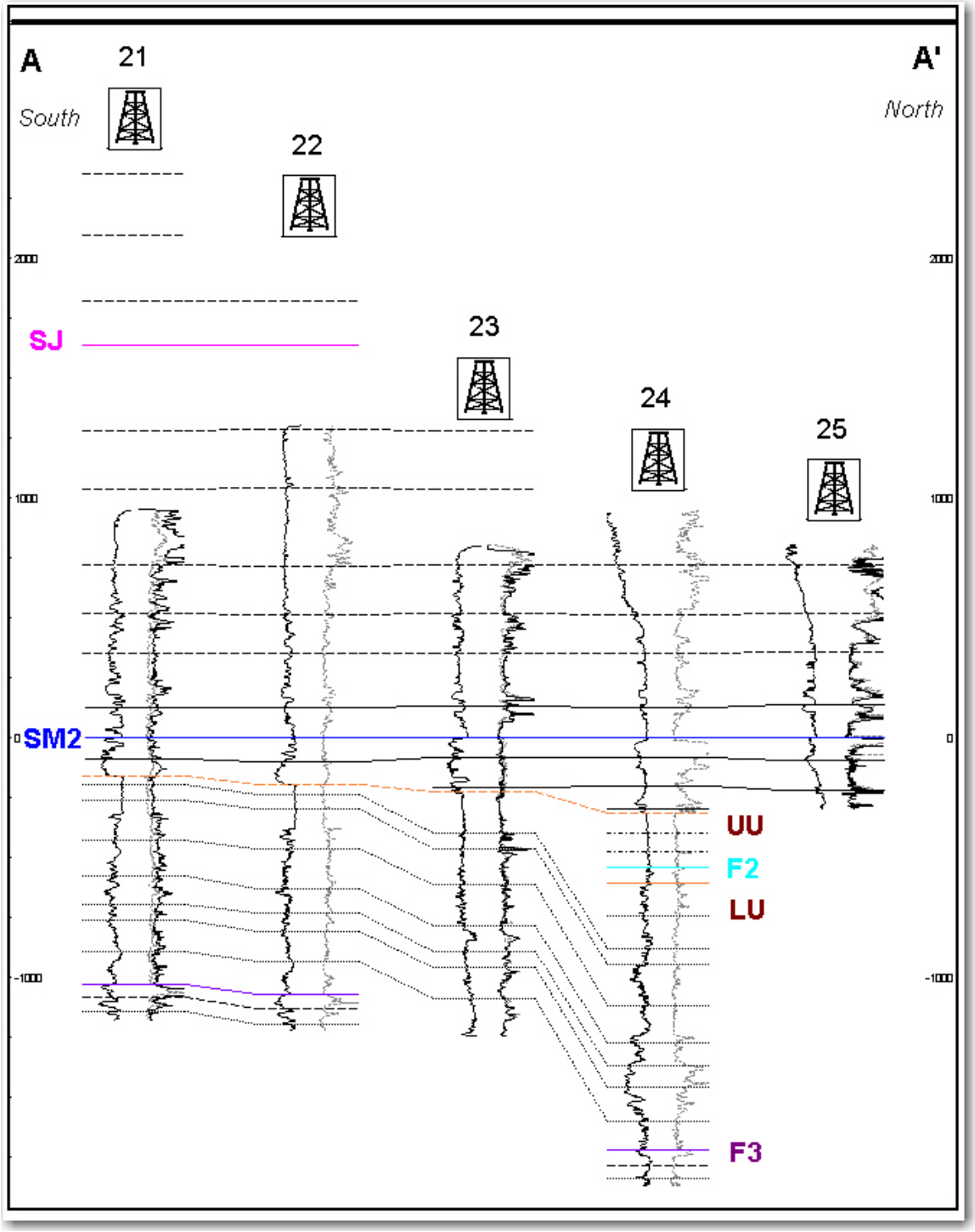

Figure 23. Stratigraphic cross section of the Santa Margarita formation, south to north, flattened on the SM2. The increased resistivity to the north is due to the presence of hydrocarbons.

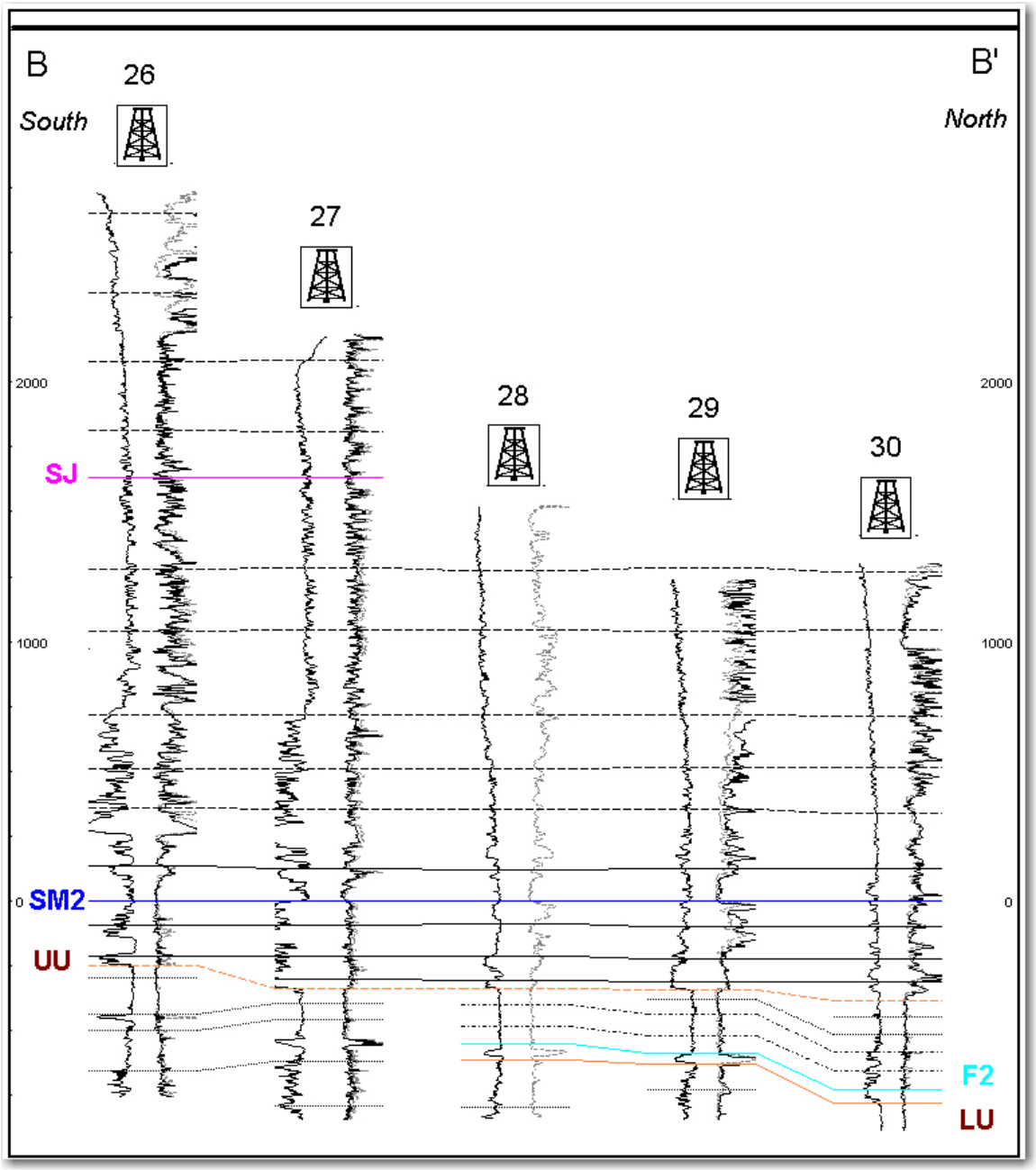

Figure 24. Stratigraphic cross section of the Santa Margarita formation, south to north, flattened on the SM2. The increased resistivity to the north is due to the presence of hydrocarbons.

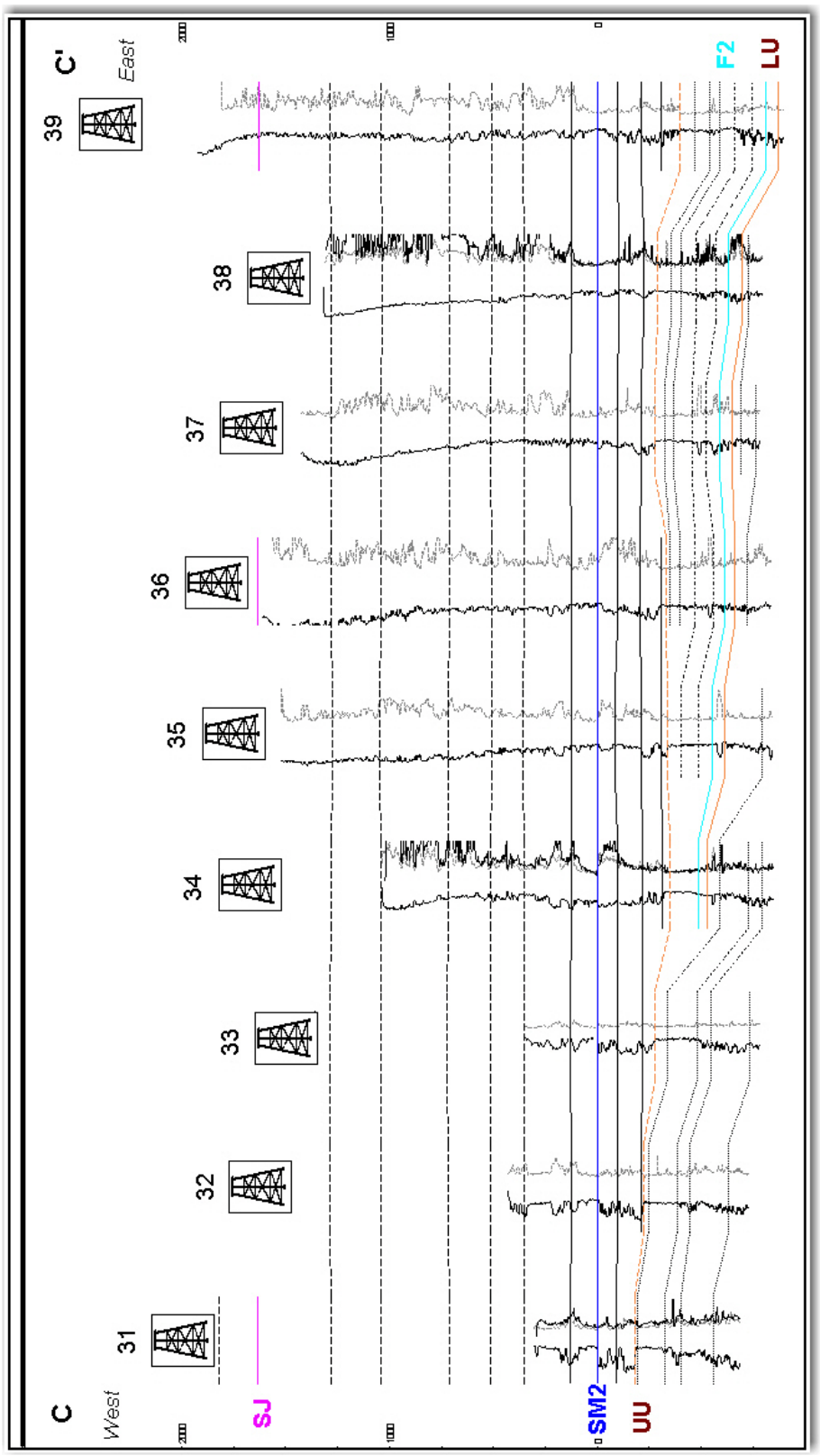

Figure 25. Stratigraphic cross section of the Santa Margarita formation, east to west, flattened on the SM2 marker. Note the increase of thickness of the SM2 and the change of upper Fruitvale formation below the base of the SM2 to the east.

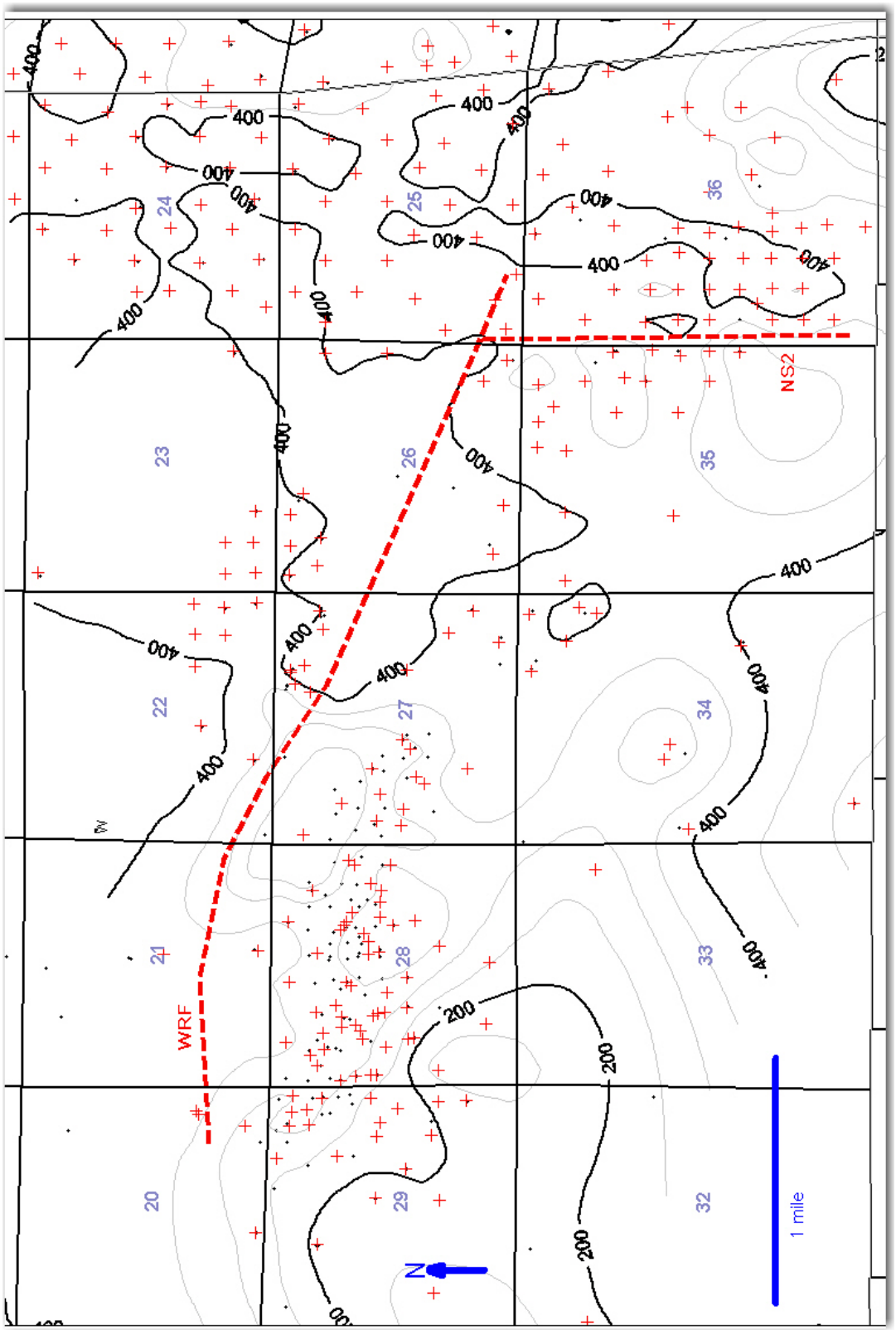

Figure 26. Isochore of the Santa Margarita Formation (SM2), excluding repeated section due to faulting. Note the increasing thickness to the north. Dashed red line shows fault intersections with SM2 H marker.

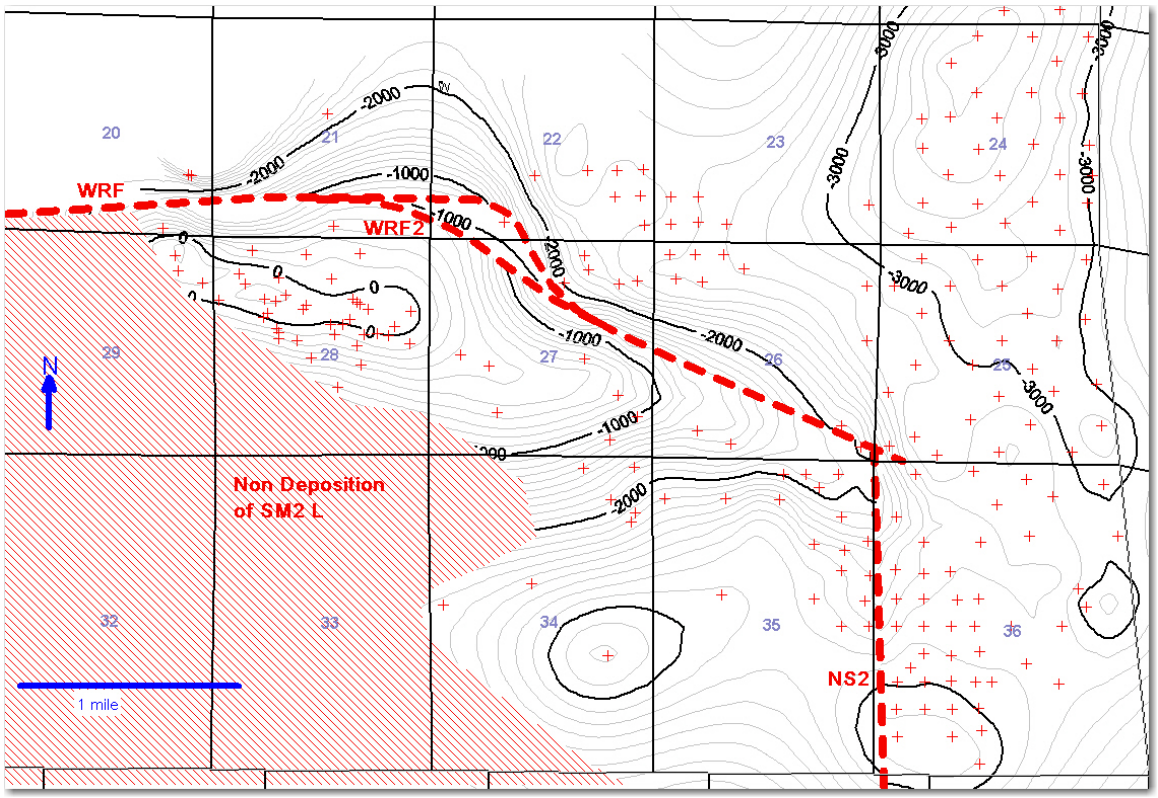

Figure 27. Structure contour map of the SM2 L marker. Note the northwest to southeast trend of the missing section to the southwest of the field.

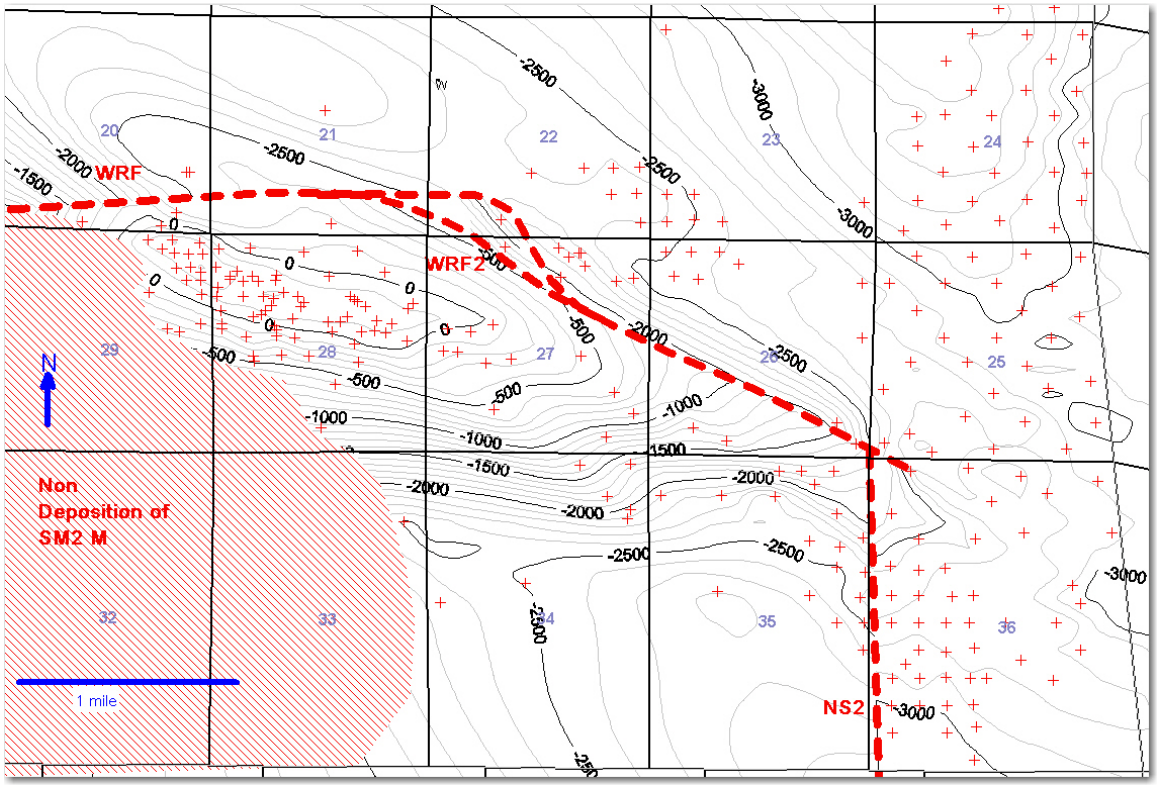

Figure 28. Structure contour map of the SM2 M marker. Note the northwest to southeast trend of the missing section to the southwest of the field.

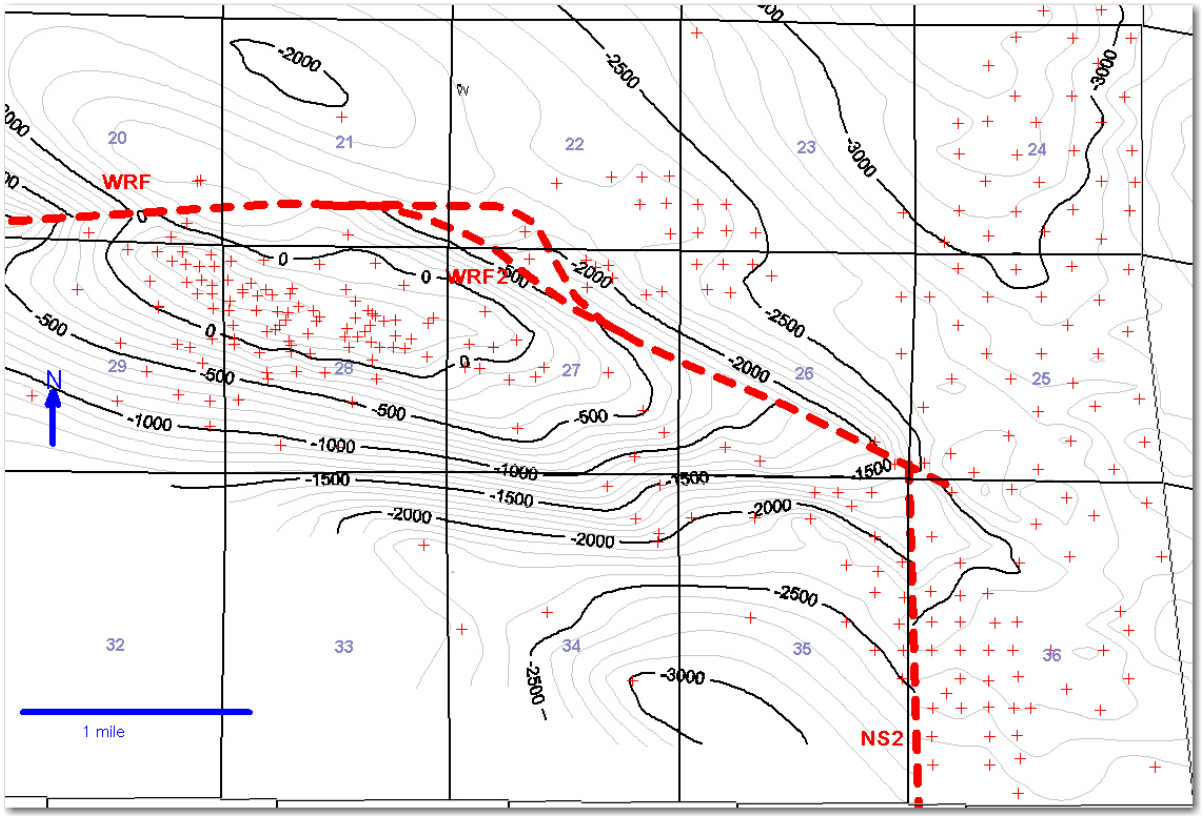

Figure 29. Structure contour map of the SM2 Z marker. This is the first SM2 sand to completely overtop the Miocene Wheeler Ridge anticline.

A map of the Santa Margarita sands was generated directly above the upper unconformity (Figure 30). The onlap of the Santa Margarita sands is strong evidence of an early history to the Wheeler Ridge anticline that has not previously been identified (see discussion section). The SM2 L appears to have been deposited next to a paleo-Wheeler Ridge anticline related to the lower and upper unconformities in the Fruitvale formation. The SM2 M onlaps further onto the structure and the SM2 Z is the first sand to completely overtop the paleo-Wheeler Ridge anticline. A study of the paleo-flow direction and source of the Santa Margarita sands was not undertaken as part of this study, but general trends in net to gross sand from evaluating logs during correlation would suggest the sediment source is from the east, possibly even southeast. The onlap is more apparent in the model in the Discussion portion of this paper.

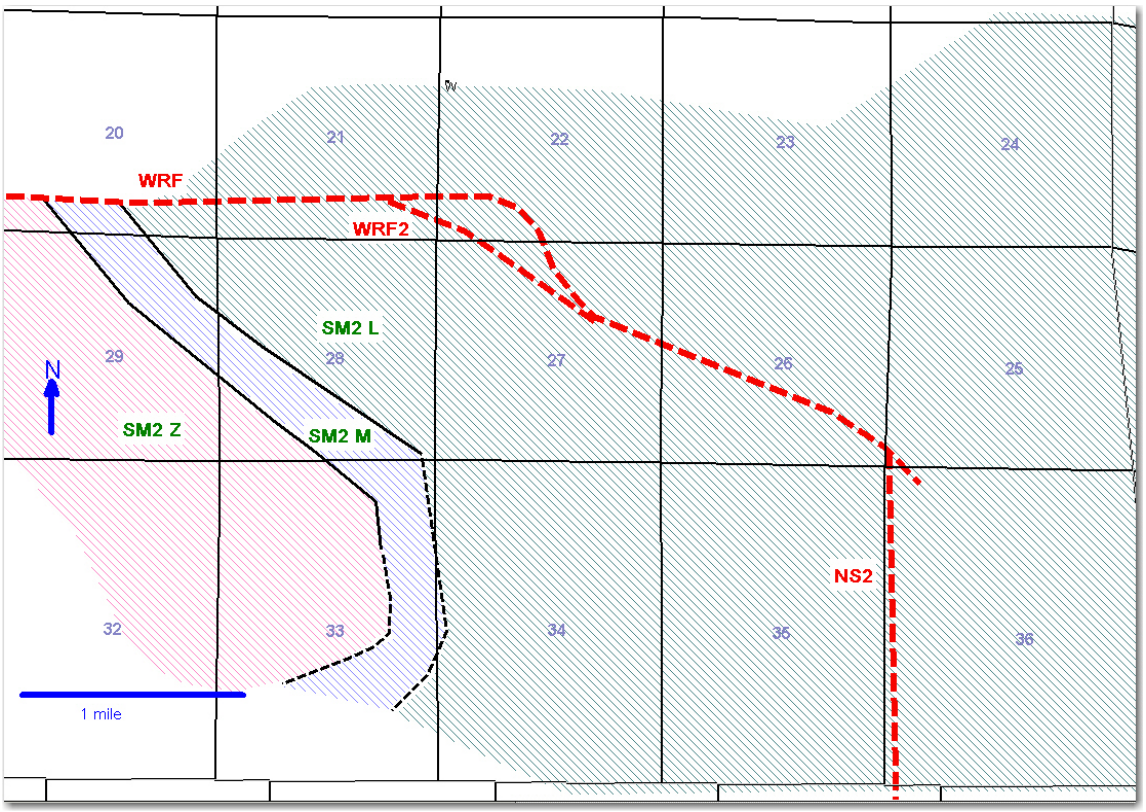

Figure 30. Santa Margarita sands deposited on top of the upper unconformity. Dashed red line shows fault intersections with SM2 H marker.

Undifferentiated Tulare, San Joaquin, and Etchegoin

The Tulare, San Joaquin, and Etchegoin (undifferentiated) conformably overly the Santa Margarita Formation. Although they are undifferentiated, time markers within the Tulare, San Joaquin, and Etchegoin (undifferentiated) have been identified and carried throughout the field area (Figures 31-33). Note that correlation within the Tulare, San Joaquin, and Etchegoin (undifferentiated) is undertaken with caution due to its nonmarine origins.

The Etchegoin, San Joaquin, and Tulare (undifferentiated) are thicker at the North Tejon and Wind Gap oil fields (Figure 34). Key structural contour maps of time markers within the Tulare, San Joaquin, and Etchegoin (undifferentiated) are shown below (Figures 35 and 36). An outcrop of the modern surface, from well logs, is shown in

Figure 37. The modern outcrop pattern bears a strong resemblance to the subcrop maps corresponding to the upper Miocene upper and lower unconformities.

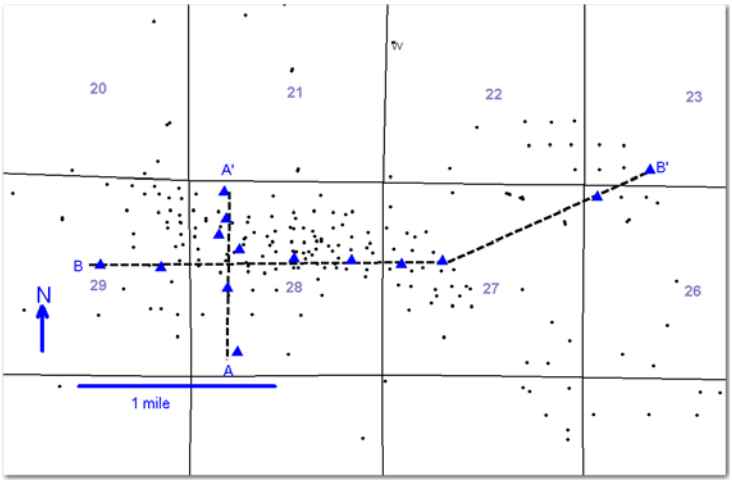

Figure 31. Location of N-S cross section of the Tulare, San Joaquin, and Etchegoin (undifferentiated).

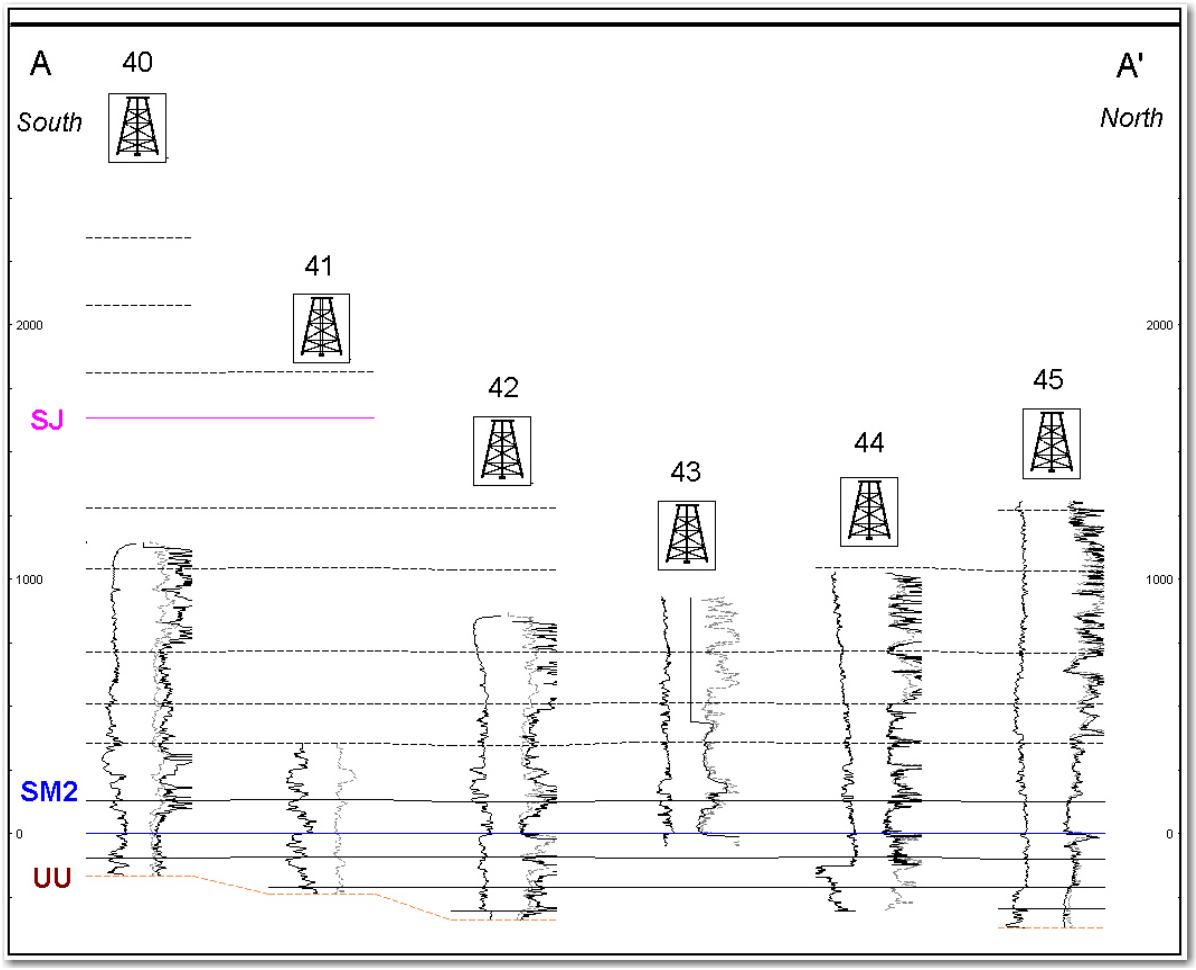

Figure 32. Stratigraphic cross sections of the Tulare, San Joaquin, and Etchegoin (undifferentiated) flattened on SM1.

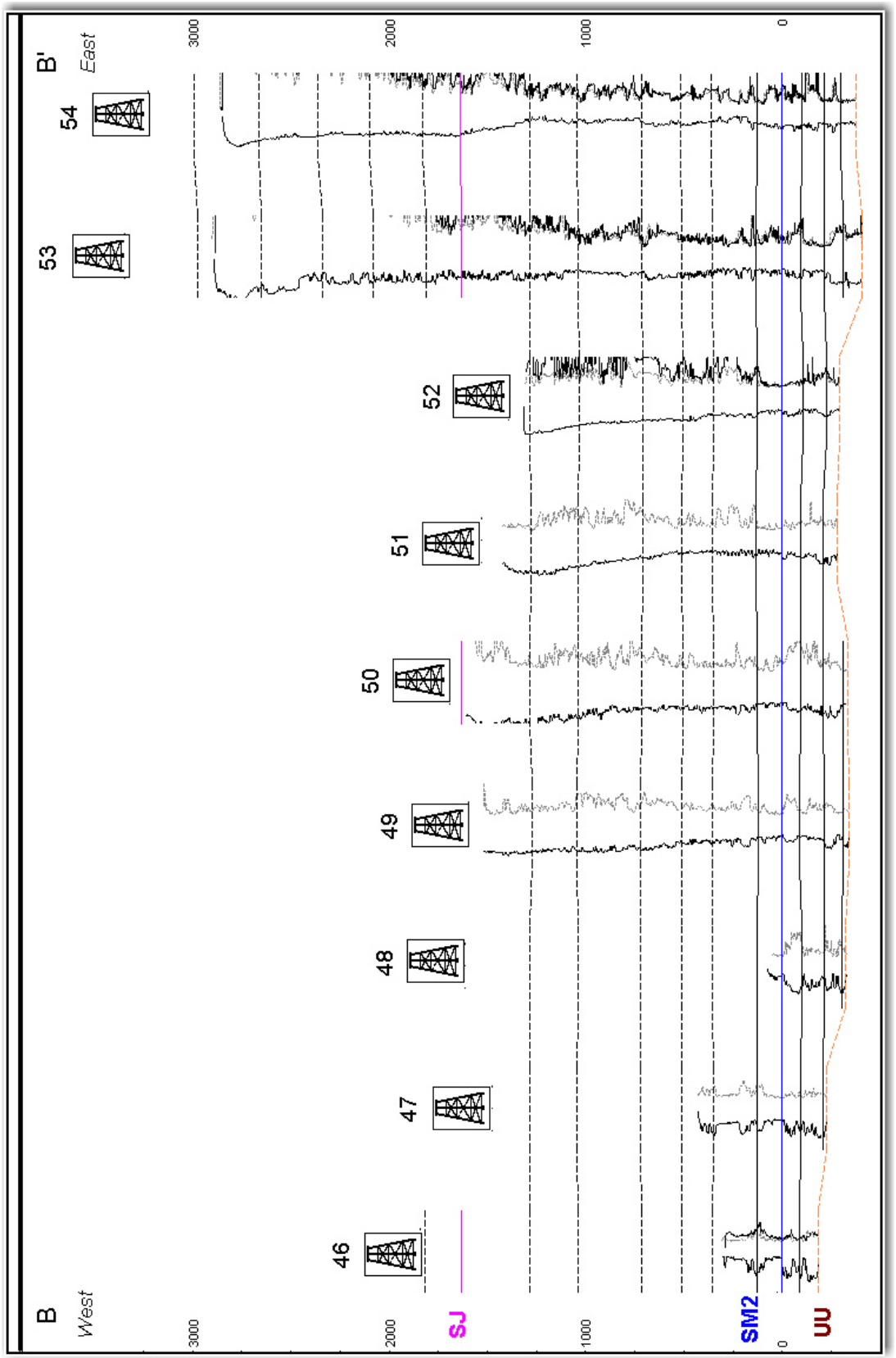

Figure 33. Stratigraphic cross sections of the Tulare, San Joaquin, and Etchegoin (undifferentiated) flattened on SM1.

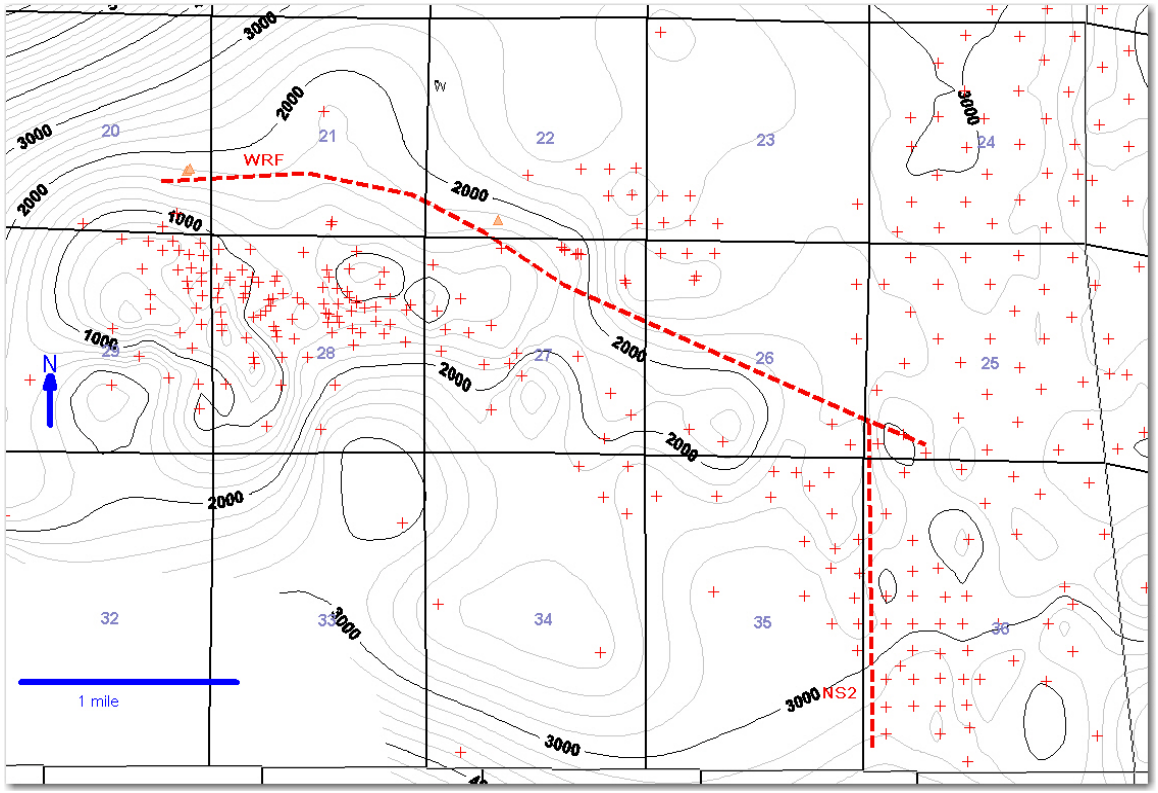

Figure 34. Isochore of Tulare, San Joaquin, and Etchegoin (undifferentiated). Dashed red line shows fault intersections with San_Joaquin marker.

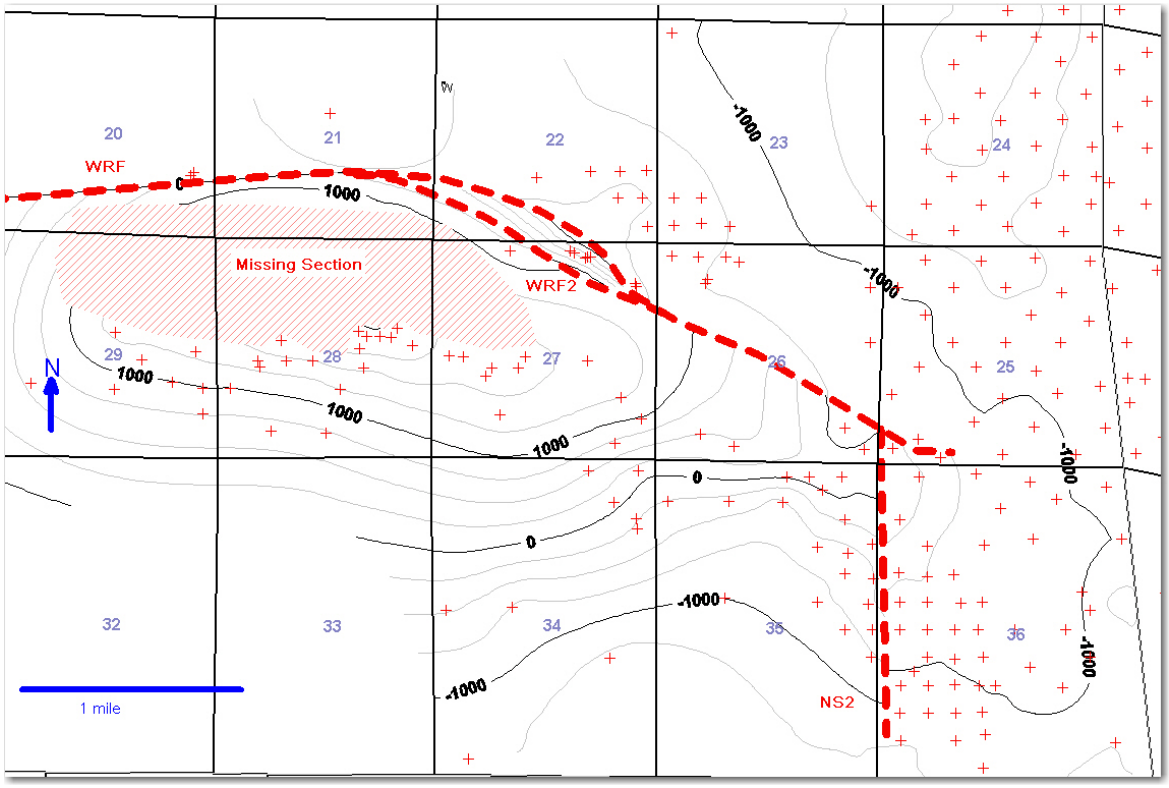

Figure 35. Structure contour map of the San Joaquin marker with missing section.

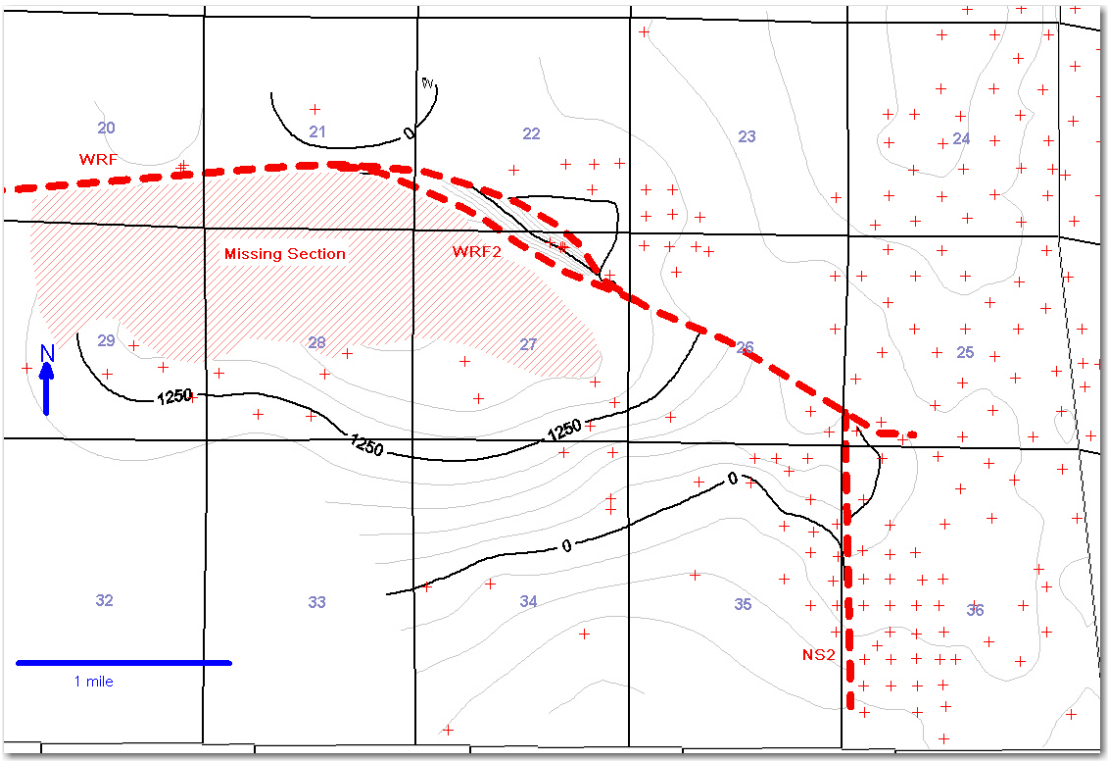

Figure 36. Structure contour map of the SJ_UP_2 marker with missing section.

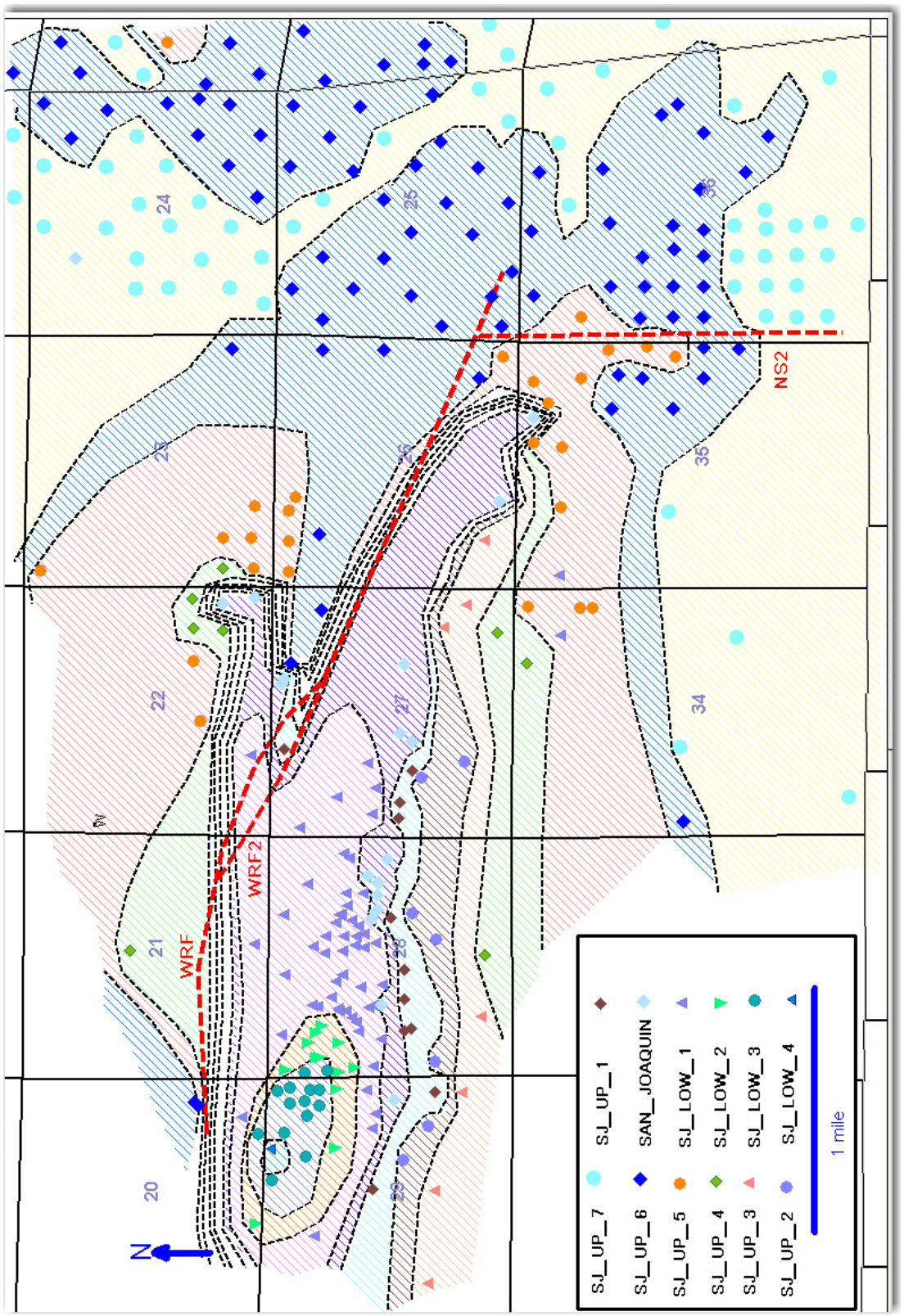

Figure 37. Unconformity subcrop map (unconformity is equivalent to current surface of anticline). Dashed red line shows fault intersections with San Joaquin marker.

Structure

To evaluate the structure of the Wheeler Ridge anticline at the Wheeler Ridge oil field three NNE to SSW cross sections have been created (Figures 38-42). The cross sections have no vertical exaggeration and are interpreted to show a fault propagation fold style for the Wheeler Ridge Fault.

The fault picks from well logs create a fairly smooth fault surface (Figure 43). The Wheeler Ridge fault dips to the south at an average angle of 30 degrees and strikes roughly east to west with a slight curve to northwest to southeast at its eastern edge. The increased repeated section near the middle of the Wheeler Ridge oil field coincides with

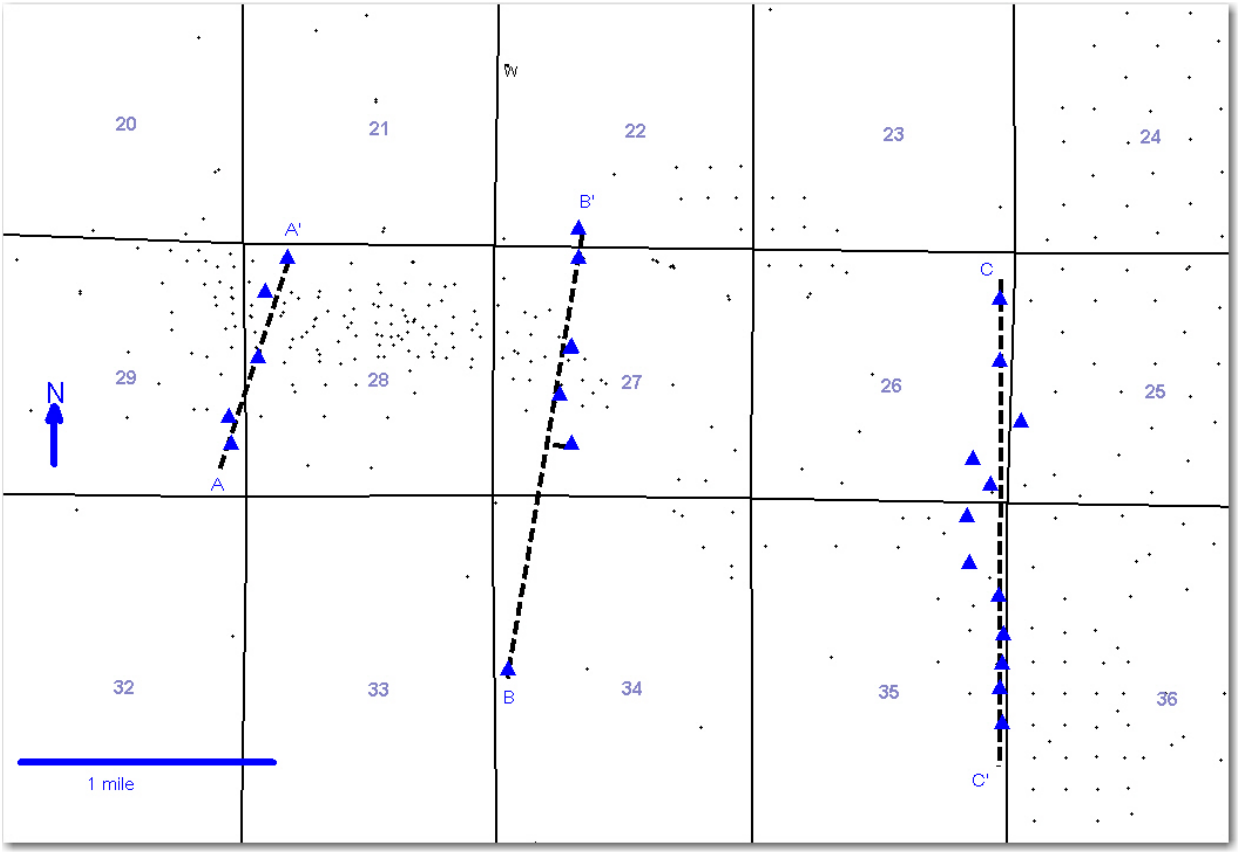

Figure 38. Location of cross sections A-A', B-B', and C-C'.

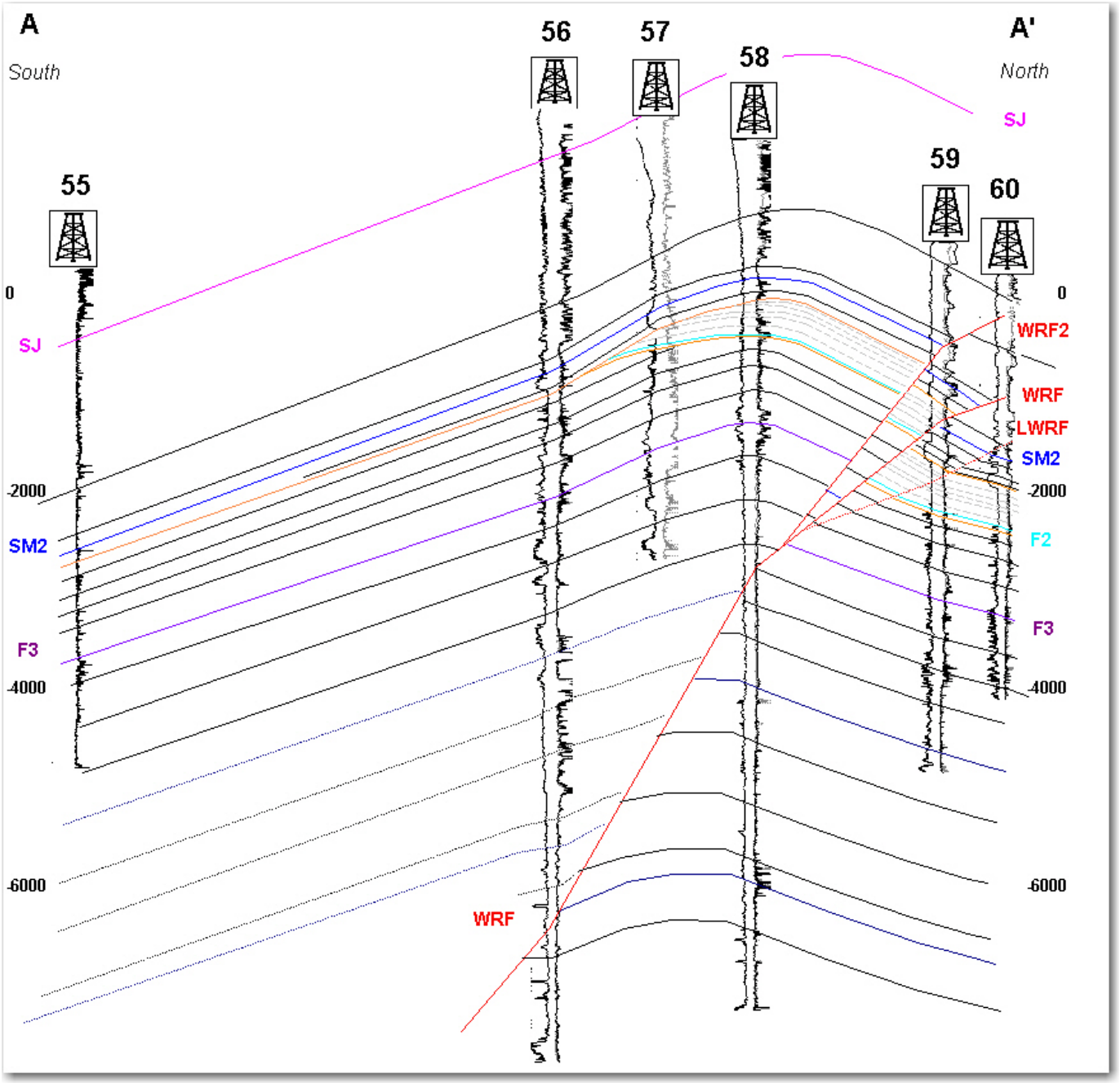

Figure 39. Cross section A-A'. Cross section shows interaction between Lower and upper unconformity. No vertical exaggeration.

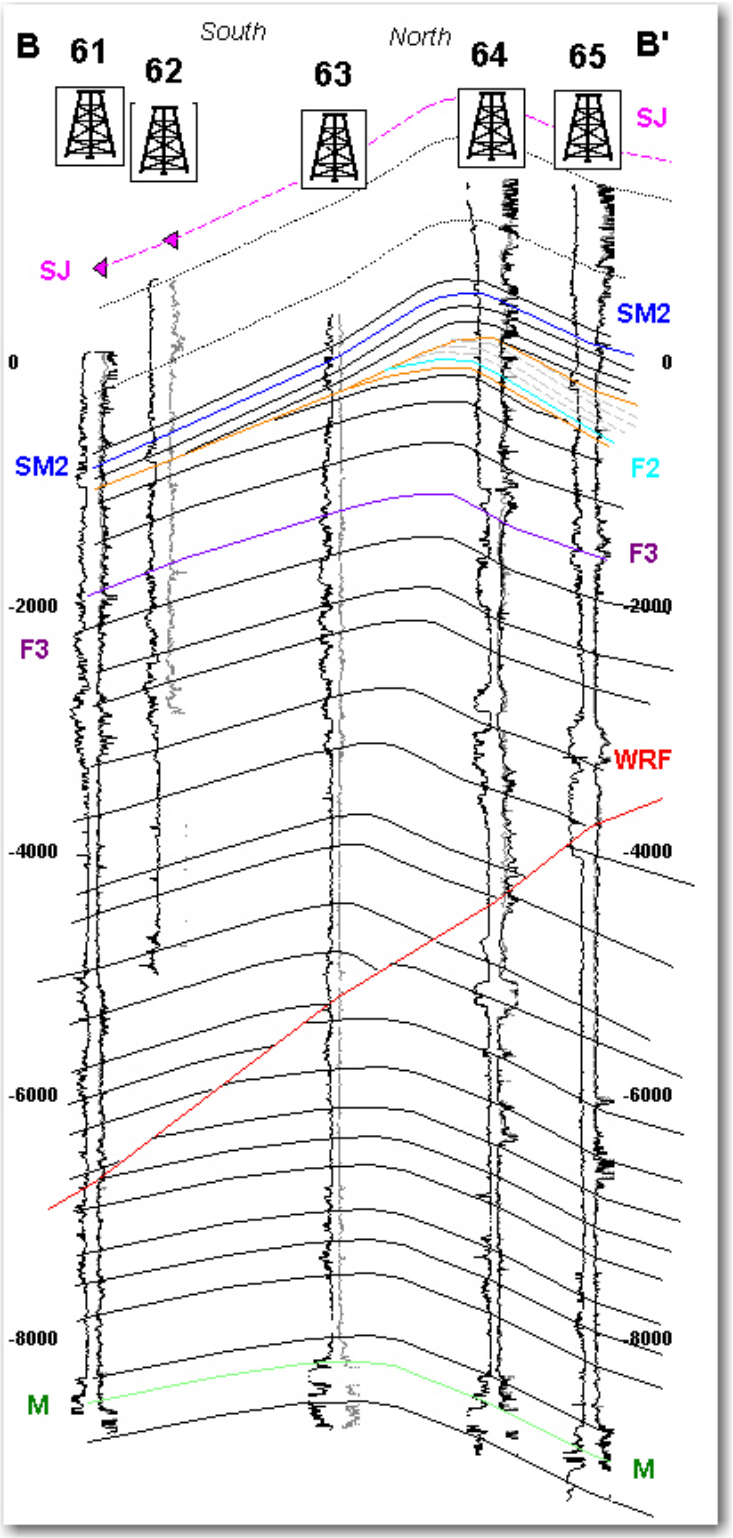

Figure 40. Cross section B-B'. Cross section shows lower unconformity cutting into a fold in the lower Fruitvale. The upper unconformity cuts out the entire upper Fruitvale and the lower unconformity. No vertical exaggeration.

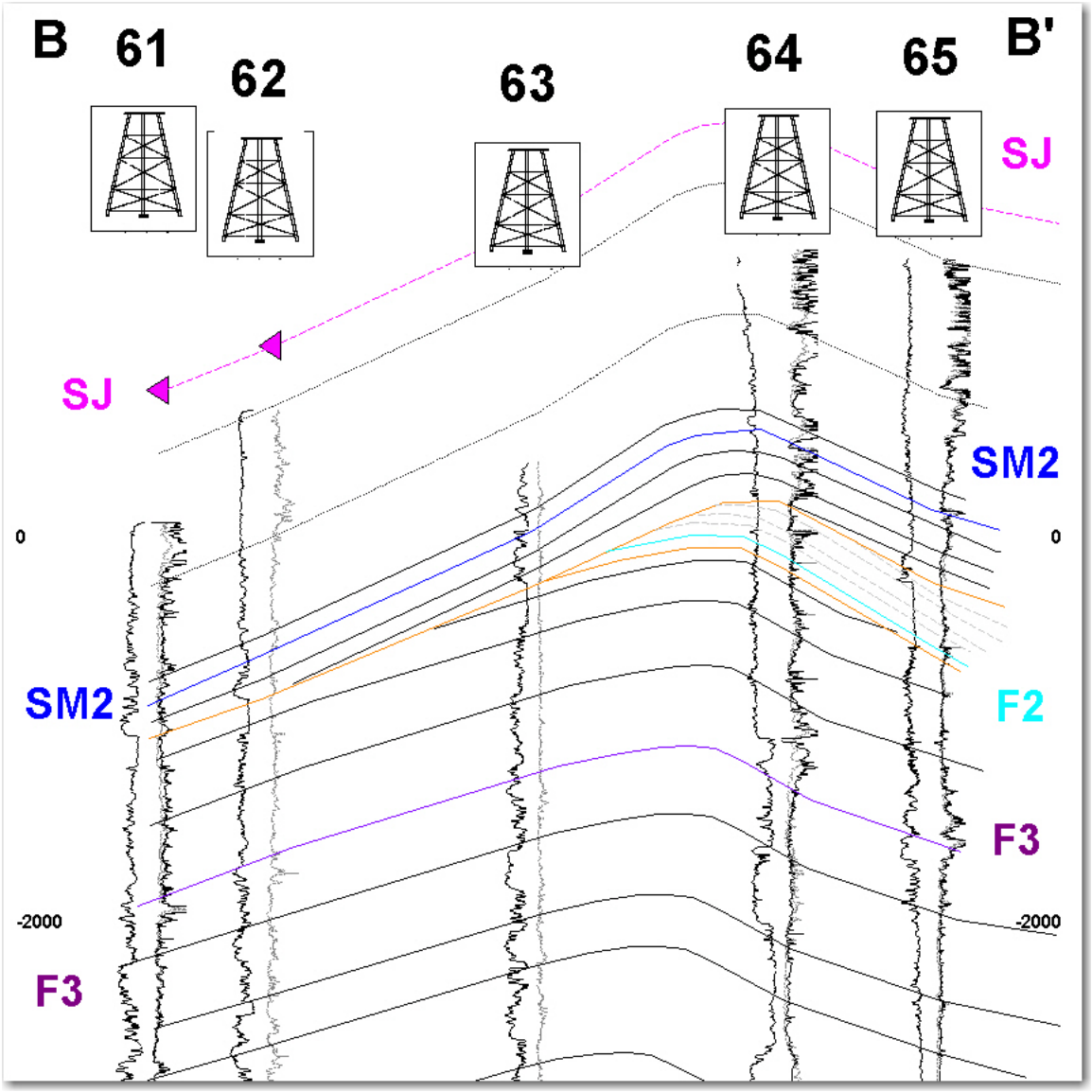

Figure 41. Cross section B-B'. Zoomed in on upper Fruitvale being truncated by upper unconformity. No vertical exaggeration.

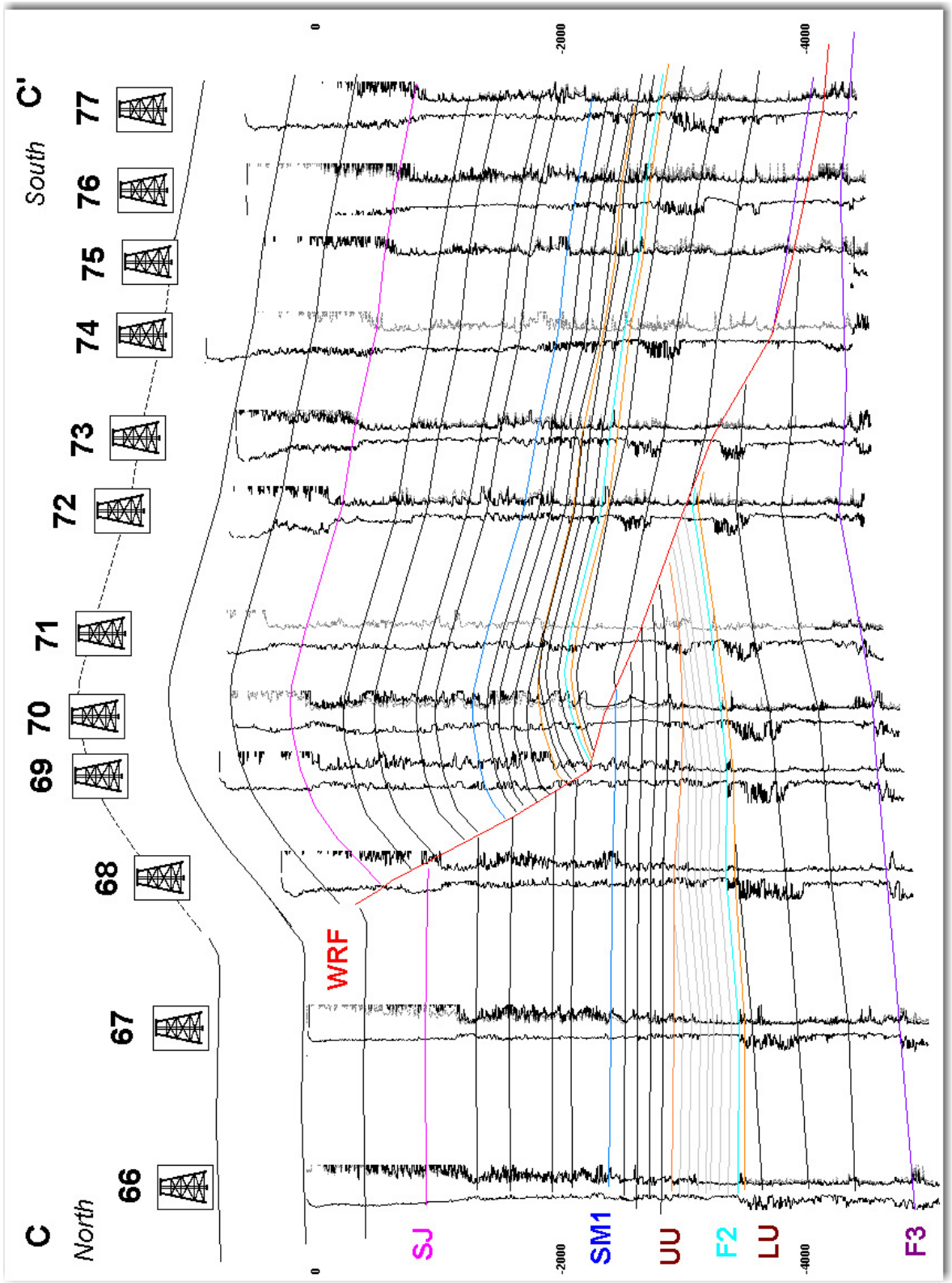

Figure 42. Cross section C-C'. North to south cross section of the Wind Gap to North Tejon oil field.

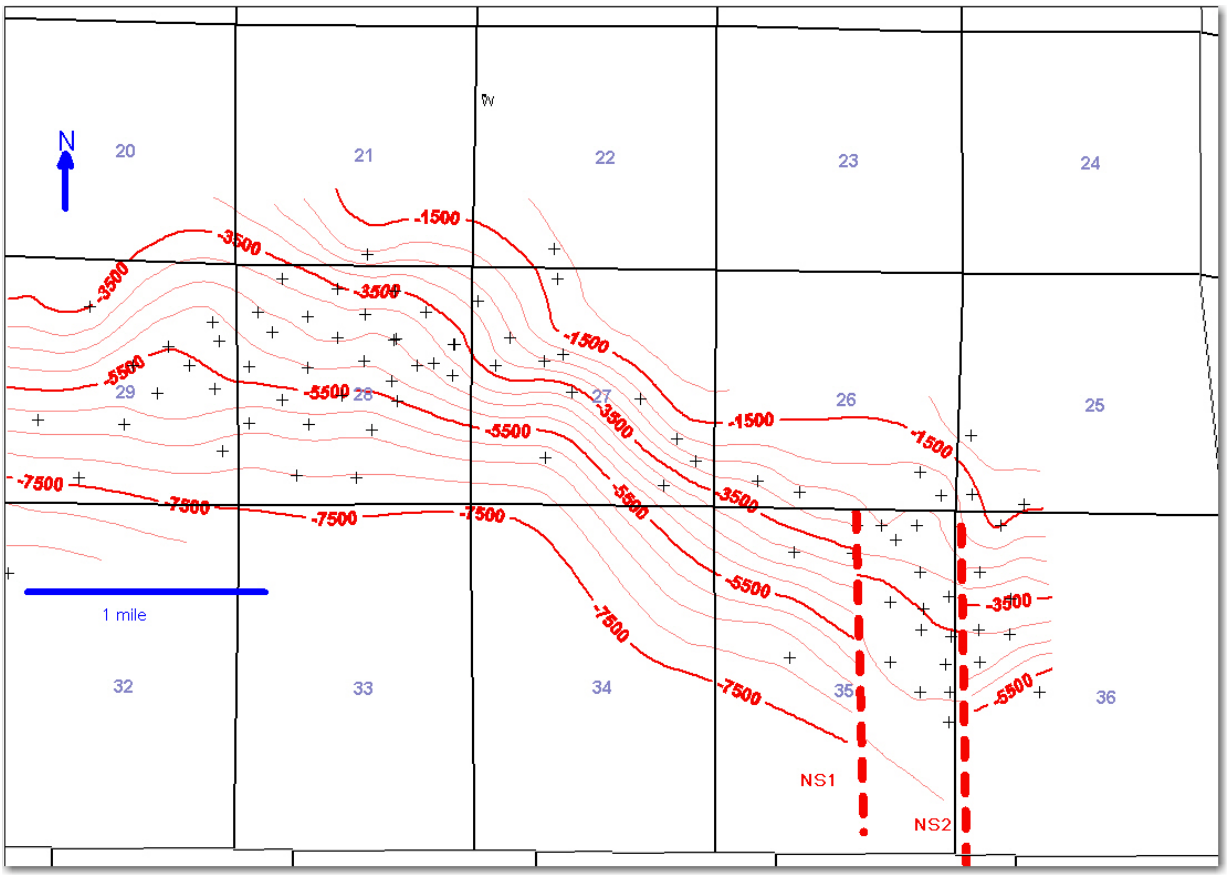

Figure 43. Wheeler Ridge Fault map. Data is from fault picks in wells using log data. In general the Wheeler Ridge fault appears fairly smooth and curves to the south at the western and eastern edges.

the maximum throw of the Wheeler Ridge fault (Figure 44). The throw of the Wheeler Ridge fault was compared to the subcrop map of the Wheeler Ridge fault (Figure 45). The maximum throw was found to lie in the same area as the lower Miocene strata in the subcrop map.

The throw of the Wheeler Ridge thrust decreases to the east and no repeated section was found past the western part of Section 36 in the Wind Gap oil field. At the eastern edge of the Wind Gap oil field there is a very distinct fault with normal fault separation, which may also have strike slip offset. The normal fault trends from north to south and dips to the west. To the east of the west dipping normal fault, the throw on the Wheeler Ridge fault quickly decreases and terminates (Figure 44-45). This is in contrast

to previous interpretations of the Wind Gap and North Tejon oil fields (Medwedeff, 1992).

The lower Miocene strata typically consists of shales with Olcese and Valv sands. The Olcese and Valv sands are likely submarine distributary channels from their coarsening upward log profile. The mixed sand and shale environment possibly suggests the stratigraphy is not localizing and controlling the location of the ramp in the Wheeler Ridge fault.

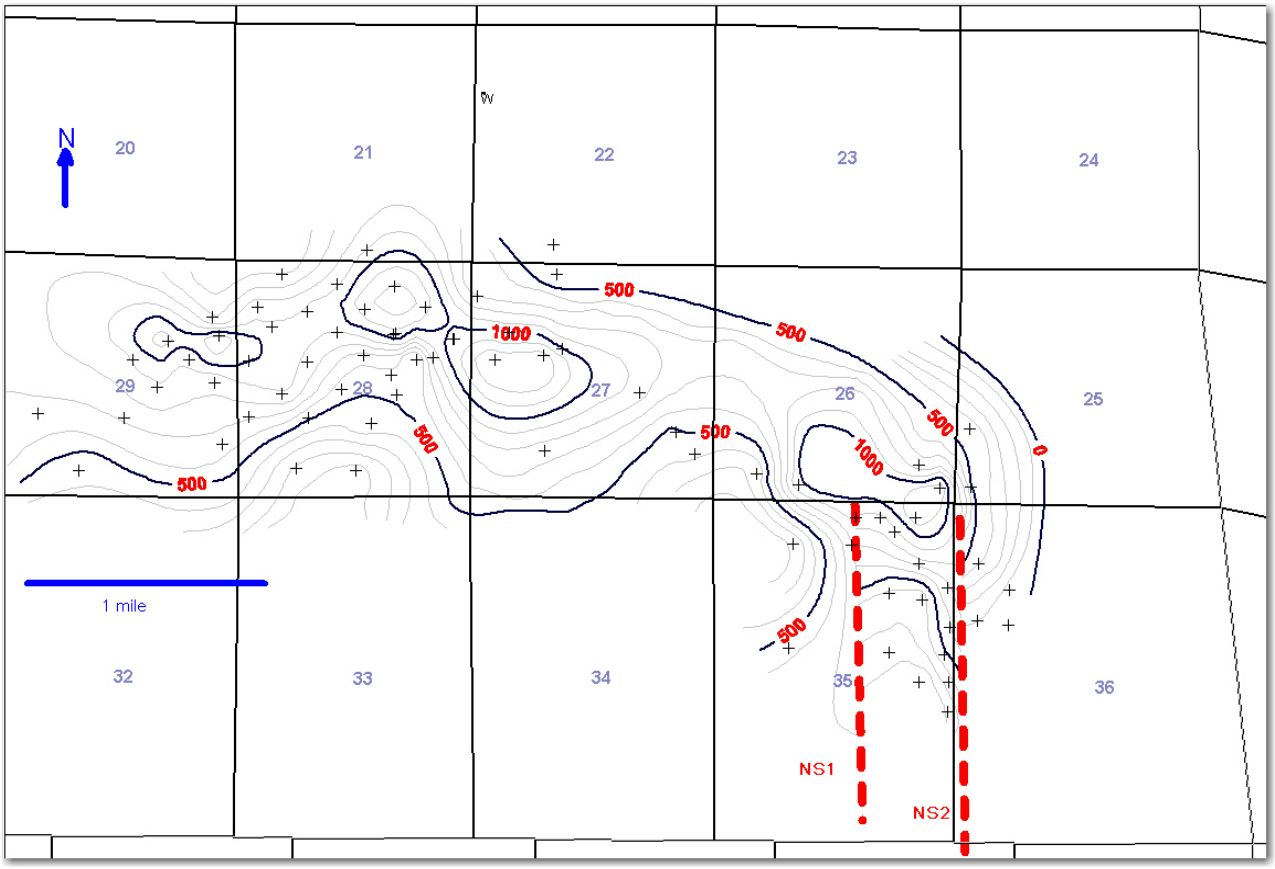

Figure 44. Wheeler Ridge Fault throw map. This figure shows the vertical separation measured in well logs of offset faulted formations. The vertical separation also represents the amount of repeated section related to the main splay of the Wheeler Ridge fault in each well. (The main splay being defined as the fault with the most repeated section).

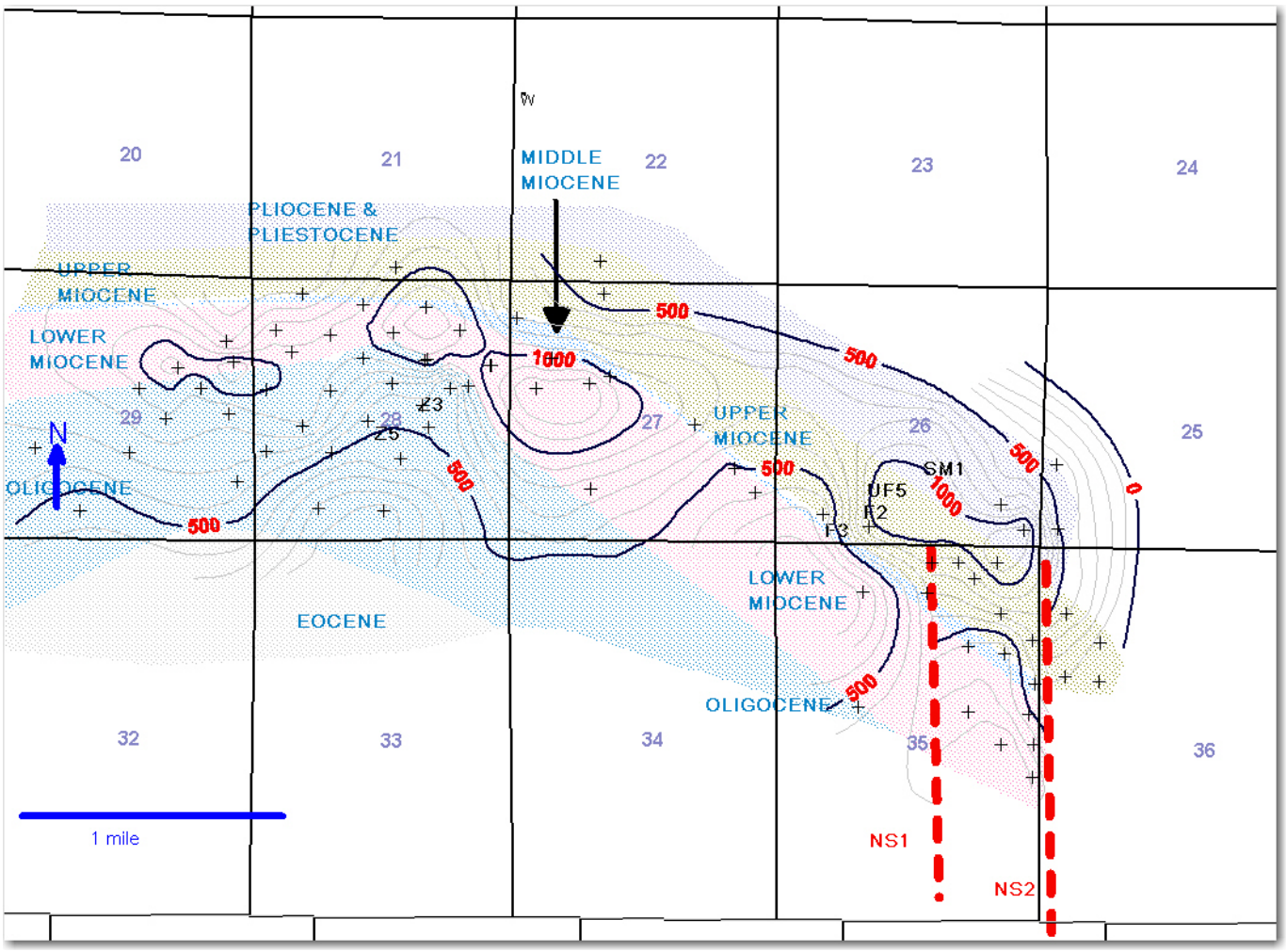

Figure 45. Wheeler Ridge Fault footwall cutoff map. Figure shows the unit directly below the Wheeler Ridge fault and is placed on top of the fault throw map from Figure 44. This figure illustrates most of the "ramping" in the fault occurs in the lower Miocene strata.

Discussion

Upper Miocene uplift has been identified in the San Emigdio Mountains (Davis, 1983; Gordon and Gerke, 2009; Medwedeff, 1992; Namson and Davis, 1988). However, the Wheeler Ridge anticline has been interpreted to be a post-Miocene fault propagation fold (Davis, 1983; Dibblee, 1986, Davis and Lagoe, 1988; Dibblee, 1986; Medwedeff, 1992; Namson and Davis, 1988). The uplift in the San Emigdio Mountains is coincident with the timing of a change in the relative motions of the North American and Pacific plates (Atwater and Stock, 1998). There is also evidence of erosion regionally that can be placed in the upper Miocene that is possibly related to uplift (Gordon and Gerke, 2009). The timing of the unconformities and facies changes at Wheeler Ridge matches the regional uplift with erosion in the Pioneer oil field and in the San Emigdio Mountains. The evidence for erosion and uplift at Wheeler Ridge during the upper Miocene will be explored in more detail below.

Structural and Stratigraphic Evidence of Uplift and Erosion

The upper Miocene shows evidence of at least two compressional events at the Wheeler Ridge oil field. The uplift events created the lower and upper unconformities (Figures 15 and 21). Approximately 600 feet of erosion was associated with the uplift related to the lower unconformity. The second uplift event in the upper Miocene corresponded to 1000 feet of erosion completely removing the upper Fruitvale in the southwest portion of the Wheeler Ridge oil field. The two uplift events produced an anticlinal structure that was subsequently onlapped and buried by the Santa Margarita (Figures 27-30).

The late Miocene Wheeler Ridge anticline appears to have a fold axis trending roughly northwest to southeast. Evidence for the late Miocene fold axis trend comes from the strike of the lower and upper unconformities where they cut formations, and the onlap of the Santa Margarita Formations. A northwest to southeast trending paleofold axis would indicate compression in a southwest to northeast direction. The current Wheeler Ridge fold axis trends roughly east to west, indicating north to south compression. Therefore, there must have been a rotation in the stress regime in the area since the upper Miocene compressional events. Both fold axes orientations are common in the region (Dibblee, 1986).

It is difficult to time exactly when the Wheeler Ridge fault began to offset formations within the Wheeler Ridge oil field. With the interpretation of the upper Miocene compression as directional southwest to northeast and the Wheeler Ridge anticline as the result of a fault propagation fold it is possible there is a deep, yet unidentified, thrust fault that strikes northwest to southeast. To test this possibility it will be necessary to evaluate the stratigraphy and structures from the Paleocene to the Middle Miocene, which is out of the scope of this research project.

Structural and Stratigraphic Model of the Wheeler Ridge Anticline

A schematic model has been put forward below to illustrate the relationship between the lower and upper unconformities and the compression and faulting in the Wheeler Ridge anticline. The model begins at the end of the middle Miocene and the deposition of the lower Fruitvale in the late Miocene (Figure 46a).

In order to create the lower unconformity identified in the PF6, PF7, and PF8 horizons there must have been uplift and erosion of the lower Fruitvale formation prior to

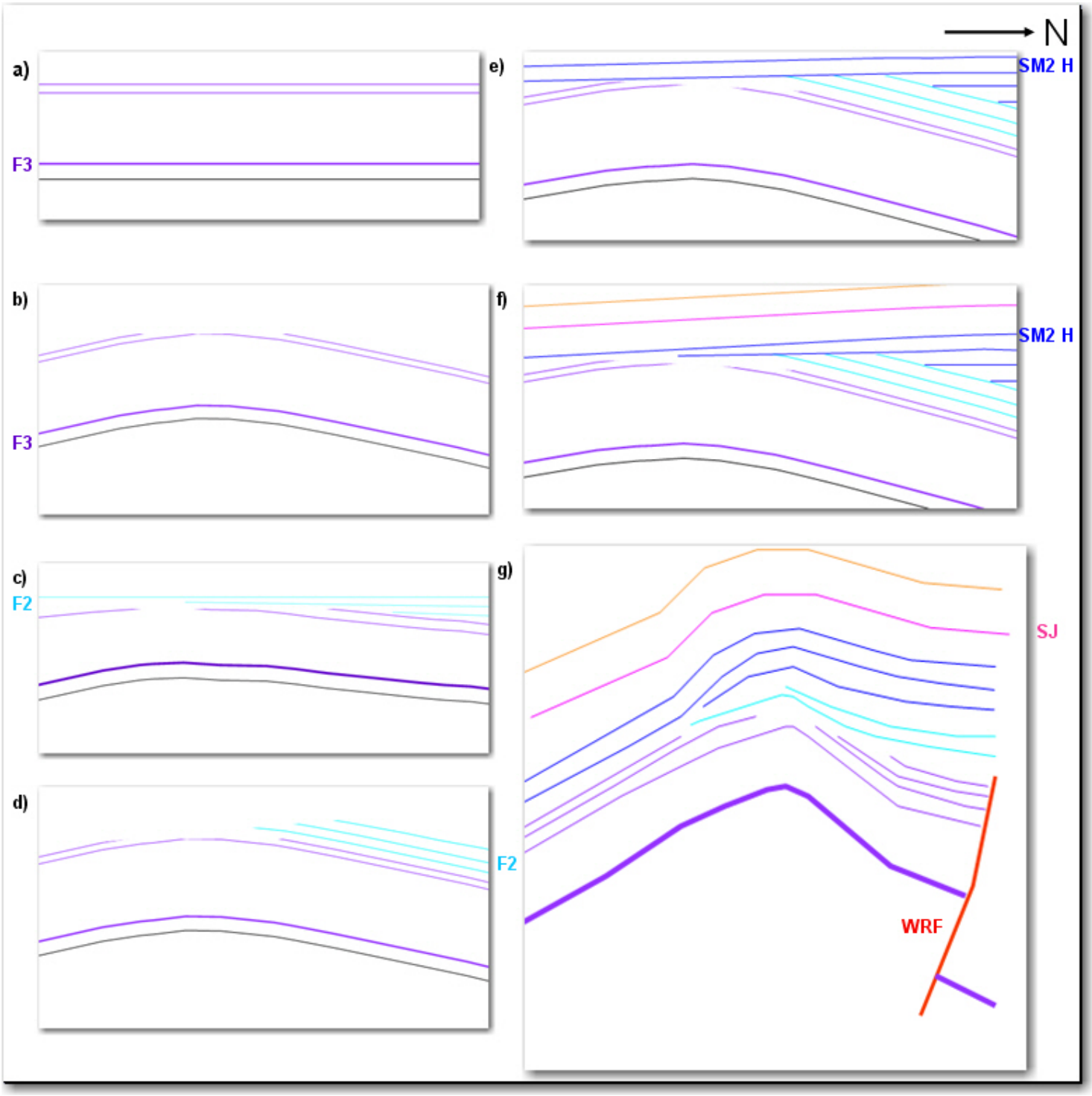

Figure 46. Model of upper Miocene to present uplift. a) Deposition of the lower Fruitvale (10-12 Mya). b) First episode of upper Miocene uplift creating the lower unconformity (10 Mya). c) Deposition of the upper Fruitvale (8-9 Mya). d) Second episode of upper Miocene uplift creating the upper unconformity (8 Mya). e) Deposition of the Santa Margarita (7-8 Mya). f) Deposition of the Etchegoin, San Joaquin, and Tulare (undifferentiated) (7-1 Mya). g) Formation of the Wheeler Ridge thrust (1-0 Mya).

the deposition of the upper Fruitvale, within the upper Miocene (Figure 46b). The uplift would have occured approximately ten million years based on the age distribution through time of the Fruitvale Formation (Childs, 1985).

After the lower unconformity and uplifting another period of deposition occurred (Figure 46c). The upper Fruitvale was deposited unconformably on top of the lower Fruitvale. The upper Fruitvale was deposited approximately eight to nine million years ago.

Another period of compression occurred between the deposition of the upper Fruitvale and the Santa Margarita formations, approximately seven to eight million years ago (Figure 46d). The uplift shows approximately the same direction of compression. The upper unconformity cuts out all of the upper Fruitvale to the south of the crest of the anticline.

After the growth of the upper Miocene paleo-Wheeler Ridge anticline there was a period of relatively little to no uplift and burial of the paleo-structure by the Santa Margarita formation (Figure 46e). Evidence of the paleo-Wheeler Ridge anticline can be seen by the onlapping of Santa Margarita sands. The SM2 L and SM2 M progressively deposit higher on the paleo-anticline. The SM2 Z is the first sand to completely overtop the paleo-anticline. The SM2 H and SM1 conformably overlie the SM2 Z sand.

The Etchegoin, San Joaquin, and Tulare (undifferentiated) are shown conformably overlying the Santa Margarita formations (Figure 46f). The Etchegoin, San Joaquin, and Tulare Formations represent the change from marine facies to non marine fluvial and alluvial systems. Without more research into this section it is not possible to identify if the recent uplift occurred episodically, as it did in the upper Miocene.

Finally we have the formation of a late Neogene to present phase of the Wheeler Ridge fault propagation and fold system (Figure 46g). The compression orientation appears to have changed by approximately 30 degrees, in a rotation eastward. A comparison of the model (Figure 46g) and current surface orientations is shows good correlation (Figure 47).

The model makes the following prediction. If the late Miocene Wheeler Ridge anticline was symmetrical about the crest of the structure then you would expect the same wedge stratigraphy to the south. Picks in wells south of the subject area strongly suggest that upper Fruitvale formation is, indeed, present. An asymmetrical fold would result from general uplift of the region from the south. Previous authors have suggested the southern and western end of the San Joaquin being uplifted during the late Miocene (Gordon and Gerke, 2009; Hirst, 1986).

The wedge shaped stratigraphy in the Santa Margarita is the result of the onlapping of a deltaic sequence onto a late Miocene Wheeler Ridge. Thus, structural complexity of the Wheeler Ridge anticline is reduced significantly from previous interpretations. In particular, the unconformity model eliminates the need for the back thrust solution proposed by previous authors (e.g. Medwedeff , 1992). The main problem with the back thrust solution at Wheeler Ridge is the need to carry the back thrust essentially up the upper unconformity surface to in between the Santa Margarita and the upper Fruitvale sections. It is highly coincidental of a back thrust to consistently cut the same amount of section in the same stratigraphic position for approximately one mile in length. Another problem with a back thrust solution is the lack of offset in the Etchegoin,

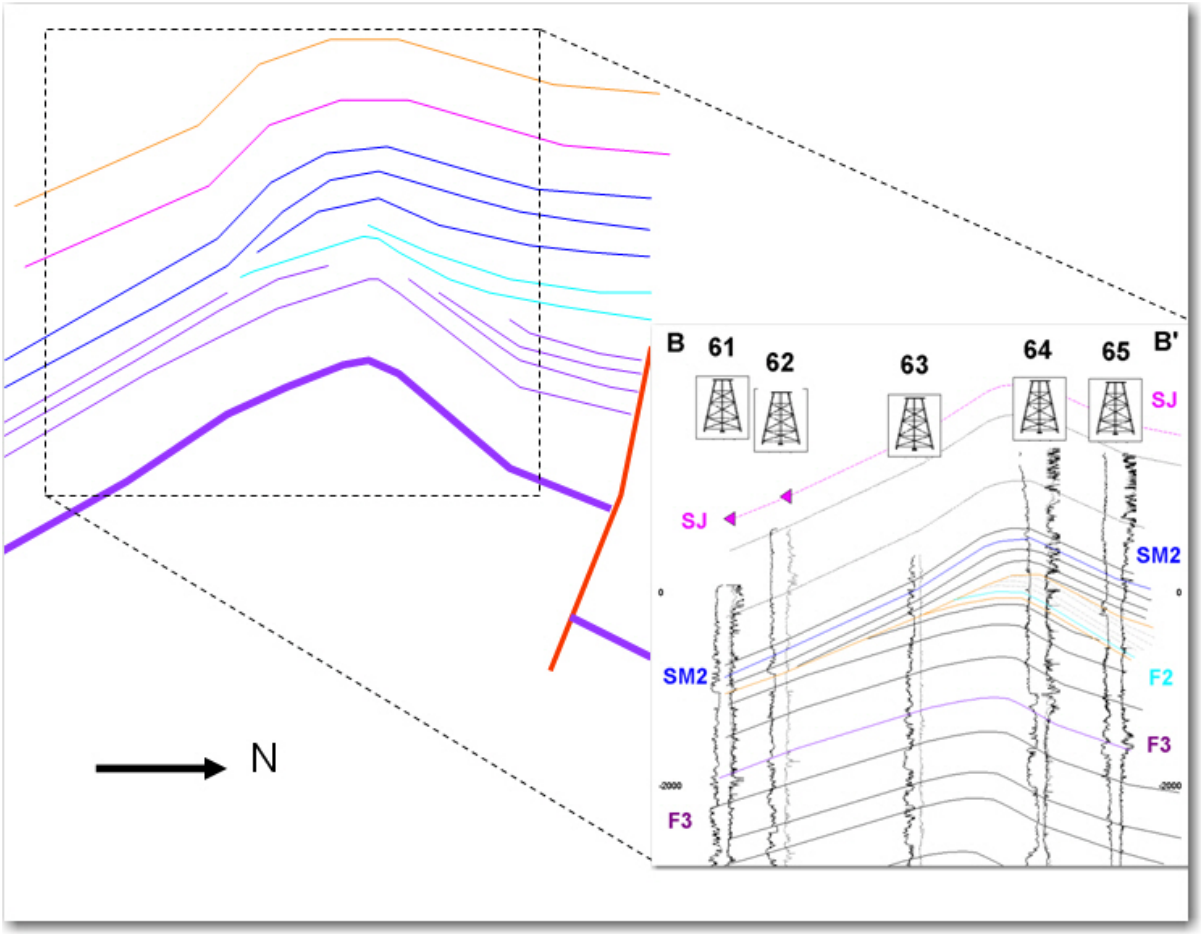

Figure 47. Model versus cross section. Model was generated by working backwards from current stratigraphic relationships and, as such, matches very well with current observations.

San Joaquin, and Tulare (undifferentiated). The increased section is more simply explained by the model put forth here.

Conclusions

Wheeler Ridge has had a longer lived Neogene tectonic history than previously thought, extending back into the late Miocene. Two periods of fold development have now been identified in the upper Miocene based on two unconformities that cut the lower and upper Fruitvale predominantly near the core of the upper Miocene Wheeler Ridge anticline. The unconformities represent surfaces that were previously described as back thrusts (DOGGR, 1992; Medwedeff, 1992). The section previously interpreted to be repeated by a back thrust in the northern part of the field is interpreted as missing section in the southern part of the field related to uplift and erosion of a upper Miocene Wheeler Ridge anticline. This reinterpretation eliminates the need for a back thrust and greatly simplifies the structure identified along the Wheeler Ridge anticline. The onlap of the Santa Margarita formation over the late Miocene anticline provide an upper age constraint of 8 Ma for the late Miocene uplift and unconformities. At least one unconformity of similar age has been previously identified in the southern part of the San Joaquin Valley (Gordon and Gerke, 2009).

The lower unconformity cuts out approximately 600 feet of section and the upper unconformity approximately 1000 feet of section. The strike of the lower unconformity, upper unconformity, and onlap of the Santa Margarita sands suggest a southwest to northeast compression direction in the upper Miocene. The contact of the SM2 L and SM2 M support an argument that the upper Miocene Wheeler Ridge anticline had a topographic expression and was eventually buried by the deposition of the SM2 Z sand.

The upper Miocene had previously been interpreted as a period of regional extension and angular unconformities (Davis and Lagoe, 1988; Goodman and Malin,

1992). However, locally there is very strong evidence of compression and angular unconformities related to uplift (Davis 1983; Gordon and Gerke, 2009). Thus, one question that still needs to be resolved is whether the uplift events in the upper Miocene observed at Wheeler Ridge are regional or local. Notably, the upper Miocene uplift at Wheeler Ridge could be coeval with the time of the change in relative North American and Pacific plate motions (Atwater and Stock, 1998). At approximately 8 Ma the Pacific plate motion rotated 30 degrees to the east, relative to the North American plate (Atwater and Stock, 1998). The change in plate motion resulted in a more compressive boundary between the North America and Pacific plates (Atwater and Stock, 1998).

Due to the scope of this project the Paleocene to Middle Miocene stratigraphy and structure was only briefly evaluated. However, this research clearly indicates normal faults present that are of the right age and orientation to be extension in the middle Oligocene to middle Miocene (Bohannon and Parsons, 1995; Davis and Lagoe, 1988; Dibblee and Nilsen, 1973; Goodman and Malin, 1992; Glazner and Bartley, 1984; Gordon and Gerke, 2009; Hirst, 1986; Hirst, 1988; Luyendyk, 1991). The normal faults tend to strike north to south in the Wheeler Ridge area dipping to the east or west. Two normal faults were mapped cutting up into the upper Miocene stratigraphy in the Wind Gap oil field, dipping to the west. Based on the structure contour maps the normal faults appear to have a right lateral strike slip component to them. The eastern edge of the Wheeler Ridge fault decreases in displacement and quickly terminates near a normal-strike slip type fault. A further evaluation of the location of normal faults in the area is necessary to test whether previously interpreted tear faults are related to the Oligocene to middle Miocene normal fault systems (Keller et al., 1998; Medwedeff, 1992).

Appendix I

Wells used in

cross sections

Wells used in cross sections

Numbers in figures	Section number	Well number	API number
Stratigraphic cross section 1 (Fig. 9)			
1	29	54	04029208010000
2	29	363	04029207970000
3	28	413	04029207610000
4	28	423	04029207520000
5	28	343	04029007100000
6	28	163	04029207740000
7	28	183	04029207320000
8	27	23	04029207340000
Stratigraphic cross section 2 (Fig. 10)			
9	28	2	04029207370000
10	28	356	04029207410000
11	28	54	04029007100000
12	28	52	04029207690000
Structural cross section 3 (Fig. 17)			
13	28	25	04029207380000
14	28	423	04029207560000
15	28	232	04029852770000
16	28	21	04029207630000
Structural cross section 4 (Fig. 18)			
17	28	356	04029207410000
18	28	65	04029207720000
19	28	163	04029207770000
20	28	61	04029207700000
Stratigraphic cross section 5 (Fig. 23)			
21	29	87	04029208060000
22	29	286	04029207990000
23	29	184	04029207960000
24	29	482	04029208000000
25	29	81	04029207890000
Stratigraphic cross section 6 (Fig. 24)			
26	28	2	04029207370000
27	28	356	04029207410000
28	28	54	04029007100000
29	28	52	04029207690000
30	21	58	04029207100000
Stratigraphic cross section 7 (Fig. 25)			
31	29	54	04029208010000
32	29	274	04029207970000
33	28	14	04029207610000
34	28	134	04029207520000
35	28	54	04029007100000
36	28	74	04029207740000
37	27	14	04029207320000
38	27	34	04029207340000
39	27	65	04029207250000
Stratigraphic cross section 8 (Fig. 32)			
40	28	21	04029207390000
41	28	132	04029207380000
42	28	23	04029041200000
43	28	133	04029207450000
44	28	25	04029207510000
45	28	28	04029207630000
Stratigraphic cross section 9 (Fig. 33)			
46	29	54	04029208010000
47	29	274	04029207970000
48	28	34	04029207650000
49	28	54	04029007100000
50	28	74	04029207740000
51	27	14	04029207320000
52	27	34	04029207340000
53	26	11	04029209260000
54	23	38	04029207220000

Structural cross section 10 (Fig. 39)

55	34	16X	04030395270000
56	27	2	04029209010000
57	27	40	04029208790000
58	27	34	04029207340000
59	27	31	04029207240000
60	22	38RD1	04029207110100

Structural cross section 11 (Fig. 40 and 41)

61	29	87	04029208060000
62	29	286	04029207990000
63	28	14	04029207610000
64	28	312	04029207800000
65	28	21	04029207630000

Structural cross section 12 (Fig. 42 and Fig.6)

66	26	82	04029205240000
67	26	84	04029204730000
68	25	16	04029204500000
69	26	77	04029204710000
70	26	88	04029204720000
71	35	71	04029208240000
72	35	72	04029208250000
73	35	83	04029208280000
74	35	84	04029208290000
75	35	85	04029208300000
76	35	86	04029646590000
77	35	87	04029208310000

Appendix II

Core Photos

and

Descriptions

Wheeler Ridge F1 was drilled by Vintage Production, LLC in February 2011 to gather core from the SM2 H, SM2 Z, and F2 intervals to evaluate future drilling and enhanced oil recovery opportunities. The well was drilled on the crest of the Wheeler Ridge anticline structure and penetrated into the lower Fruitvale. The core was prepared by Core Lab in Bakersfield, CA. The author supervised the coring operations. Brief lithologic descriptions, by the author, are included with the core photos. Below is a summary of the coring operations and the core taken.

During coring at the top of the SM2 H a hard shale was encountered. During the start of the coring operations a pressure spike was observed. When the core barrel was retrieved it was jammed with a very hard shale. The jam was at the bottom of the barrel and would have prevented any further core being recovered if the core barrel had been advanced beyond the point at which the pressure spike had been observed. The shale was very dense, dark black in color, and had a strong petroleum odor. The second core run went without any pressure spikes. In general it was observed the pressure spikes resulted in a hard streak being encountered, either shale or cemented sandstone. If the core barrel was advanced beyond the pressure spike then core recovery was adversely affected. This resulted in an average core recovery per run of 20-25 feet, the maximum possible core being 30 feet per run.

The core was slabbed in three foot intervals. All depths are calculated as measured depths from the Kelly Bushing (KB) of the drilling rig (1821'). A photo was taken of each three foot interval in both plain light, displayed on the left, and ultraviolet light, displayed on the right. In ultraviolet light hydrocarbons will fluoresce and look

very bright, while non hydrocarbon bearing rock will look dark. Other minerals can fluoresce, but in general this correlation works very well.

The SM2 H and SM2 Z are very sandy intervals with few shaly intervals. In general, the SM2 H and SM2 Z are very well sorted with bimodal very fine to fine grained and medium to coarse grain intervals. The medium to coarse grain intervals occasionally have pebbles and massive to normal bedding, massive being more common. The very fine to fine grained intervals occasionally have cross bedding and planar bedding. The SM2 H and SM2 Z have a slight reddish tint to them suggesting oxidation, which would mean they would have been deposited in an environment with occasional exposure to the atmosphere (near shore environment). Other key depositional observations within the Santa Margarita Formations are the presence of roots, coquina layers, charcoal, and slightly imbricated pebbles. The high degree of sorting would suggest a wave dominated environment, such as a beach environment. From this information it seems likely the Santa Margarita sands at Wheeler Ridge oil field are near shore deltaic to beach deposits.

The upper Fruitvale section cored was shaly with one small sand interval, F2 sand. The shale was highly bioturbated. There was one nearly vertical fissure in the core that was approximately one inch wide and six feet long. The F2 sand shows five Bouma sequences. The Bouma sequences present suggest an edge of a distal turbidite fan was penetrated by the Wheeler Ridge F1 well.

The lower unconformity is present in the Wheeler Ridge F1 core. The upper Fruitvale highly bioturbated shale is followed abruptly by hard shale and chert layers that are highly fractured and contain hydrocarbons. To date, no analysis of the siliceous chert

has been made to identify if it is in opal A, opal Ct, or quartz phase. It was also noted the potassium content of the compensated spectral natural gamma log sharply decreased at the unconformity. The Thorium/Uranium ratio in the upper portion of the lower Fruitvale is ~0.5 with Uranium values ranging from 8-18ppm and Potassium at ~1 percent (Wheeler Ridge F1). The lower Fruitvale is interpreted to be a deep marine depositional sequence.

WR F1 CORE
(SM2 1490-1629)

SM2 H top at 1485'

Corresponds to Maximum Flooding Surface (MFS)- defines upper Sequence Boundary of SM2 depositional sequence. Mechanically very hard shale, siliceous?

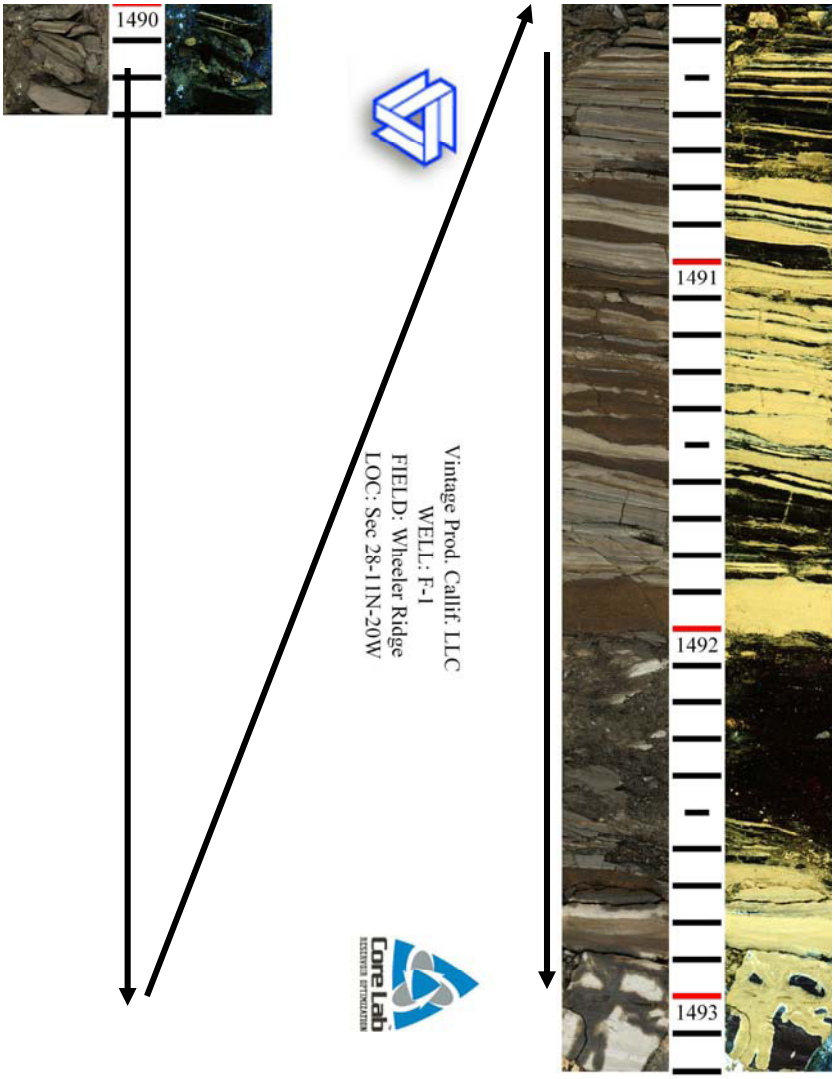

Interbedded sands and silts (1mm-15mm thickness) planar bedding, sands cemented. Well sorted.

VF-F with M sand. Massive bedding. Well sorted. Slight coarsening downward.

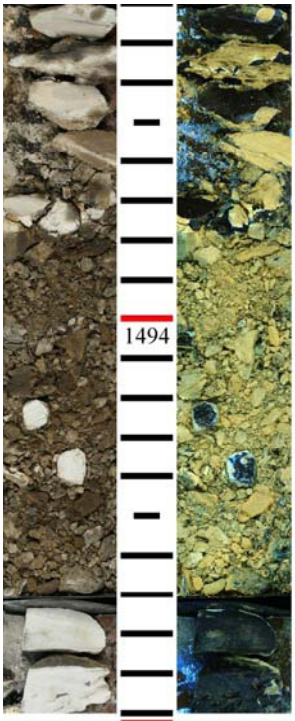

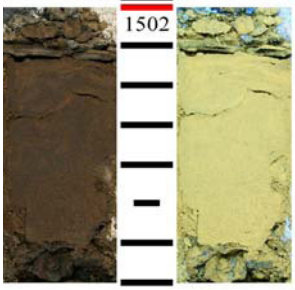

M-C sand. Massive bedding. Very well sorted.

Vintage Prod. Calif. LLC
WELL: F-1
FIELD: Wheeler Ridge
LOC: Sec 28-11N-20W

M-C sand. Massive bedding. Very well sorted.

M-C sand. Massive bedding. Very well sorted.

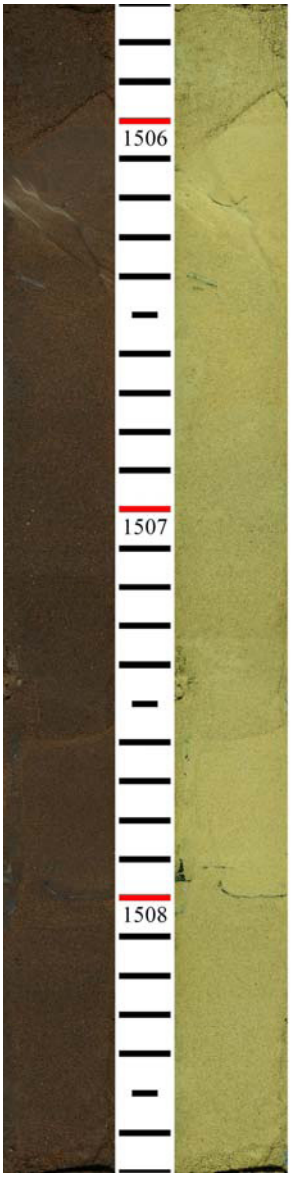

Vintage Prod. Callif. LLC
WELL: F-1
FIELD: Wheeler Ridge
LOC: Sec 28-11N-20W

Core Lab

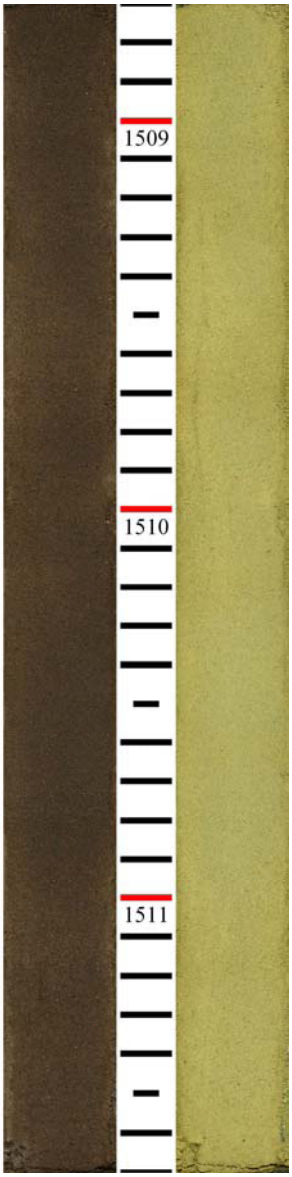

M-C sand.
Massive bedding.
Very well sorted.

M-C sand. Massive bedding. Very well sorted.

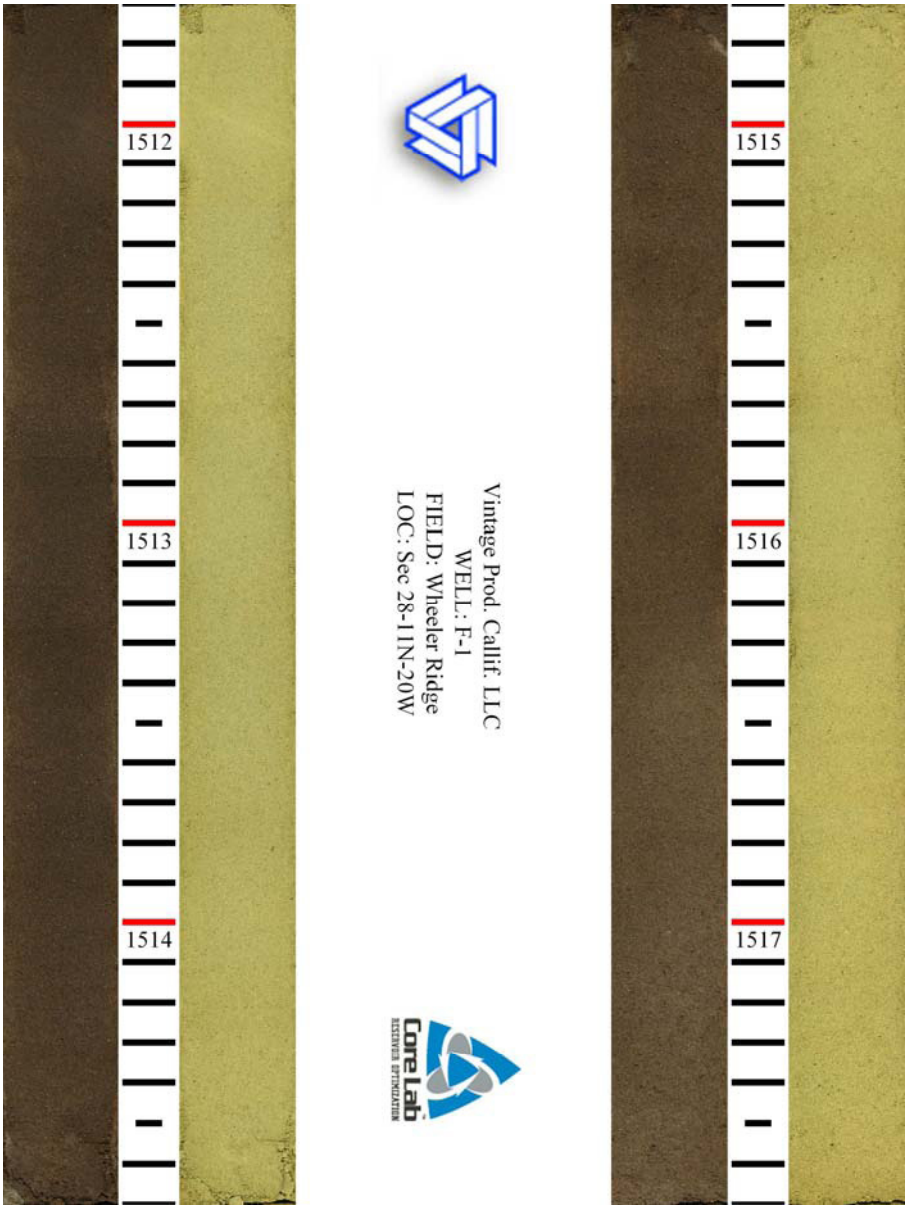

M-C sand. Massive bedding. Very well sorted.

M-C sand with pebbles. Massive bedding. Very well sorted.

Silt lense (2cm thick). Planar bedding.

M-C sand. Massive bedding. Very well sorted.

VF-F sand. Cross bedding (beds dip at 22°). Very well sorted.

Vintage Prod. Calif. LLC
WELL: F-1
FIELD: Wheeler Ridge
LOC: Sec 28-11N-20W

M-C sand. Massive bedding. Very well sorted.

M-C sand with pebbles. Massive bedding. Very well sorted.

M-C sand. Massive bedding. Very well sorted.

Interbedded sands and silts. Wavy to planar bedding with beds dipping at ~10° grading into VF-M sand with similar dips. Possible dewatering structure? Scour?

M-C sand. Massive bedding. Very well sorted. Scour at base into silt lense.

Interbedded sands and silts. Wavy to planar bedding with beds dipping at ~5° grading into VF-M sand with similar dips.

M-C sand. Massive bedding. Very well sorted. Scour at base into silt lense.

M-C sand. Massive bedding. Very well sorted.

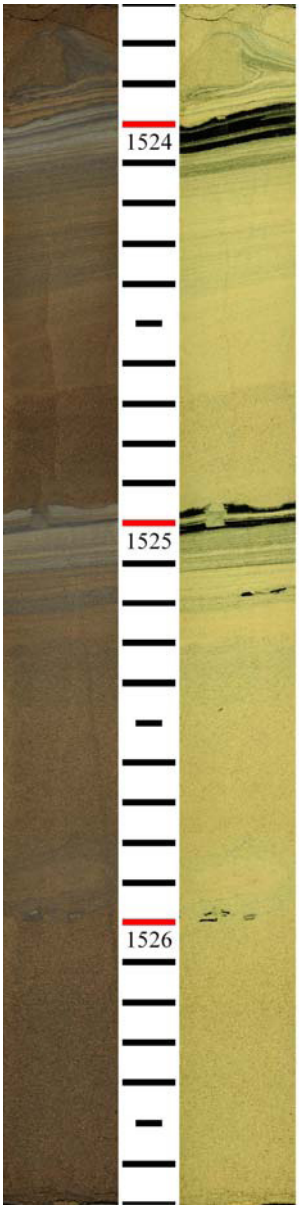

Vintage Prod. Callif. LLC
WELL: F-1
FIELD: Wheeler Ridge
LOC: Sec 28-11N-20W

Core Lab

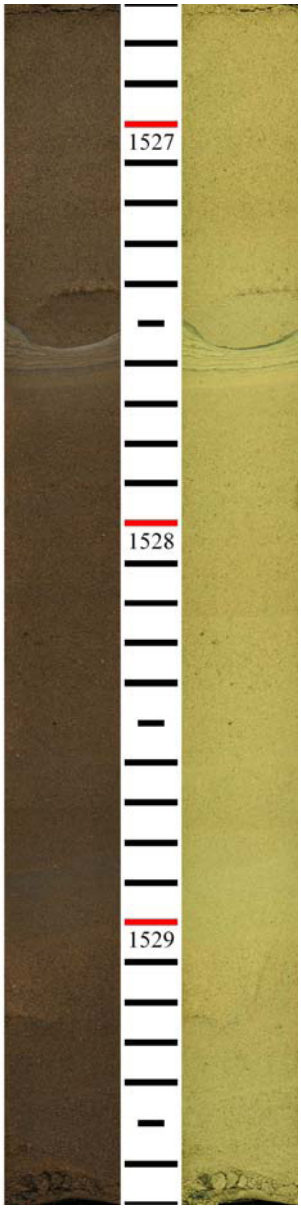

M-C sand. Massive bedding. Very well sorted. Scour at base into silt lense.

Interbedded sands and silts. Planar bedding with beds dipping at ~5° grading into VF-M sand with similar dips.

M-C sand. Massive bedding. Very well sorted.

Interbedded sands and silts. Wavy to planar bedding with beds dipping at ~5° grading into VF-M sand with similar dips.

M-C sand. Massive bedding. Very well sorted.

Interbedded sands and silts. Wavy to planar bedding with beds dipping at ~5° grading into VF-M sand with similar dips.

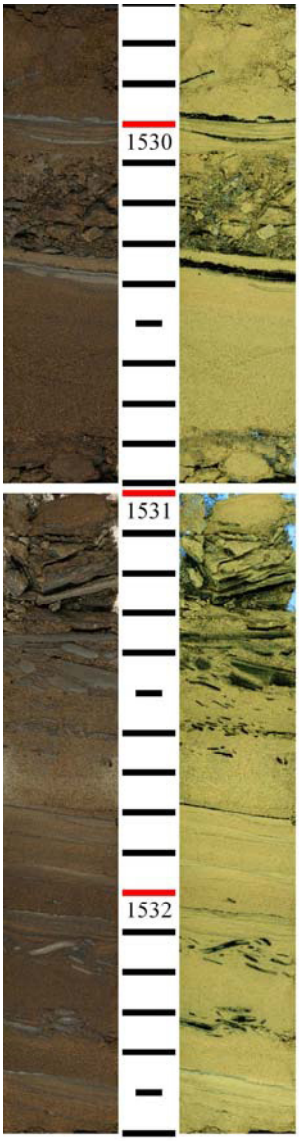

Vintage Prod. Callif. LLC
WELL: F-1
FIELD: Wheeler Ridge
LOC: Sec 28-11N-20W

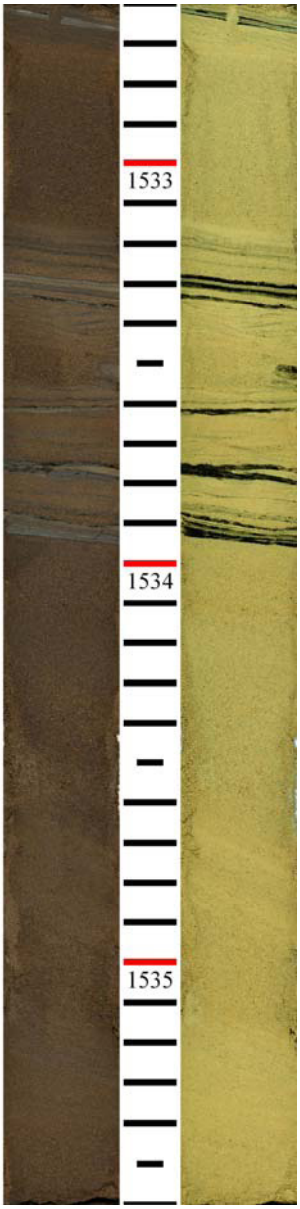

Interbedded sands and silts. Wavy to planar bedding with beds dipping at ~5° grading into VF-M sand with similar dips.

Interbedded sands and silts. Wavy to planar bedding with beds dipping at ~10° grading into F-M sand with similar dips.

F-M sand. Cross bedding with 30 ° dips. Very well sorted.

M-C sand. Massive bedding. Very well sorted.

M-C sand with pebbles. Massive bedding. Very well sorted.

Vintage Prod. Callif. LLC
WELL: F-1
FIELD: Wheeler Ridge
LOC: Sec 28-11N-20W

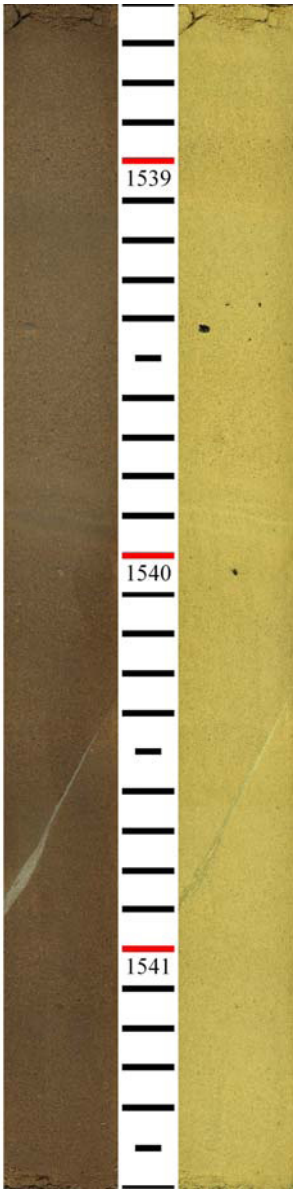

F-M sand. Cross bedding with ~20° dips.

M-C sand. Massive bedding. Very well sorted.

Dendritic root.

M-C sand.
Massive bedding.
Very well sorted.

Dendritic root.

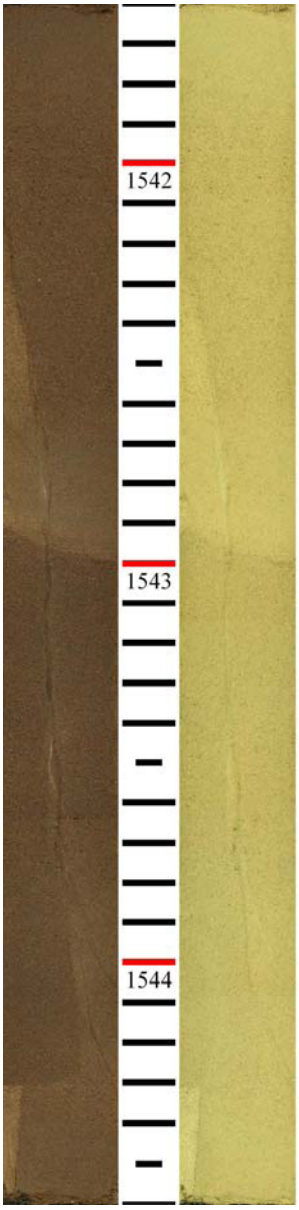

Vintage Prod. Callif. LLC
WELL: F-1
FIELD: Wheeler Ridge
LOC: Sec 28-11N-20W

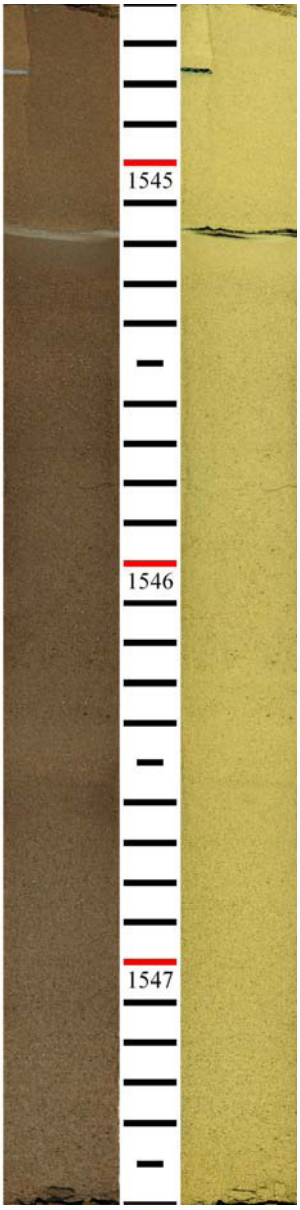

M-C sand. Massive bedding. Very well sorted.

Thin silt lense.
Planar bedding.

M-C sand with pebbles. Massive bedding. Very well sorted.

M-C sand with pebbles. Massive bedding. Very well sorted.

Silt lense. Planar bedding dipping at ~10°.

M-C sand. Massive bedding. Very well sorted.

Silt lense. Planar bedding dipping at ~5°.

M-C sand. Massive bedding. Very well sorted.

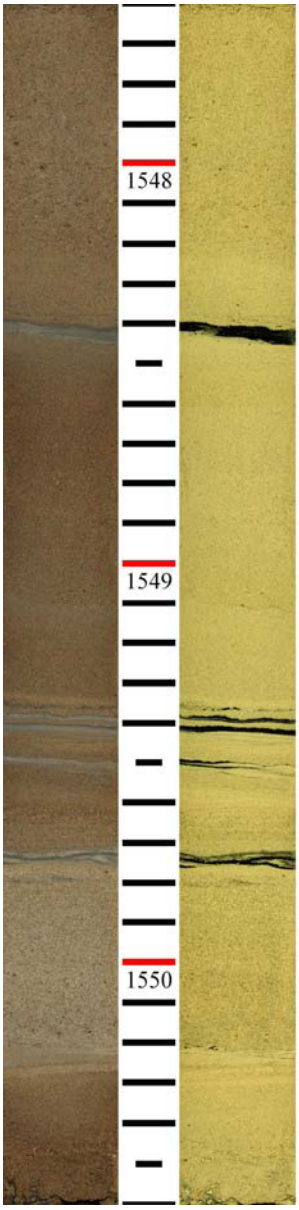

Vintage Prod. Callif. LLC
WELL: F-1
FIELD: Wheeler Ridge
LOC: Sec 28-11N-20W

M-C sand with pebbles. Massive bedding. Very well sorted.

M-C sand. Massive bedding. Very well sorted.

M-C sand. Massive bedding. Very well sorted.

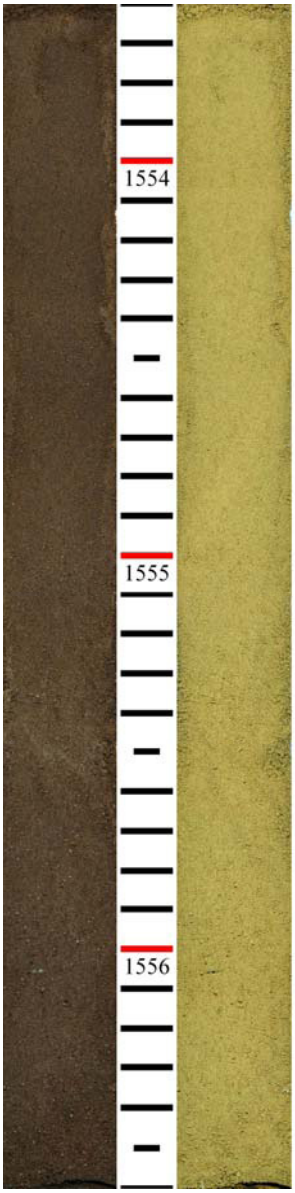

Vintage Prod. Callif. LLC
WELL: F-1
FIELD: Wheeler Ridge
LOC: Sec 28-11N-20W

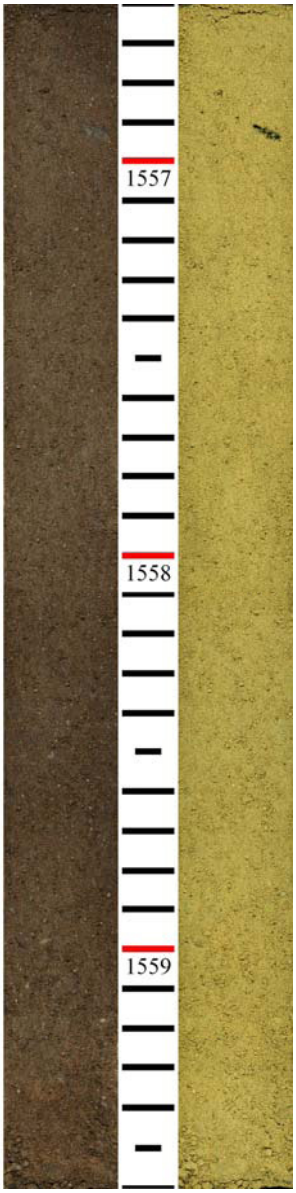

M-C sand with pebbles. Massive bedding. Very well sorted.

Cemented zone.

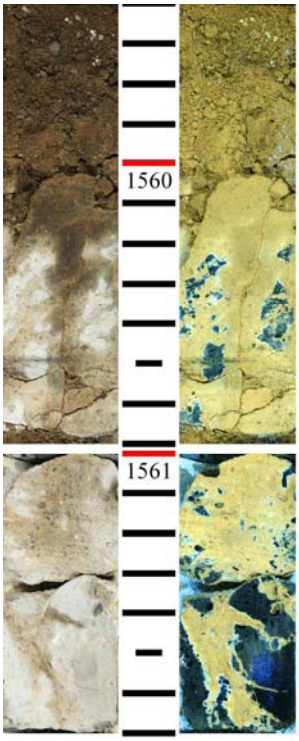

Vintage Prod. Calif. LLC
WELL: F-1
FIELD: Wheeler Ridge
LOC: Sec 28-11N-20W

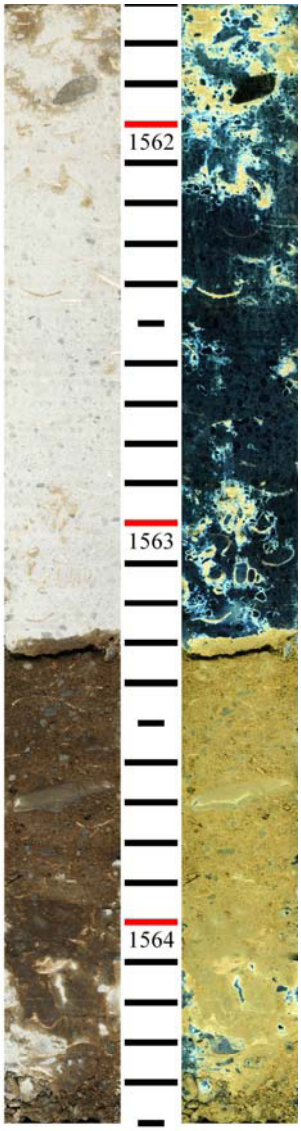

Cemented zone. Bivalve and gastropods apparent.

M-C sand with pebbles. Massive bedding. Very well sorted.

Gravel with M-VC sand, ~1cm pebbles.

M-C sand with pebbles and cementing. Massive bedding. Very well sorted.

M-C sand with pebbles. Massive bedding. Very well sorted.

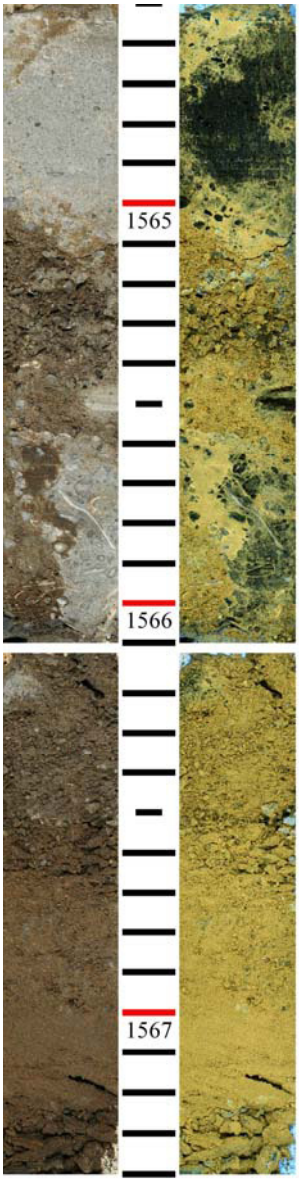

Vintage Prod. Callif. LLC
WELL: F-1
FIELD: Wheeler Ridge
LOC: Sec 28-11N-20W

M-C sand. Massive bedding. Very well sorted.

F-M sand. Normal grading. Very well sorted.

M-C sand. Massive bedding. Very well sorted.

Cement nodule at least 20cm across.

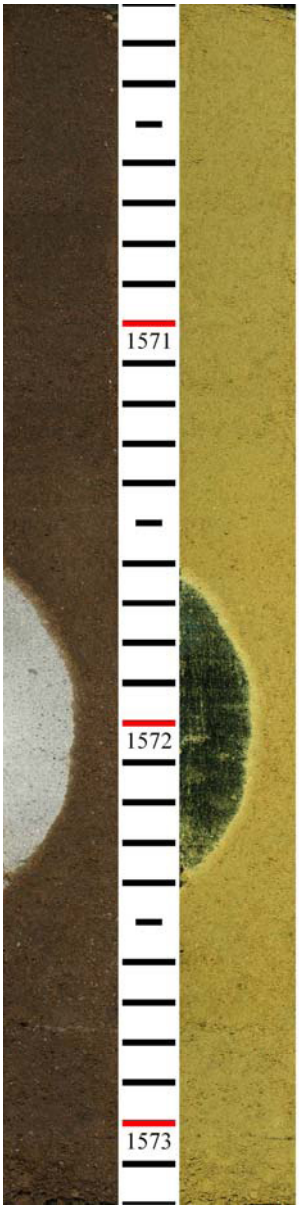

Vintage Prod. Callif. LLC
WELL: F-1
FIELD: Wheeler Ridge
LOC: Sec 28-11N-20W

M-C sand with pebbles. Massive bedding. Very well sorted.

M-C sand. Massive bedding. Very well sorted.

Cement nodule at 4cm across.

Vintage Prod. Callif. LLC
WELL: F-1
FIELD: Wheeler Ridge
LOC: Sec 28-11N-20W

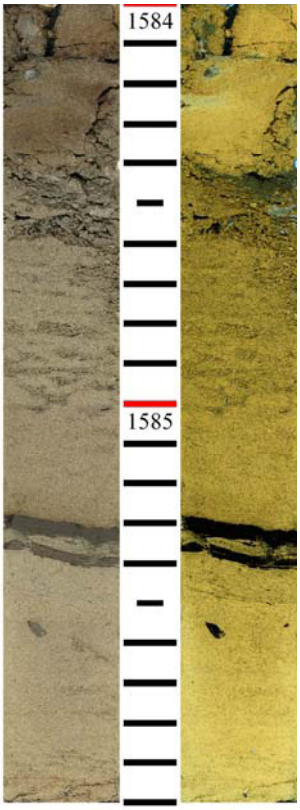

VF silt -VF sand. Poorly sorted. Roots, with charcoal?

VF-F sand. Possible crossbedding. Well sorted.

Silt lense. Planar bedding dipping at ~10°. 1cm in thickness.

VF-F sand. Well sorted.

SM2 Z top at 1584'

No recovery. During coring it was noted that the shales tended to be mechanically very hard and the sands were unconsolidated. When a thick shale was encountered during coring we lost recovery.

Silt lense. Planar bedding dipping at ~5°. 1cm in thickness.

VF-F sand. Well sorted.

VF-F sand with cement clasts. Well sorted.

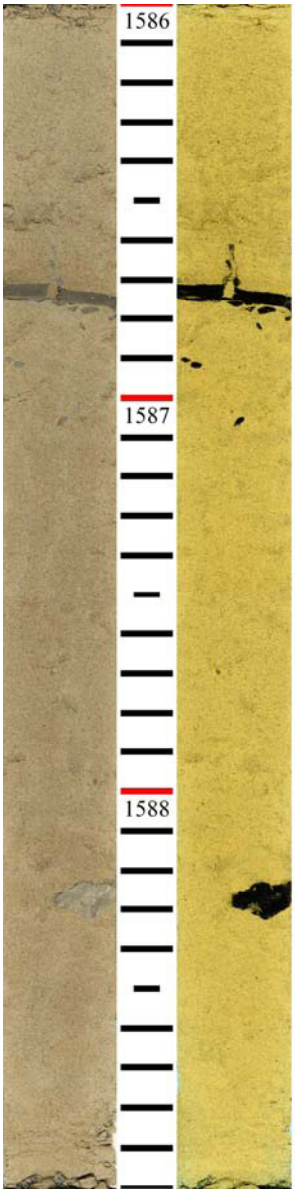

Vintage Prod. Califf. LLC
WELL: F-1
FIELD: Wheeler Ridge
LOC: Sec 28-11N-20W

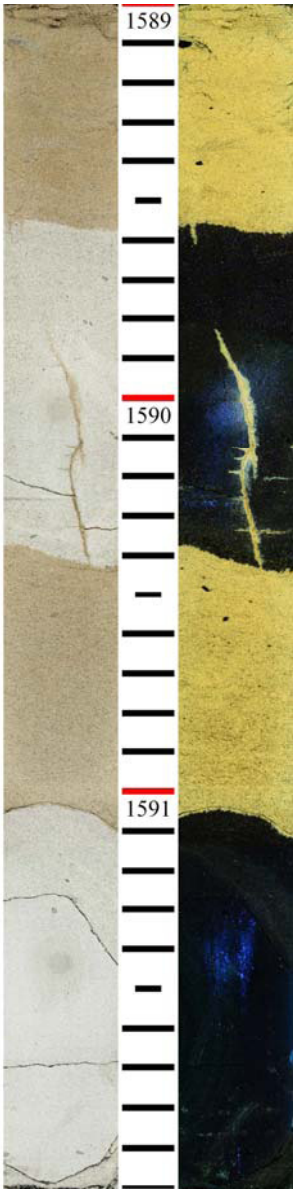

VF-F sand. Well sorted.

Cement nodule at least 20cm across.

Cement nodule at least 40cm across.

VF-F sand. Well sorted.

Silt lense. Planar bedding. 3cm in thickness. Rip up shale clasts. Storm deposit?

VF-F sand with shale clasts. Poorly sorted.

Silt lense. Planar bedding. 2cm in thickness.

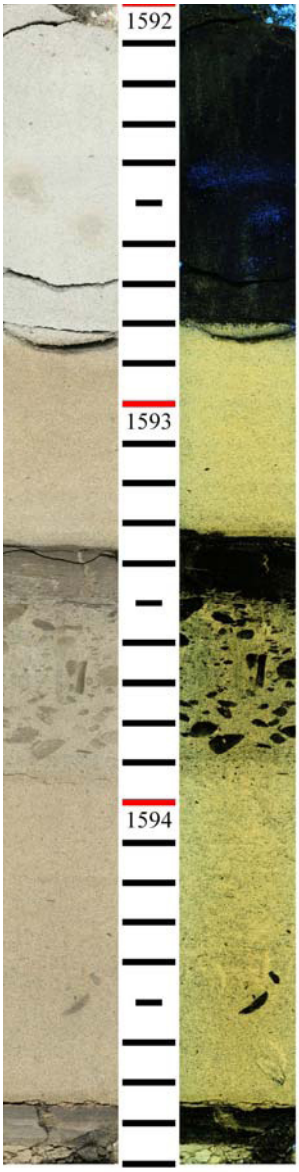

Vintage Prod. Callif. LLC
WELL: F-1
FIELD: Wheeler Ridge
LOC: Sec 28-11N-20W

VF-F sand with shale clasts. Massive bedding. Well sorted.

Cement nodule at least 20cm across.

Silt lense. Planar bedding. 2cm in thickness.

VF-F sand with shale clasts. Massive bedding. Well sorted.

Silt lense. Planar bedding. 2cm in thickness.

VF-F sand with shale clasts. Massive bedding. Well sorted.

Silt. Planar bedding.

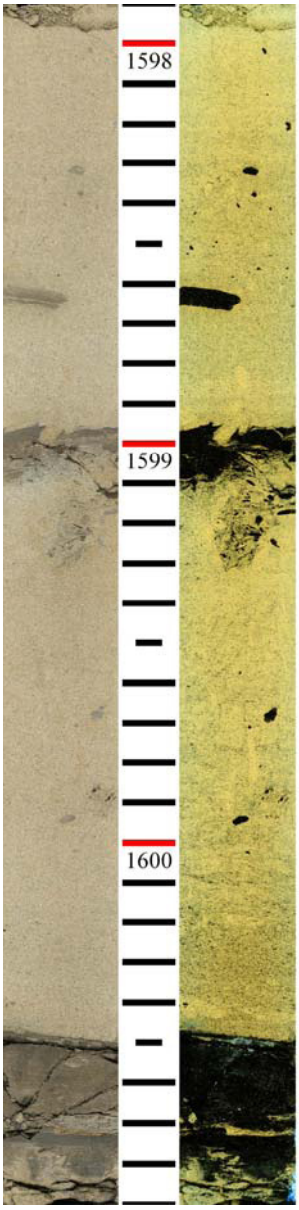

Vintage Prod. Callif. LLC
WELL: F-1
FIELD: Wheeler Ridge
LOC: Sec 28-11N-20W

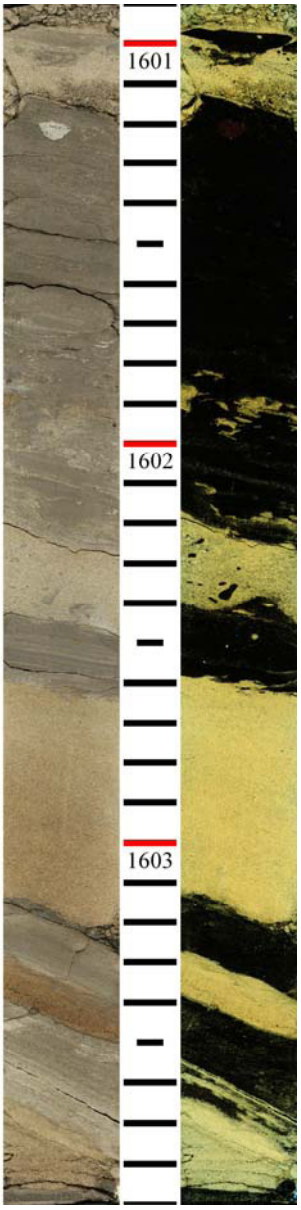

VF-F sand with shale clasts. Crossbedding with dips at 20°. Well sorted.

Silt. Planar bedding with dips at 20°.

VF-F sand with shale clasts. Crossbedding with dips at 20°. Well sorted.

Interbedded VF-F sand with silt. Crossbedding with dips at 20°. Well sorted.

VF-F sand. Planar bedding dipping 0-5°. Well sorted.

Cemented zone.

M-C sand. Massive bedding. Very well sorted.

VF-F sand. Planar bedding dipping 0-5°. Well sorted.

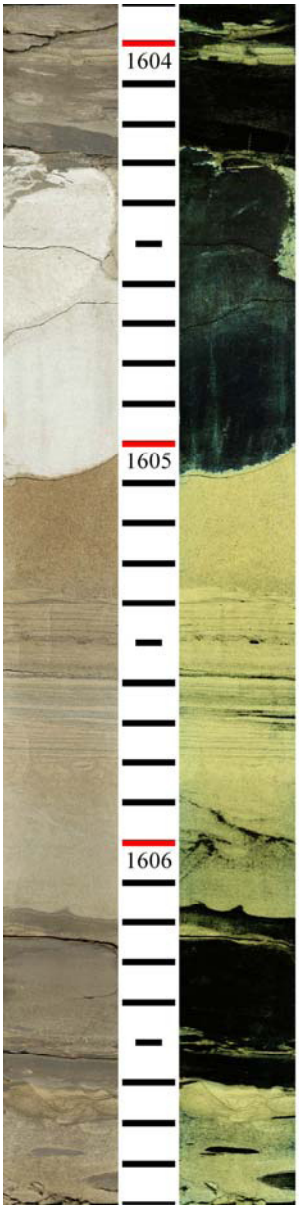

Vintage Prod. Callif. LLC
WELL: F-1
FIELD: Wheeler Ridge
LOC: Sec 28-11N-20W

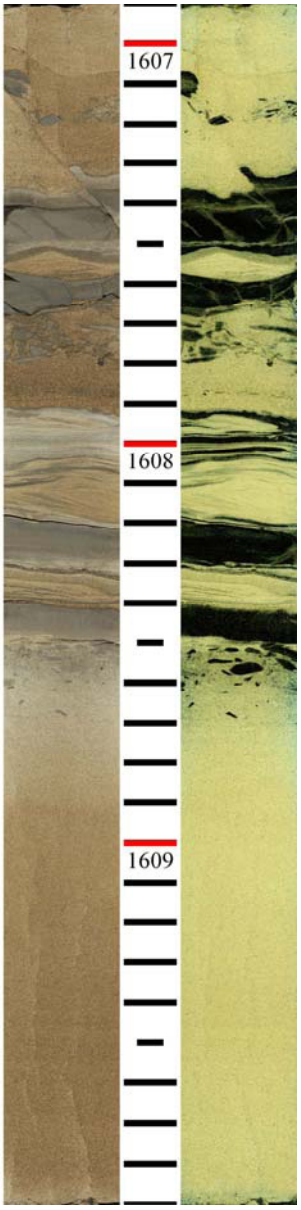

Small thrust fault. Offsets silt bed with approximately 2 cm of throw.

VF-F sand. Cross bedding with 30° dips. Well sorted.

Interbedded VF-F sand and silt. Planar to wavy bedding dipping 10°. Well sorted.

M-C sand. Massive bedding. Very well sorted.

M-C sand. Massive bedding. Very well sorted.

Interbedded VF-F sand and silt. Planar bedding dipping 0-5°. Well sorted.

Dewatering structure?

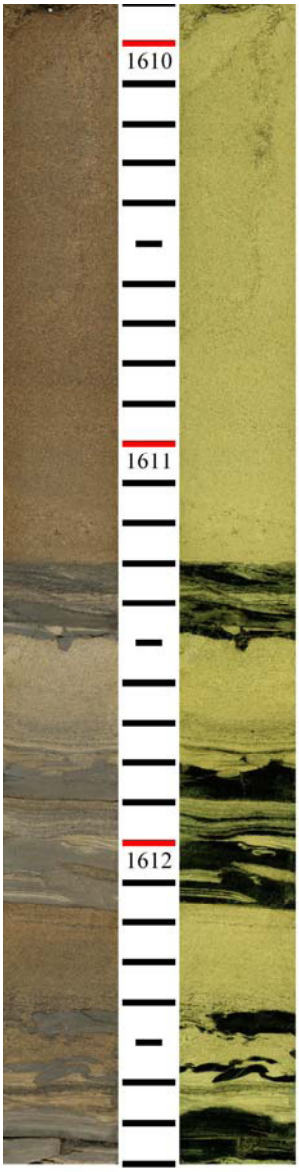

Vintage Prod. Califf. LLC
WELL: F-1
FIELD: Wheeler Ridge
LOC: Sec 28-11N-20W

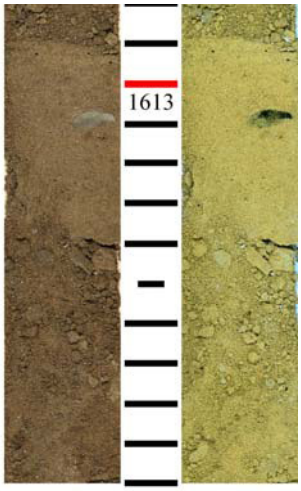

M-C sand with pebbles. Massive bedding. Well sorted.

M-C sand. Massive bedding. Very well sorted.

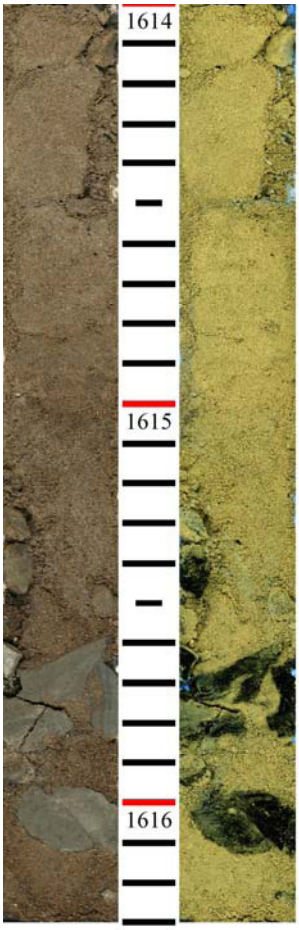

Rip up shale clasts? Storm deposits?

Vintage Prod. Callif. LLC
WELL: F-1
FIELD: Wheeler Ridge
LOC: Sec 28-11N-20W

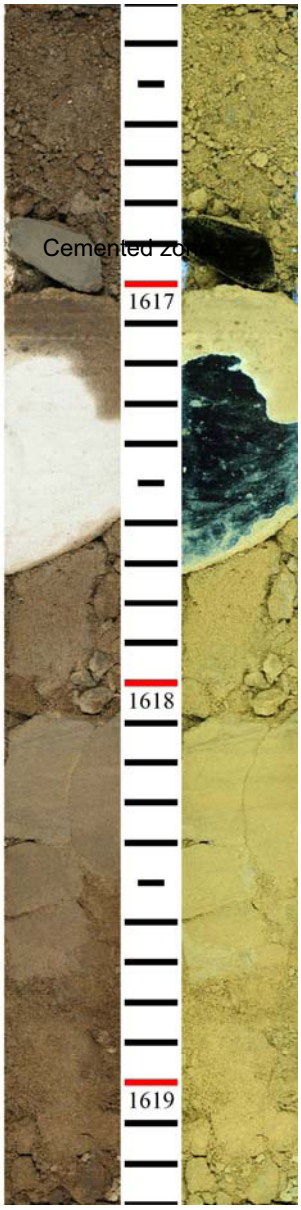

M-C sand with pebbles. Massive bedding. Very well sorted.

Cement nodule.

M-C sand. Massive bedding. Very well sorted.

M-C sand.
Massive bedding.
Very well sorted.

Vintage Prod. Callif. LLC
WELL: F-1
FIELD: Wheeler Ridge
LOC: Sec 28-11N-20W

M-C sand. Massive bedding. Very well sorted.

Root.

M-C sand with pebbles. Massive bedding. Very well sorted.

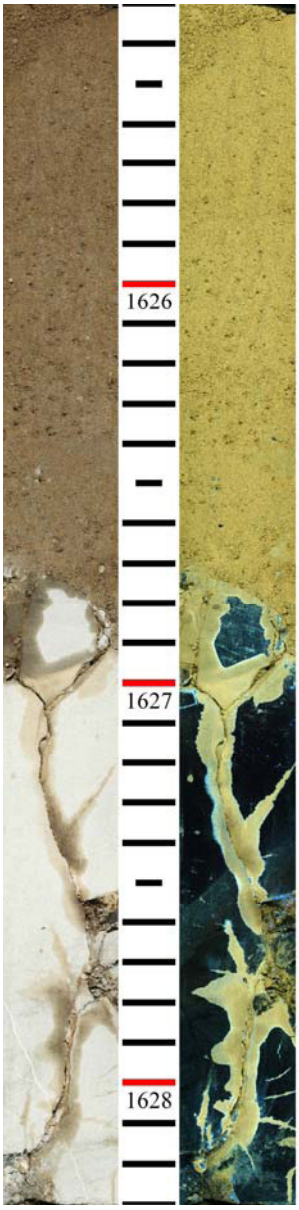

Cemented zone.

Vintage Prod. Callif. LLC
WELL: F-1
FIELD: Wheeler Ridge
LOC: Sec 28-11N-20W

M-C sand with pebbles. Massive bedding. Very well sorted.

Cemented zone.

(F2 2052-2124)

Upper Fruitvale.

Siltstone with bedding parallel laminations. Numerous burrows.

Near vertical fissure, at least six feet in length.

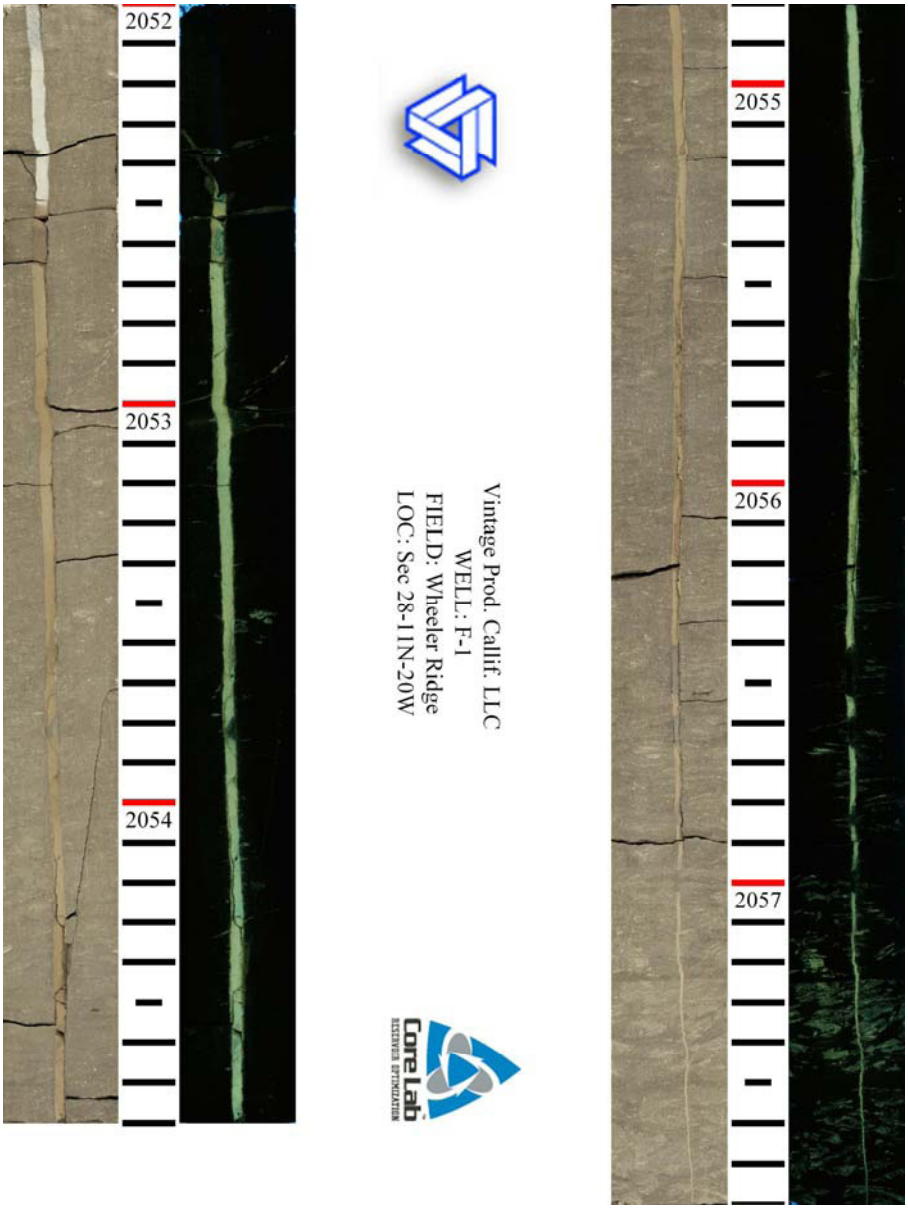

Siltstone with bedding parallel laminations. Numerous burrows.

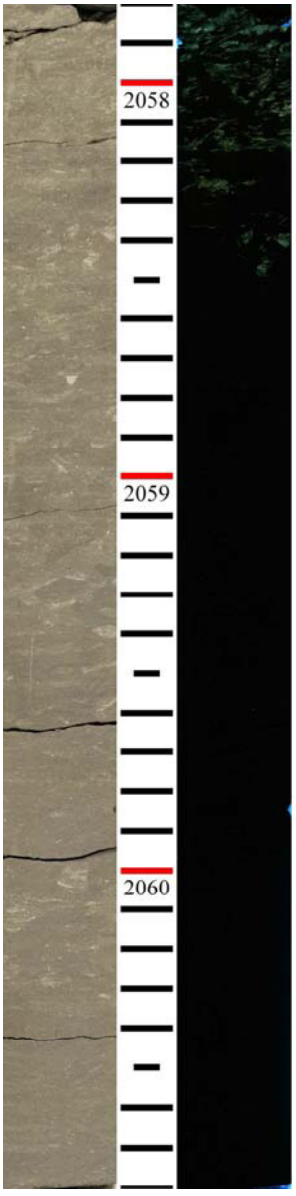

Bedding parallel fracturing.

Vintage Prod. Callif. LLC
WELL: F-1
FIELD: Wheeler Ridge
LOC: Sec 28-11N-20W

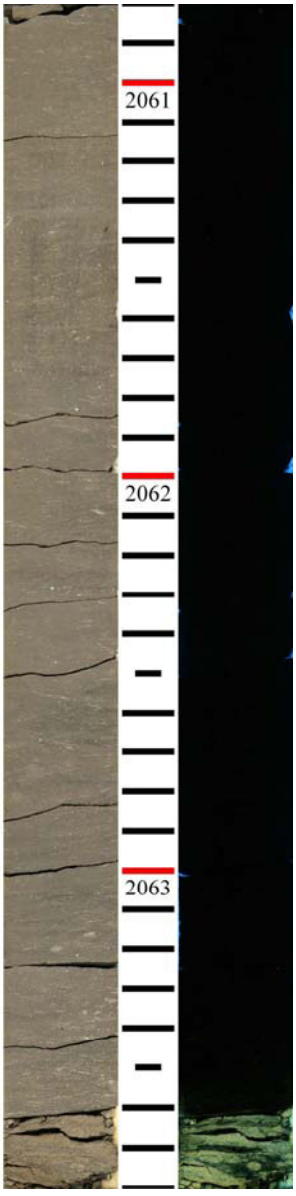

Siltstone with bedding parallel laminations. Numerous burrows.

Bedding parallel fracturing.

Siltstone with bedding parallel laminations. Numerous burrows.

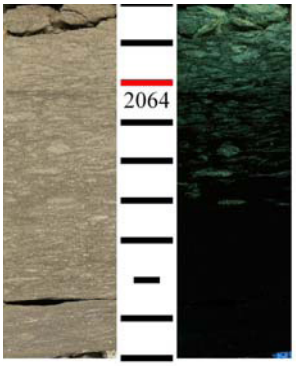

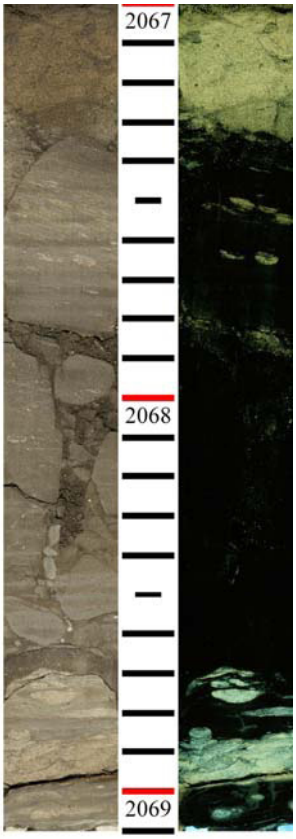

Siltstone with bedding parallel laminations. Numerous burrows.

Vintage Prod. Califf. LLC
WELL: F-1
FIELD: Wheeler Ridge
LOC: Sec 28-11N-20W

F2 top at 2069.3’

F2 is interpreted to be a turbidite deposit. The WR F1 well penetrated a distal edge of the F2 sand and is

Tb

VF-M sand with planar bedding. Well sorted.

Ta

VF-M sand with gravel. Normally graded bedding. Moderately sorted.

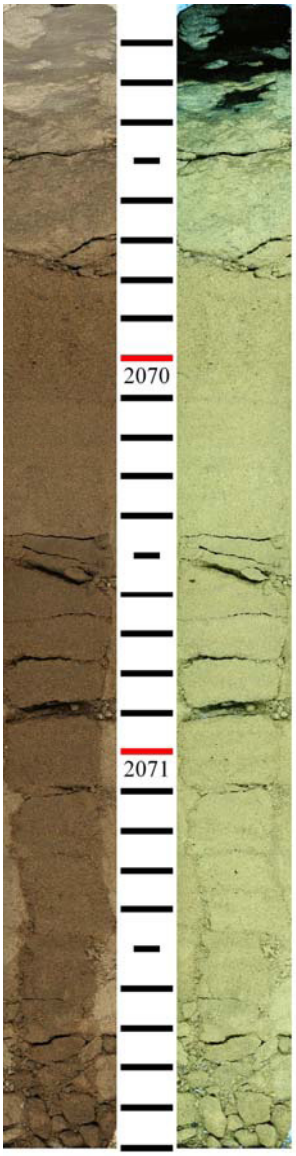

Vintage Prod. Calif. LLC
WELL: F-1
FIELD: Wheeler Ridge
LOC: Sec 28-11N-20W

Ta

VF-M sand with gravel. Normally graded bedding. Moderately sorted.

Td

Silt with bedding parallel laminations.

Tc

VF-M sand with trough cross bedding. Well sorted.

Td

Silt with bedding parallel laminations.

Tc

VF-M sand with cross bedding. Well sorted.

Tb

VF-M sand with planar bedding. Well sorted.

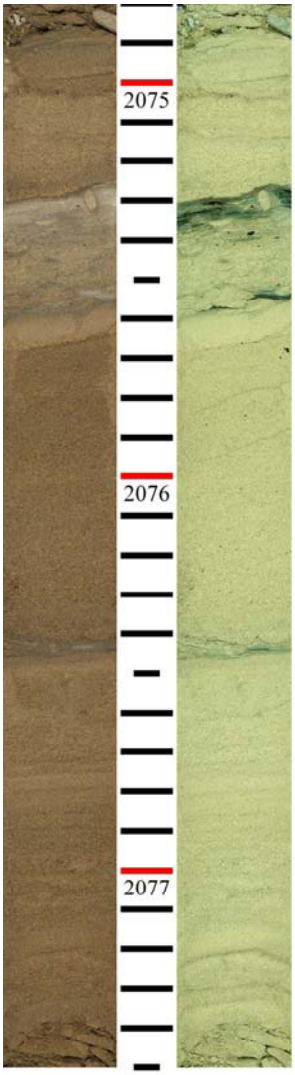

Vintage Prod. Califf. LLC
WELL: F-1
FIELD: Wheeler Ridge
LOC: Sec 28-11N-20W

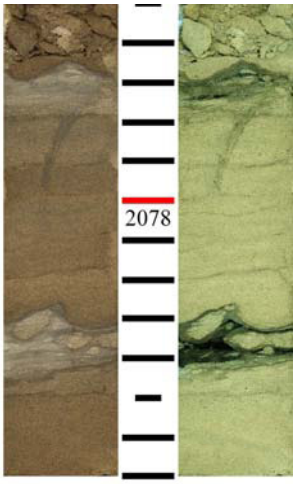

Td

Silt with bedding parallel laminations.

Tc

VF-M sand with cross bedding. Well sorted.

Td

Silt with bedding parallel laminations.

Td

Silt with bedding parallel laminations.

Tc

VF-M sand with cross bedding. Well sorted.

Tb

VF-M sand with planar bedding. Well sorted.

Ta

M-C sand with normally graded bedding. Well sorted.

Vintage Prod. Califf. LLC
WELL: F-1
FIELD: Wheeler Ridge
LOC: Sec 28-11N-20W

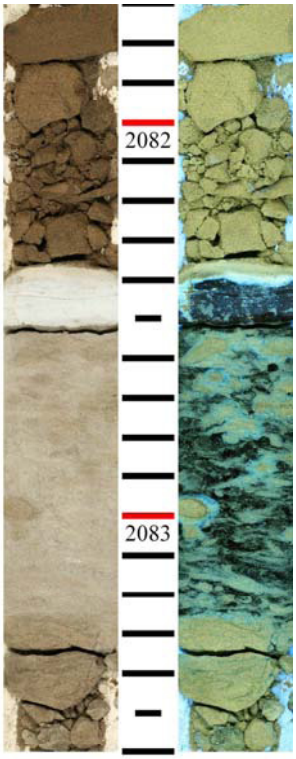

Siltstone. High degree of bioturbation.

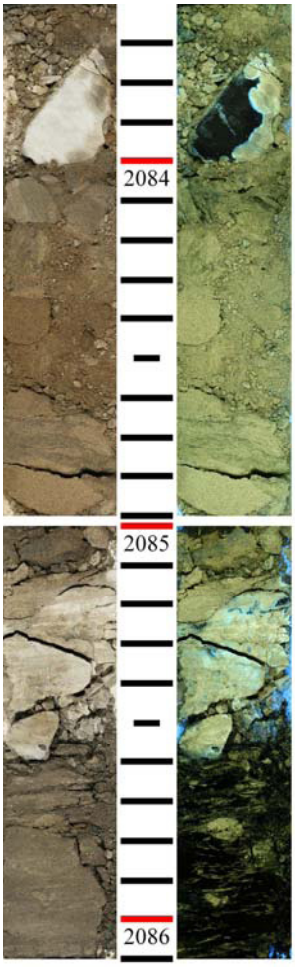

Siltstone. High degree of bioturbation.

Siltstone. High degree of bioturbation.

Vintage Prod. Califf. LLC
WELL: F-1
FIELD: Wheeler Ridge
LOC: Sec 28-11N-20W

Siltstone. High degree of bioturbation.

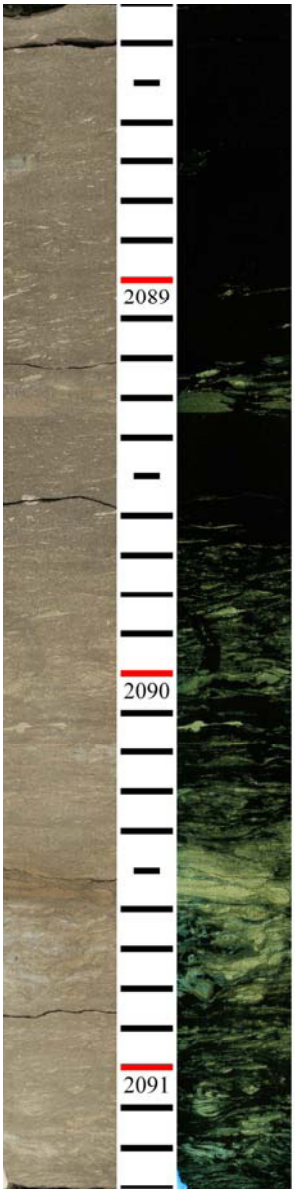

Vintage Prod. Califf. LLC
WELL: F-1
FIELD: Wheeler Ridge
LOC: Sec 28-11N-20W

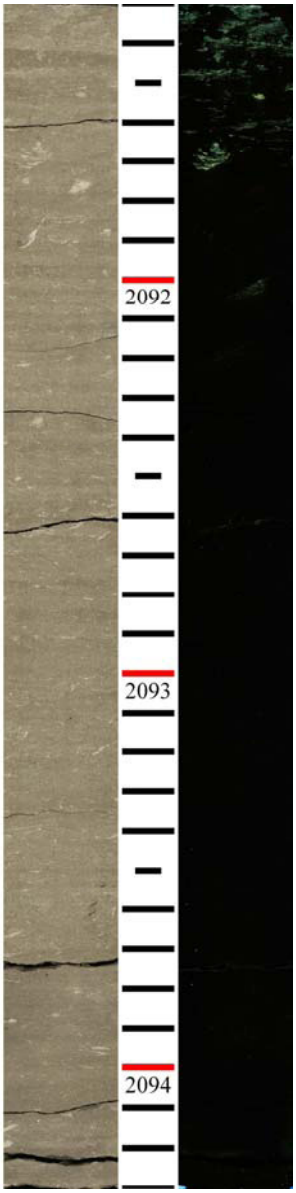

Siltstone. High degree of bioturbation.

Siltstone. High degree of bioturbation.

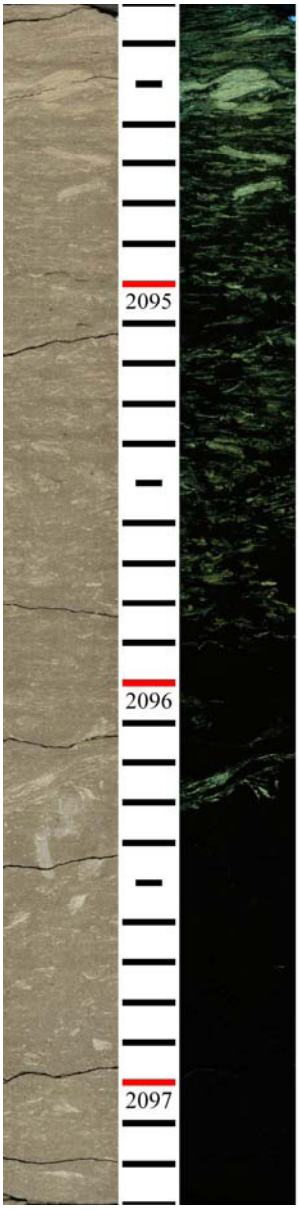

Vintage Prod. Callif. LLC
WELL: F-1
FIELD: Wheeler Ridge
LOC: Sec 28-11N-20W

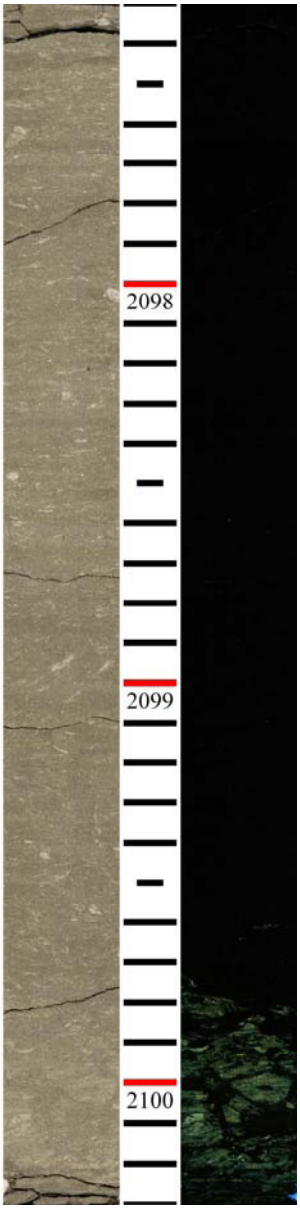

Siltstone. High degree of bioturbation.

Siltstone. High degree of bioturbation.

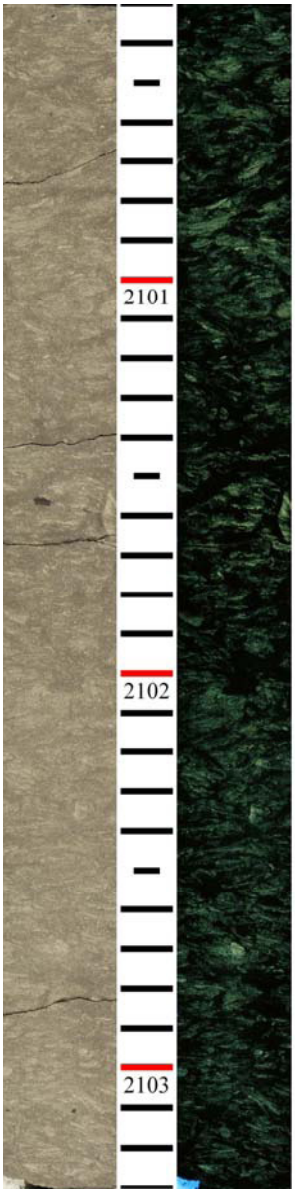

Vintage Prod. Califf. LLC
WELL: F-1
FIELD: Wheeler Ridge
LOC: Sec 28-11N-20W

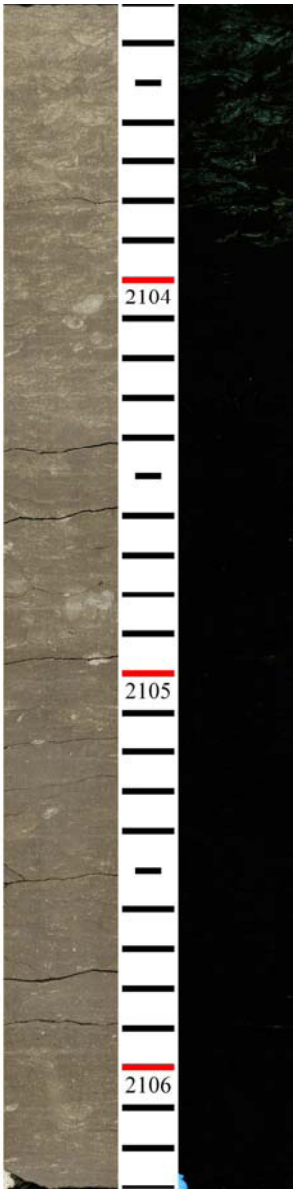

Siltstone. High degree of bioturbation.

Siltstone. High degree of bioturbation.

Lower unconformity.

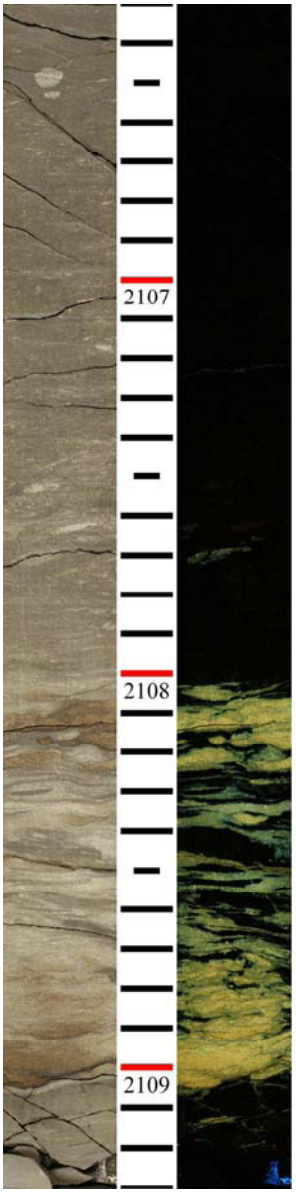

Vintage Prod. Calif. LLC
WELL: F-1
FIELD: Wheeler Ridge
LOC: Sec 28-11N-20W

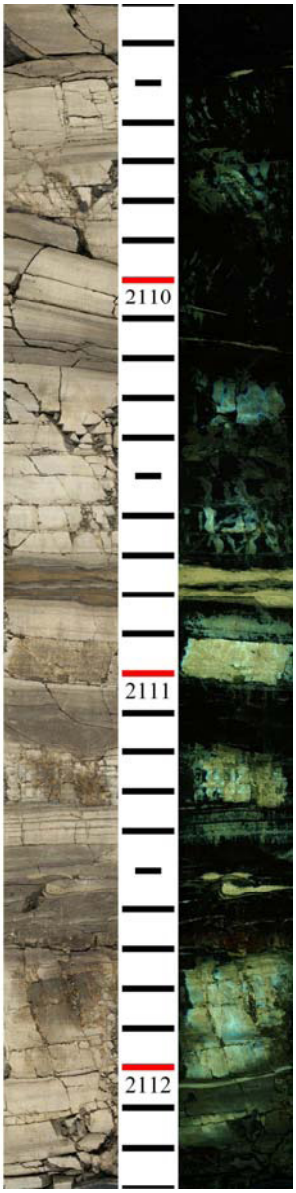

Top of lower Fruitvale at 2109'

Interbedded siltstone with chert? Bedding parallel laminations.

High fracture density.

Vintage Prod. Callif. LLC
WELL: F-1
FIELD: Wheeler Ridge
LOC: Sec 28-11N-20W

Core Lab
RESERVOIR OPTIMIZATION